Engineering artificial gauge fields with ultracold atoms - part III

Monika Aidelsburger

Ludwig-Maximilians Universität München
Munich Center for
Quantum Science & Technology

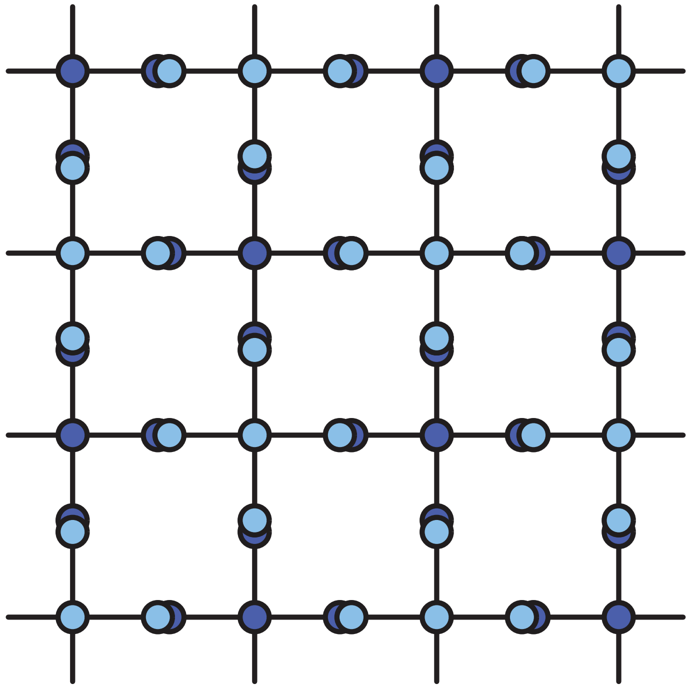

Hofstadter model

$$\hat{H} = -J \sum_{m,n} \left(\mathrm{e}^{in\Phi} \hat{a}^{\dagger}_{m+1,n} \hat{a}_{m,n} + \hat{a}^{\dagger}_{m,n+1} \hat{a}_{m,n} + \mathrm{h.c.} \right)$$

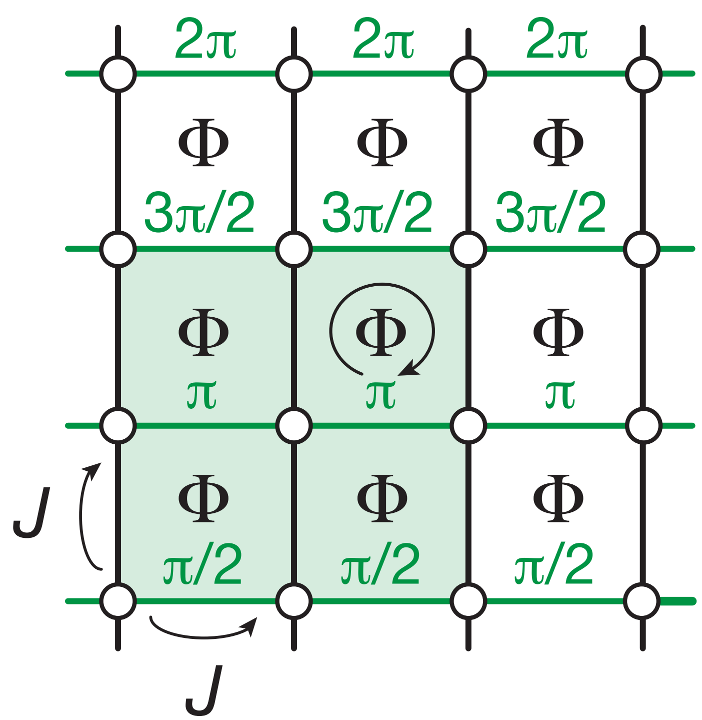

Discrete translational symmetry
no longer determined by lattice vectors

- Magnetic translation operators!
- Increased magnetic unit cell (flux 2π)

P.G. Harper, Proc. Phys. Soc., Sect.A 68, 874 (1955);
M.Y. Azbel, Zh. Eksp. Teor. Fiz. 46, 929 (1964); D.R. Hofstadter, Phys. Rev. B14, 2239 (1976)

Hofstadter model

Single-particle energy spectrum: Hofstadter-butterfly

- For $\Phi_B/\Phi_0 = p/q$, the band splits into q subbands

- For $\Phi_B/\Phi_0 = \Phi/2\pi = 1/4$:

  » Lowest band has a Chern number 1

  » Large flatness ratio: $E_{\mathrm{gap}}/E_{\mathrm{bw}} \simeq 7$

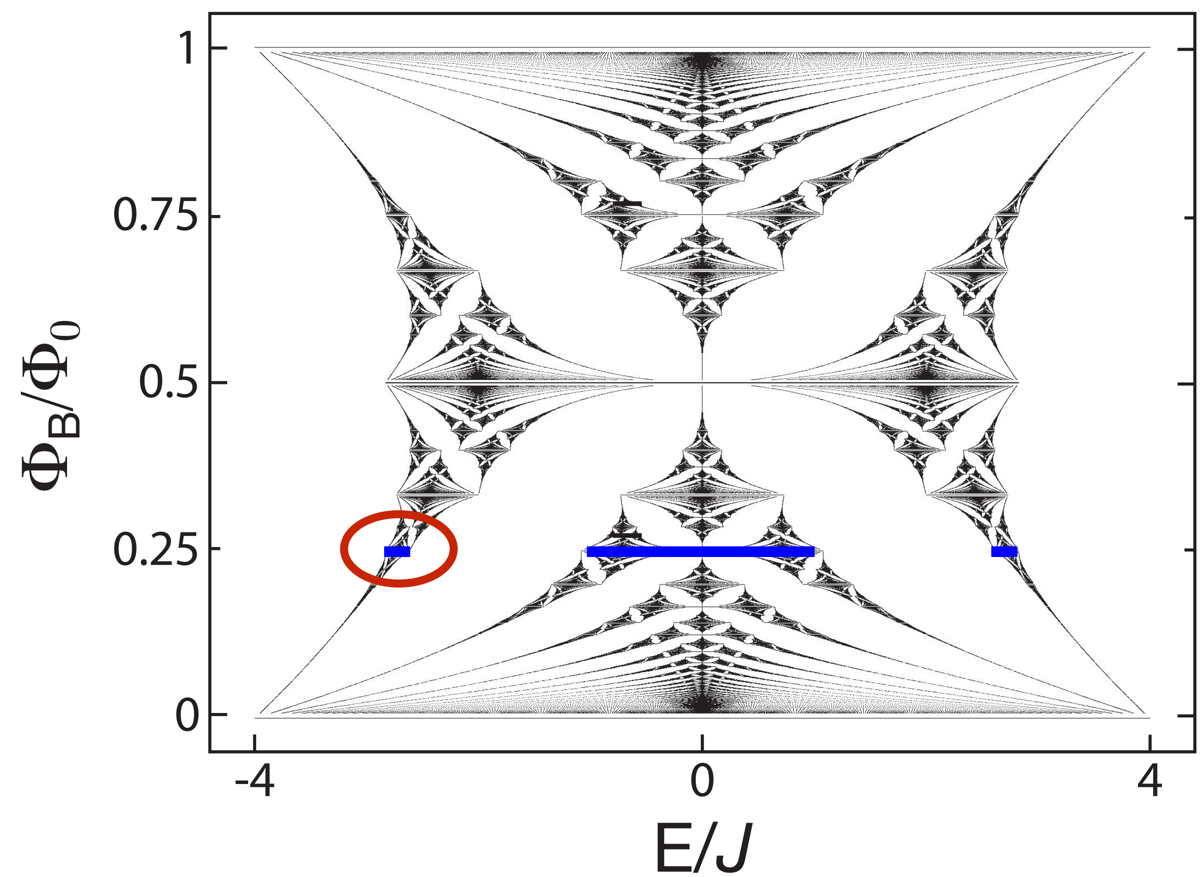

P.G. Harper, Proc. Phys. Soc., Sect.A 68, 874 (1955);
M.Y. Azbel, Zh. Eksp. Teor. Fiz. 46, 929 (1964); D.R. Hofstadter, Phys. Rev. B14, 2239 (1976)

Topology in hexagonal optical lattices

Hexagonal lattice

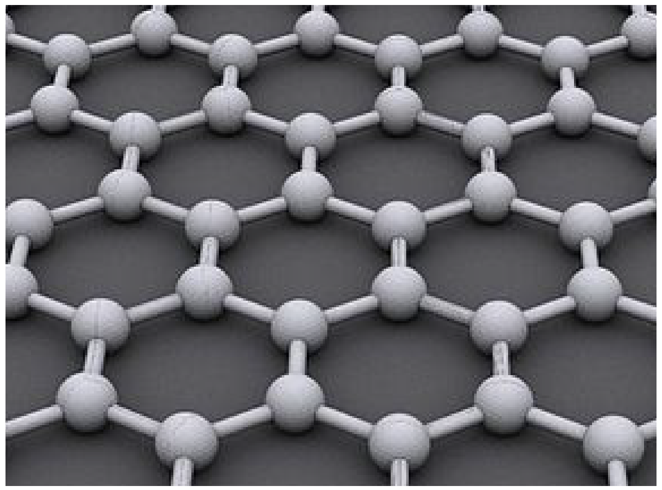

Lattice: A and B degenerate sublattices

$$H = H_0 - J \sum_{\mathbf{R}} \sum_{i=1}^{3} \left(\hat{a}_{\mathbf{R}} \hat{b}^{\dagger}_{\mathbf{R}+\mathbf{d}_i} + \text{h.c.} \right)$$

Two sublattices → two lowest energy bands

Real Space

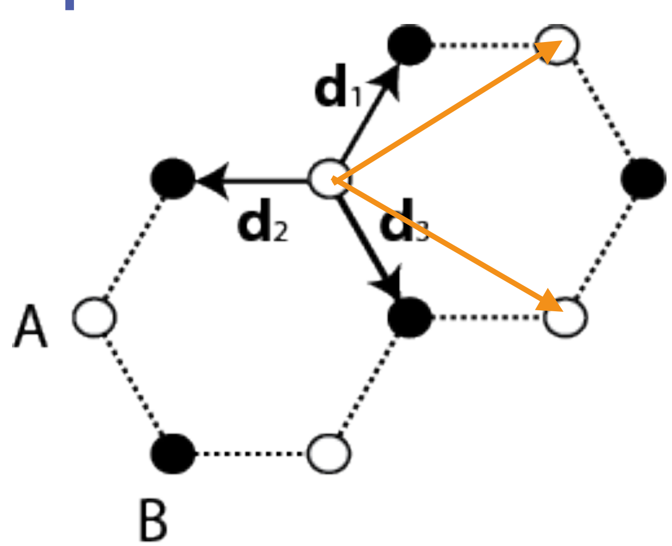

Reciprocal Space

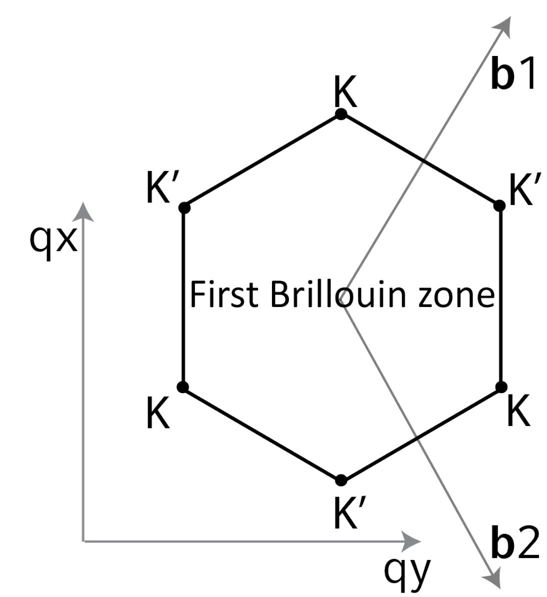

A. Castro Neto et al., Rev. Mod. Phys. **81**, 109 (2009)
cold atoms: K. Sengstock (Hamburg), T. Esslinger (Zürich)

Hexagonal lattice

Band dispersion

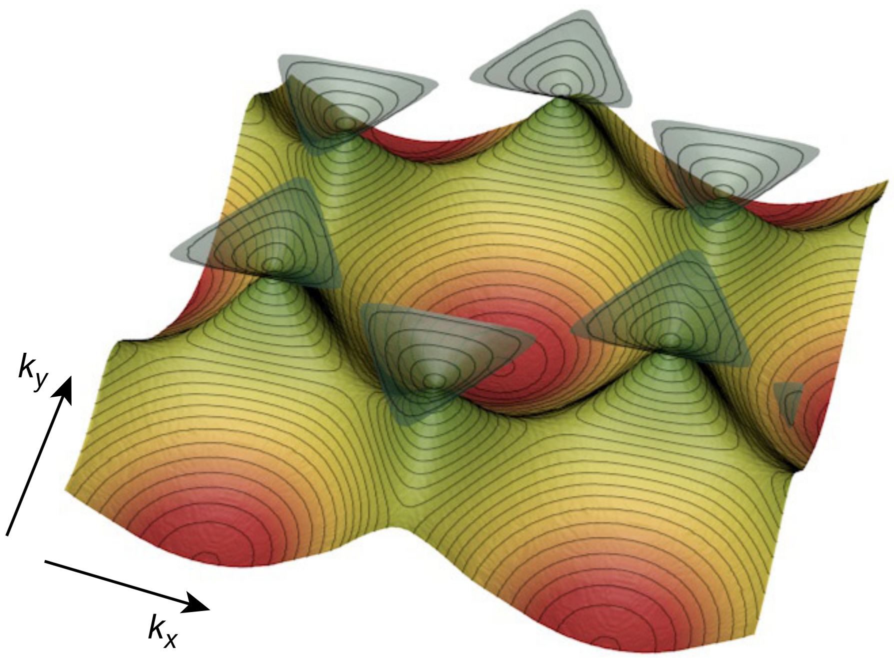

$$E_{\mathbf{q},n}$$

Berry curvature

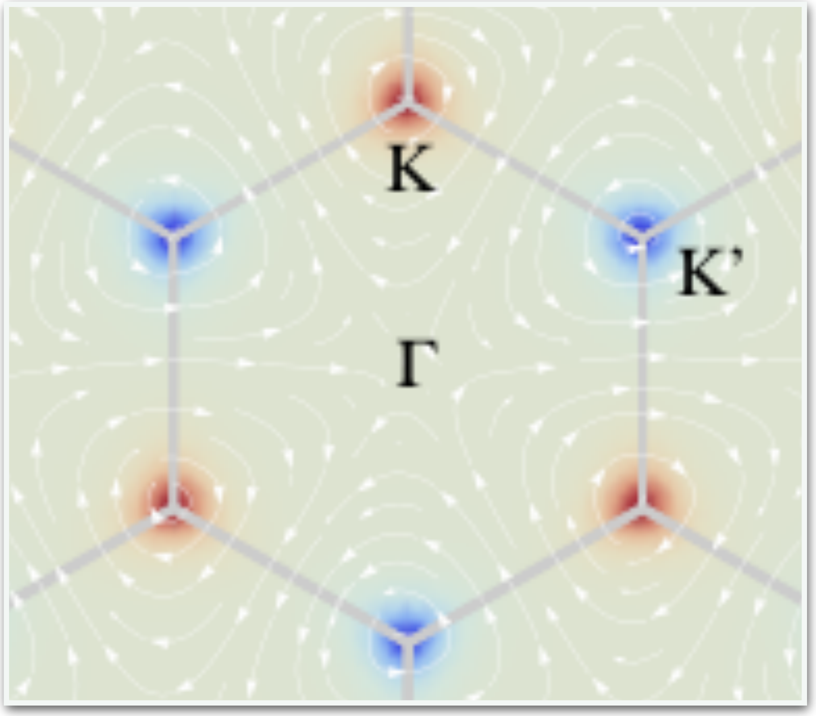

$$\Omega_n(\mathbf{q}) = \nabla_{\mathbf{q}} \times \mathbf{A_n}(\mathbf{q}) \cdot \mathbf{e}_z$$

Dirac points at the corners of the first BZ

Hexagonal lattice

Berry curvature concentrated at Dirac cones
with alternating sign at K and K' point.

- Berry Phase around K-Dirac cone

$$\varphi_{\text{Berry},\mathbf{K}} = \oint_C \mathbf{A}(\mathbf{q})\,d\mathbf{q} = \pi$$

Berry connection

- Berry Phase around K'-Dirac cone

$$\varphi_{\text{Berry},\mathbf{K}'} = -\pi$$

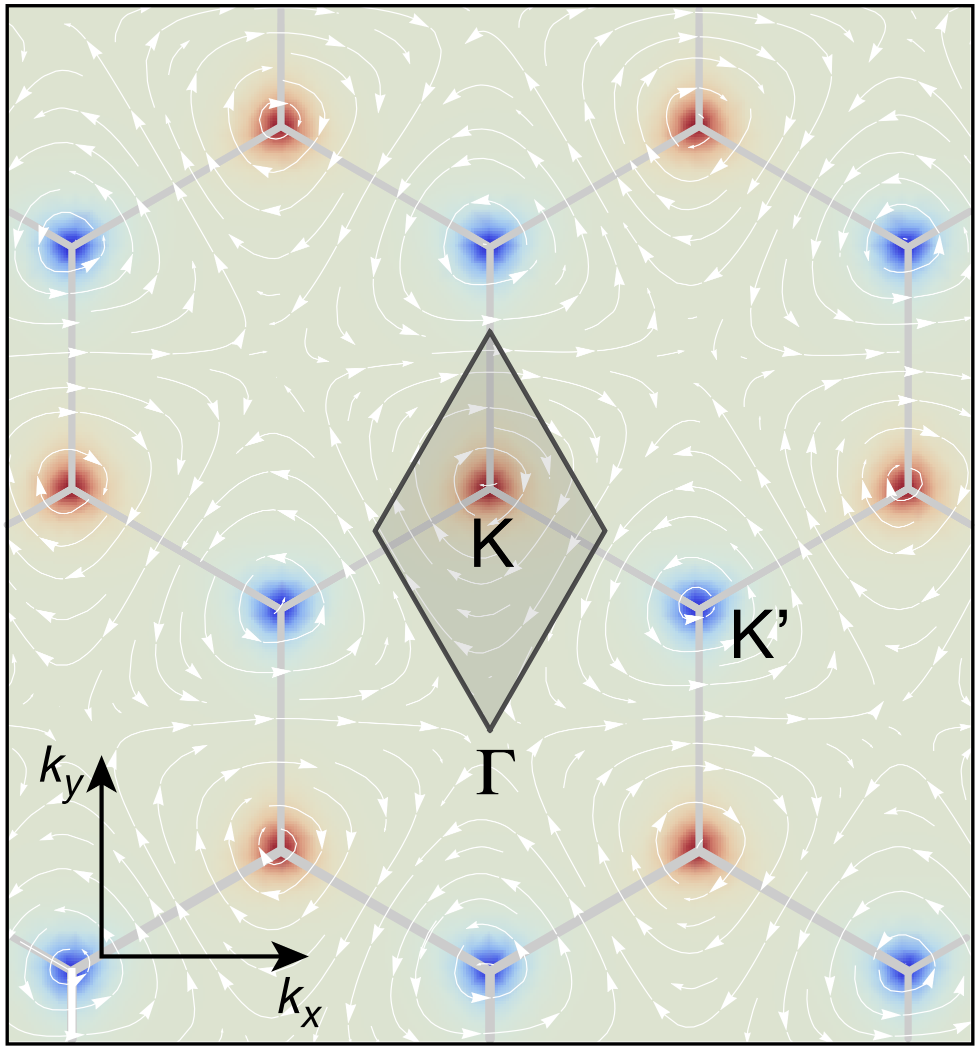

L Tarruell *et al.* Nature **483**, 302-305 (2012)
T. Uehlinger *et al.* Eur. Phys. J Special Topics **217**, 121-133 (2013)

Hexagonal lattice

Experimental realization:

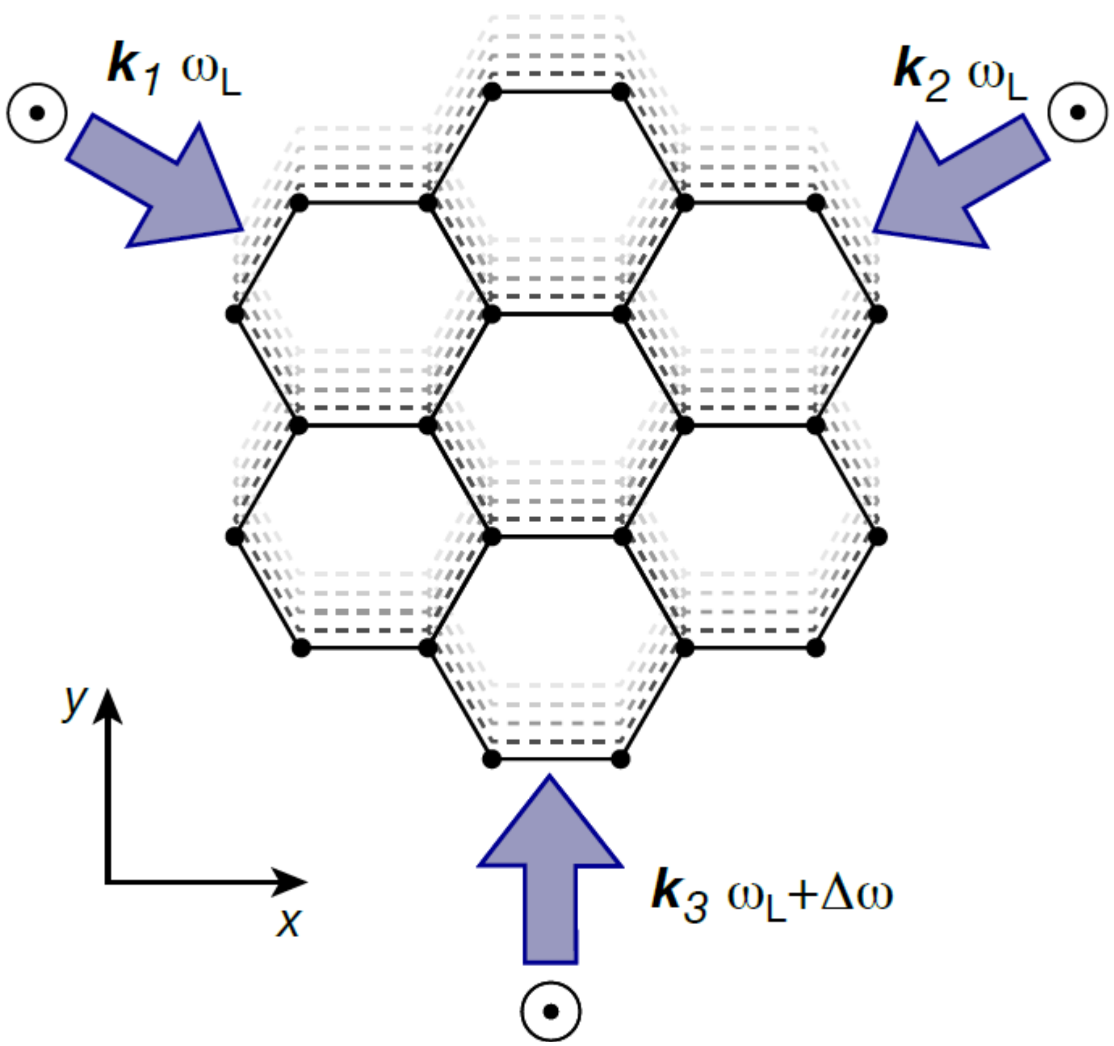

Arbitrary accelerations by t-dep. frequency shift

$$\frac{d}{dt}\Delta\omega = \mathrm{cst.}$$

→ constant acceleration

PhD thesis L. Duca (2015)

Lattice acceleration

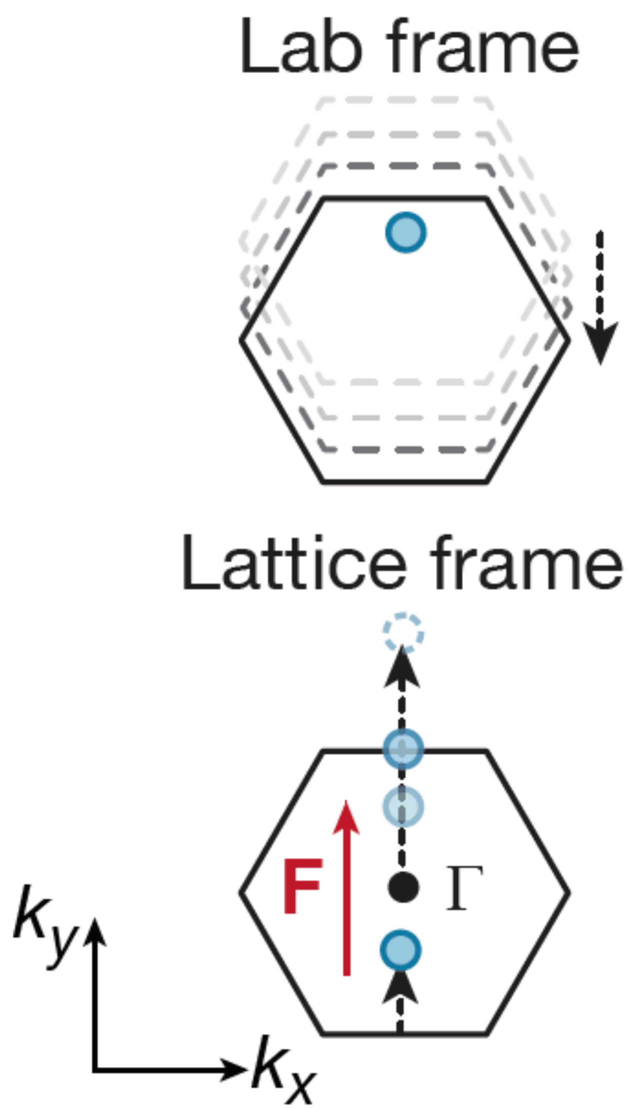

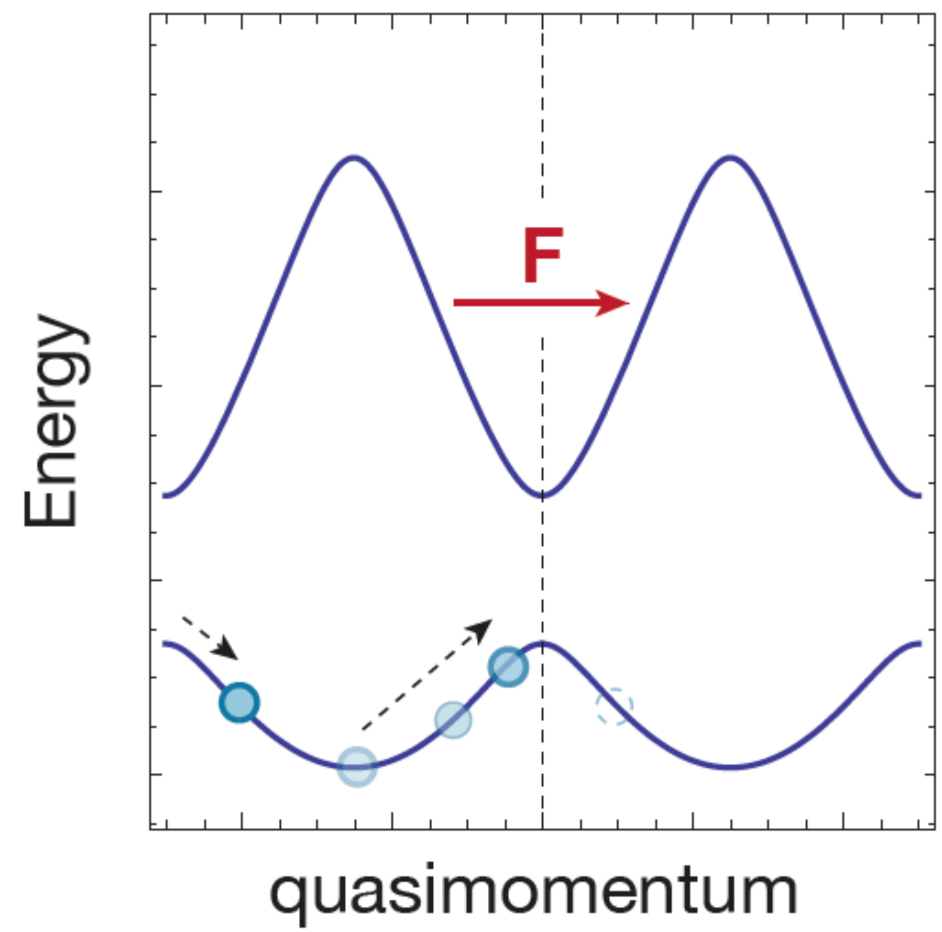

Constant force in reference frame of co-moving lattice

$$\mathbf{q}(t) = \mathbf{q}_0 + \frac{\mathbf{F}t}{\hbar}$$

PhD thesis L. Duca (2015)

Hexagonal lattice

Stückelberg oscillations:

- *Landau-Zener transitions as beam-splitters*
- Oscillations as a function of hold time at q_f=Q reveal energy gap E_Q

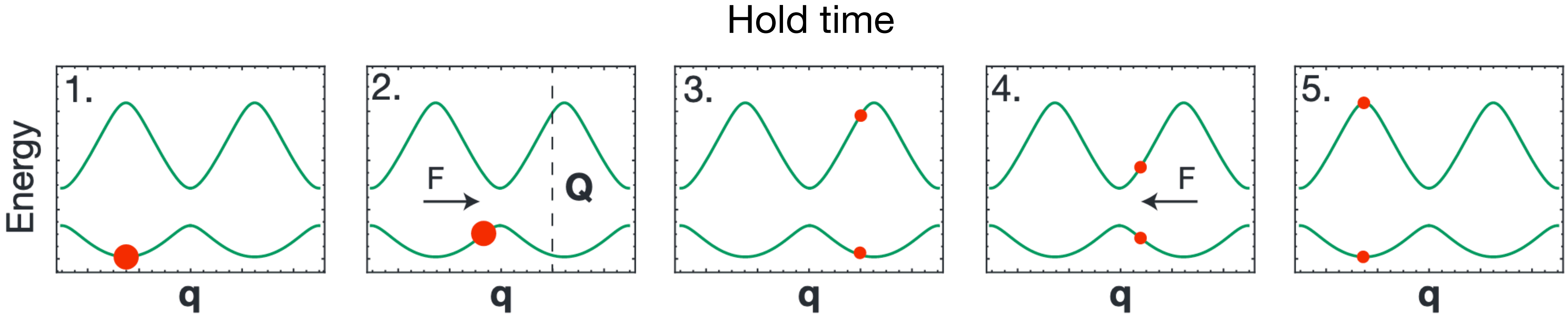

Determine band occupations!

Stückelberg, Helv. Phys. Acta 5, 369 (1932)
Shevchenko et al., Phys. Rep. 492, 1 (2010)
Zanesini et al., PRA 82, 065601, (2010), Weitz PRL 105, 215301 (2010)

Hexagonal lattice

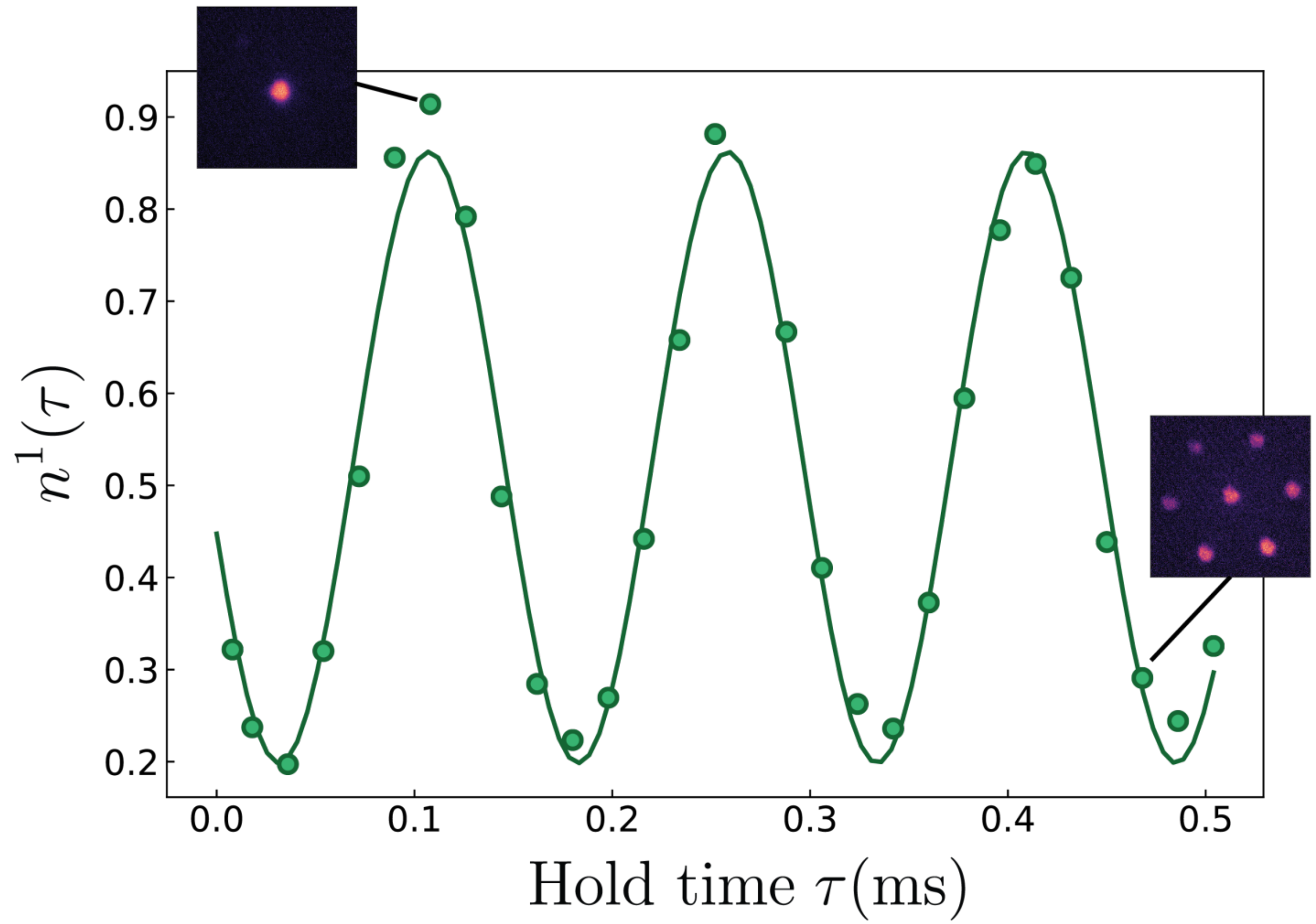

$$n^1(\tau) \propto \cos\left(\frac{E_Q^2 - E_Q^1}{\hbar}\tau\right)$$

Stückelberg, Helv. Phys. Acta 5, 369 (1932)
Shevchenko et al., Phys. Rep. 492, 1 (2010)
Zanesini et al., PRA 82, 065601, (2010), Weitz PRL 105, 215301 (2010)

Hexagonal lattice

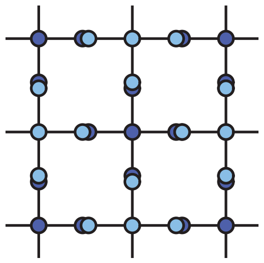

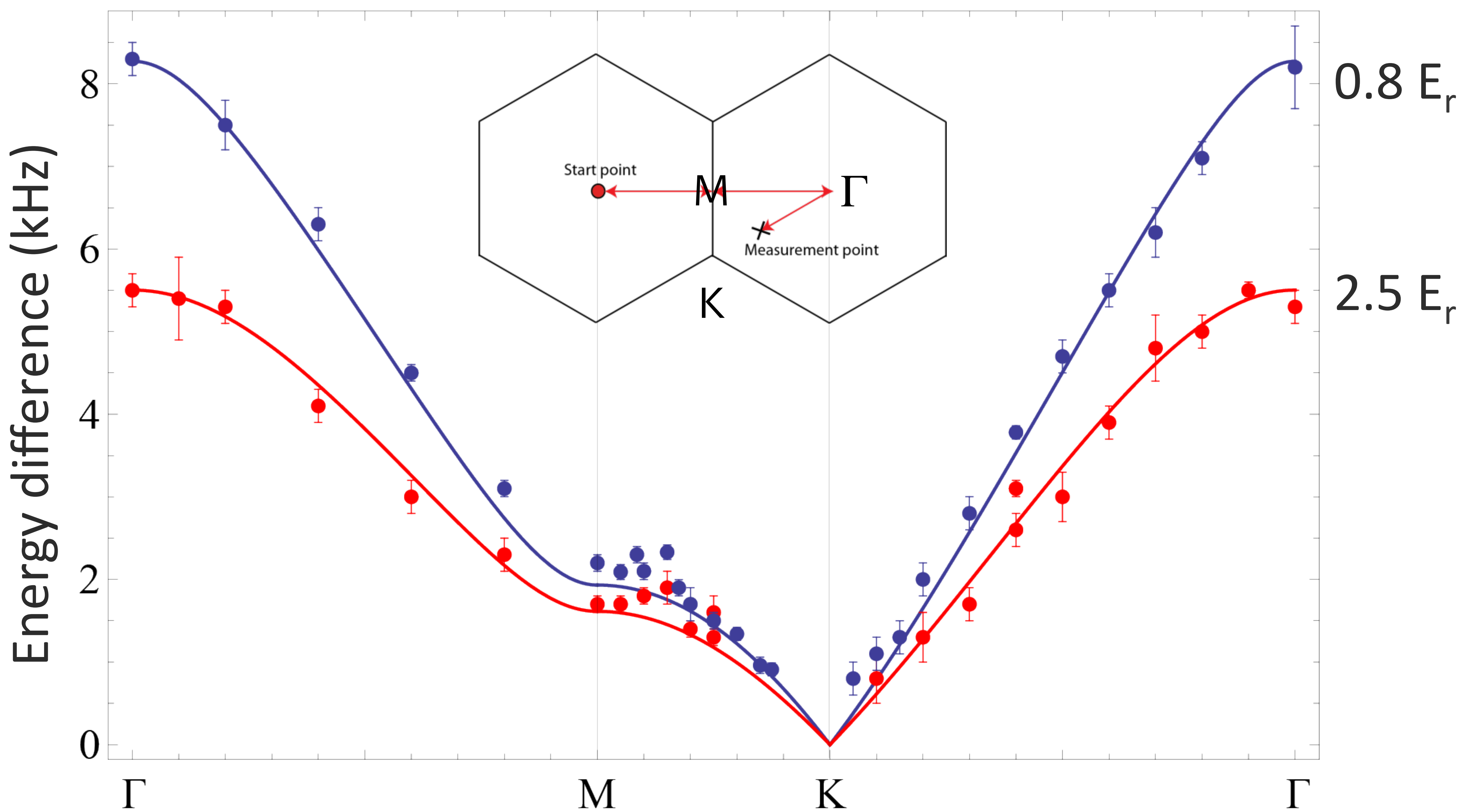

'Aharonov-Bohm' interferometer

Real Space

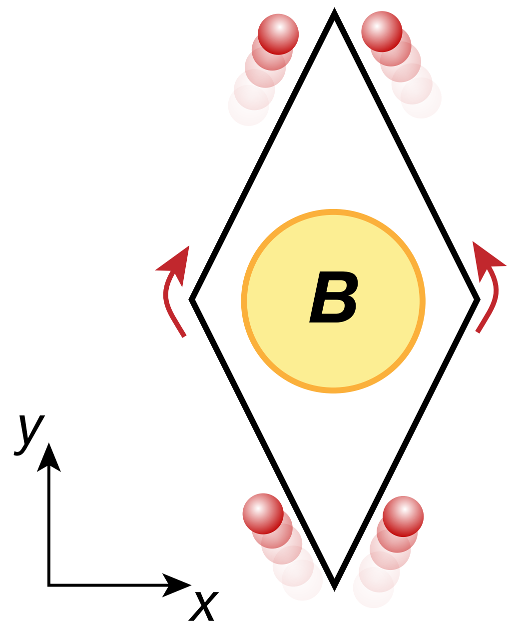

$$\varphi_{AB} = \frac{q}{\hbar}\oint_C \mathbf{A}(\mathbf{r})\,d\mathbf{r}$$

$$\varphi_{AB} = \frac{q}{\hbar}\int \mathbf{B}\,d\mathbf{S} = 2\pi\Phi/\Phi_0$$

Momentum Space

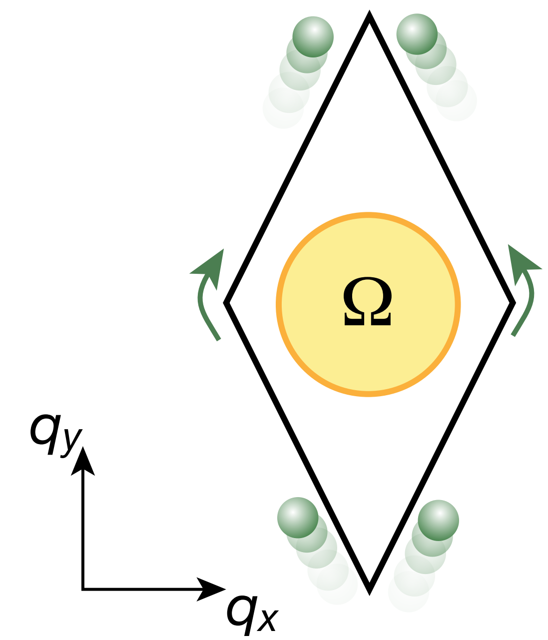

$$\varphi_{\mathrm{Berry}} = \oint_C \mathbf{A}_n(\mathbf{q})\,d\mathbf{q}$$

$$\varphi_{\mathrm{Berry}} = \int \Omega_n(\mathbf{q})\,d\mathbf{S}_q$$

Interferometer in momentum space

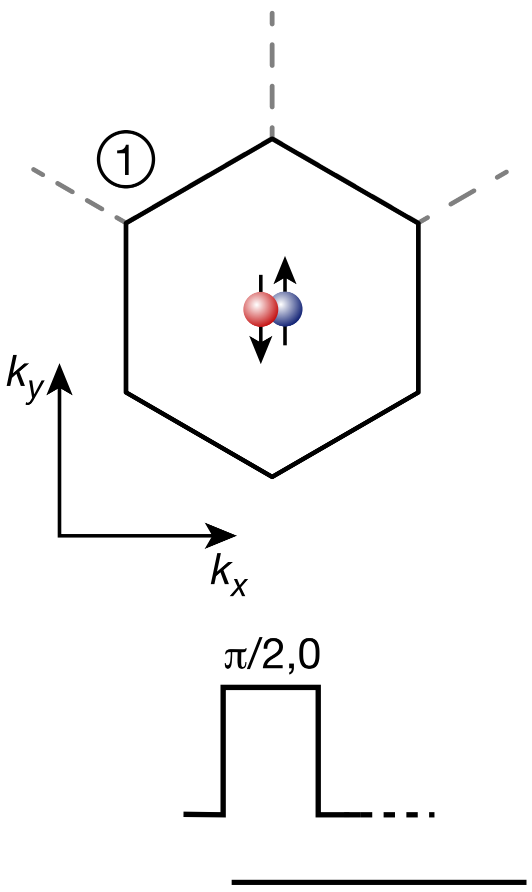

Forces applied by lattice acceleration and magnetic gradients!

L. Duca *et al.* Science **347**, 288 (2015)

Interferometer in momentum space

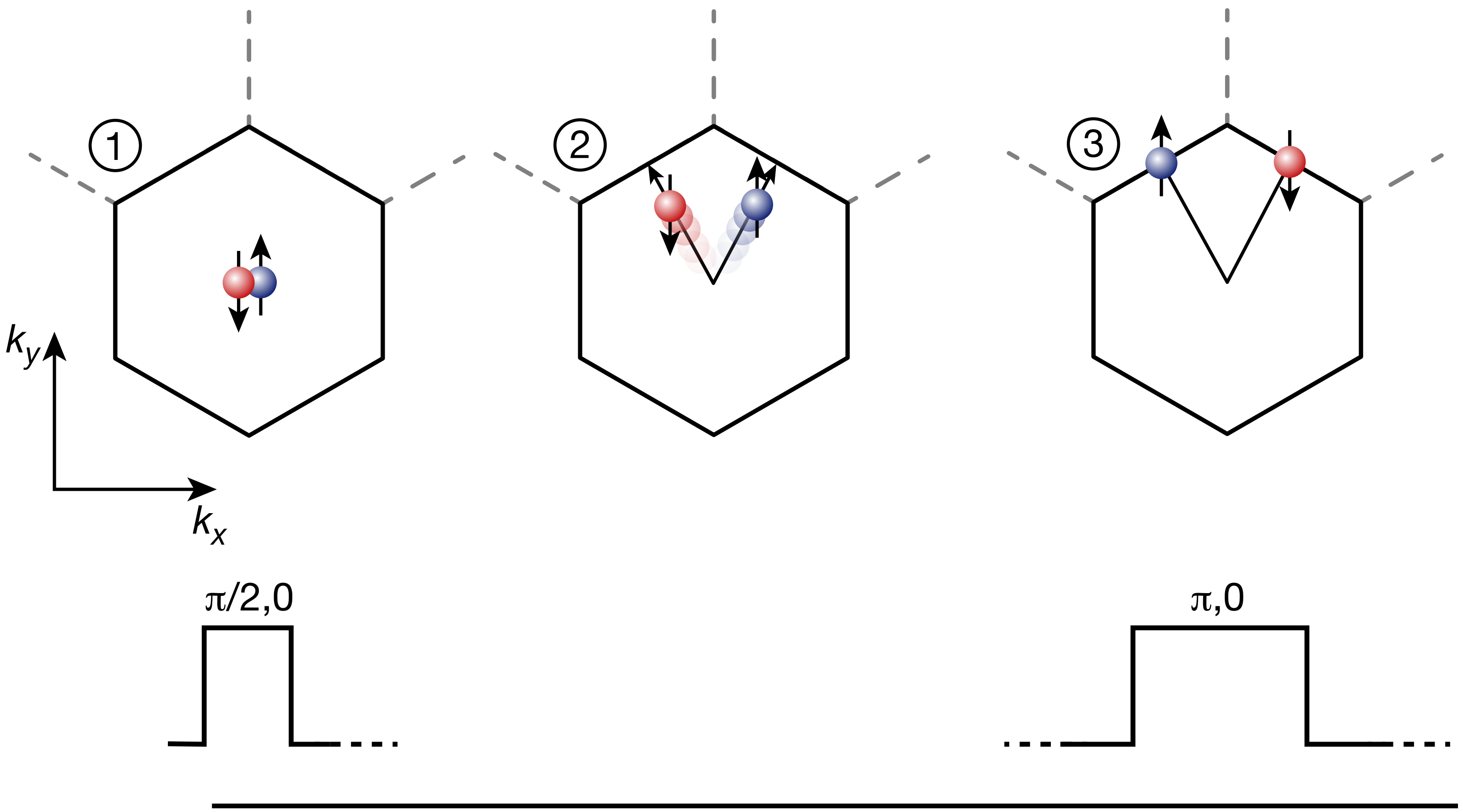

Forces applied by lattice acceleration and magnetic gradients!

L. Duca *et al.* Science **347**, 288 (2015)

Interferometer in momentum space

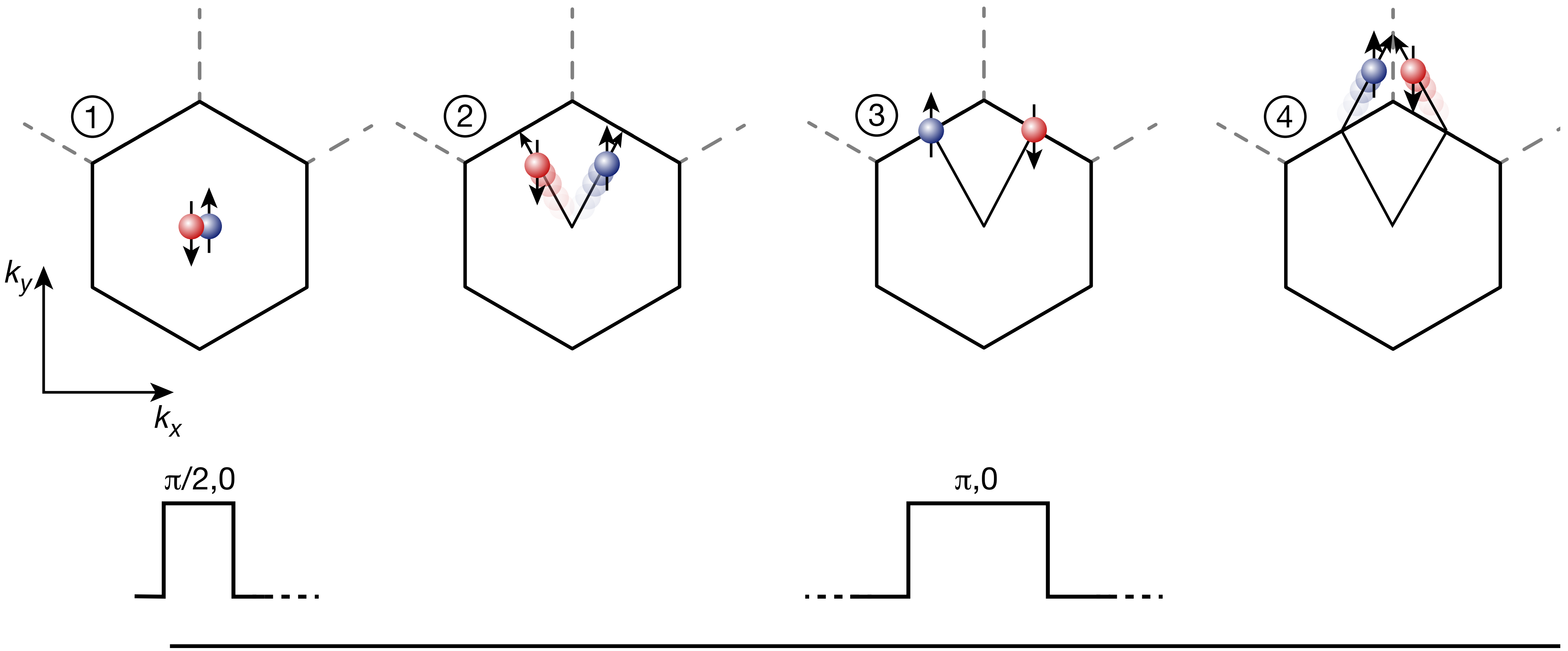

Forces applied by lattice acceleration and magnetic gradients!

L. Duca *et al.* Science **347**, 288 (2015)

Interferometer in momentum space

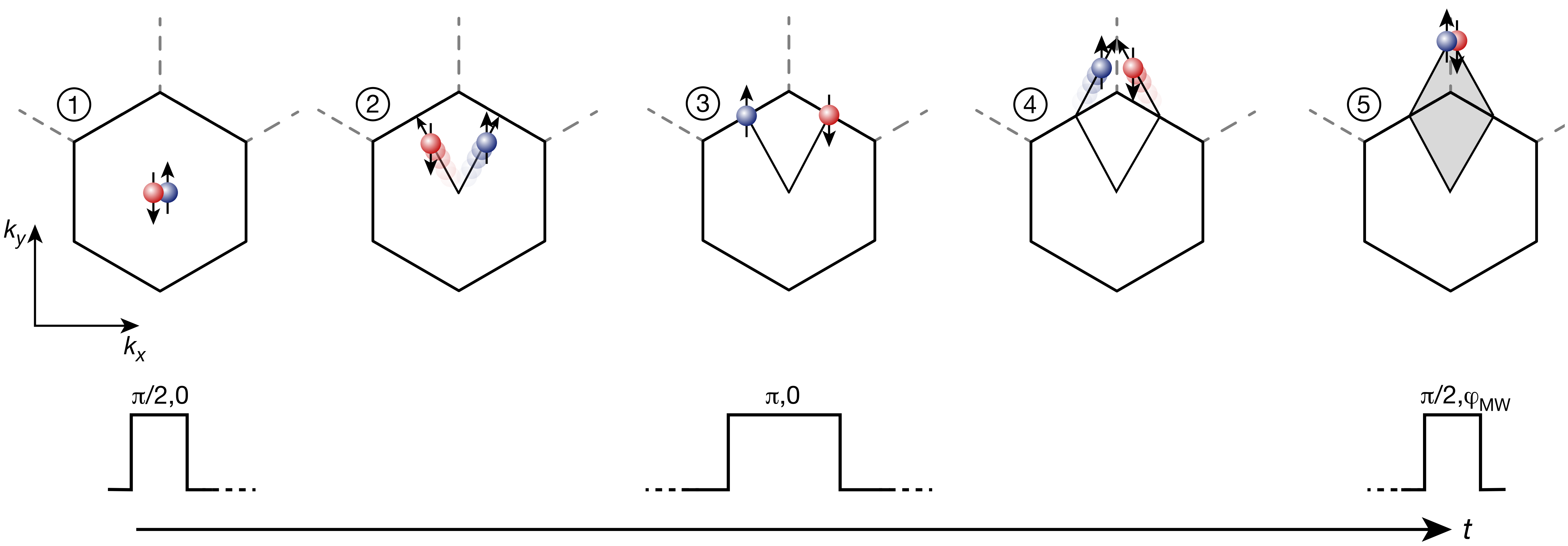

Forces applied by lattice acceleration and magnetic gradients!

L. Duca *et al.* Science **347**, 288 (2015)

Interferometer in momentum space

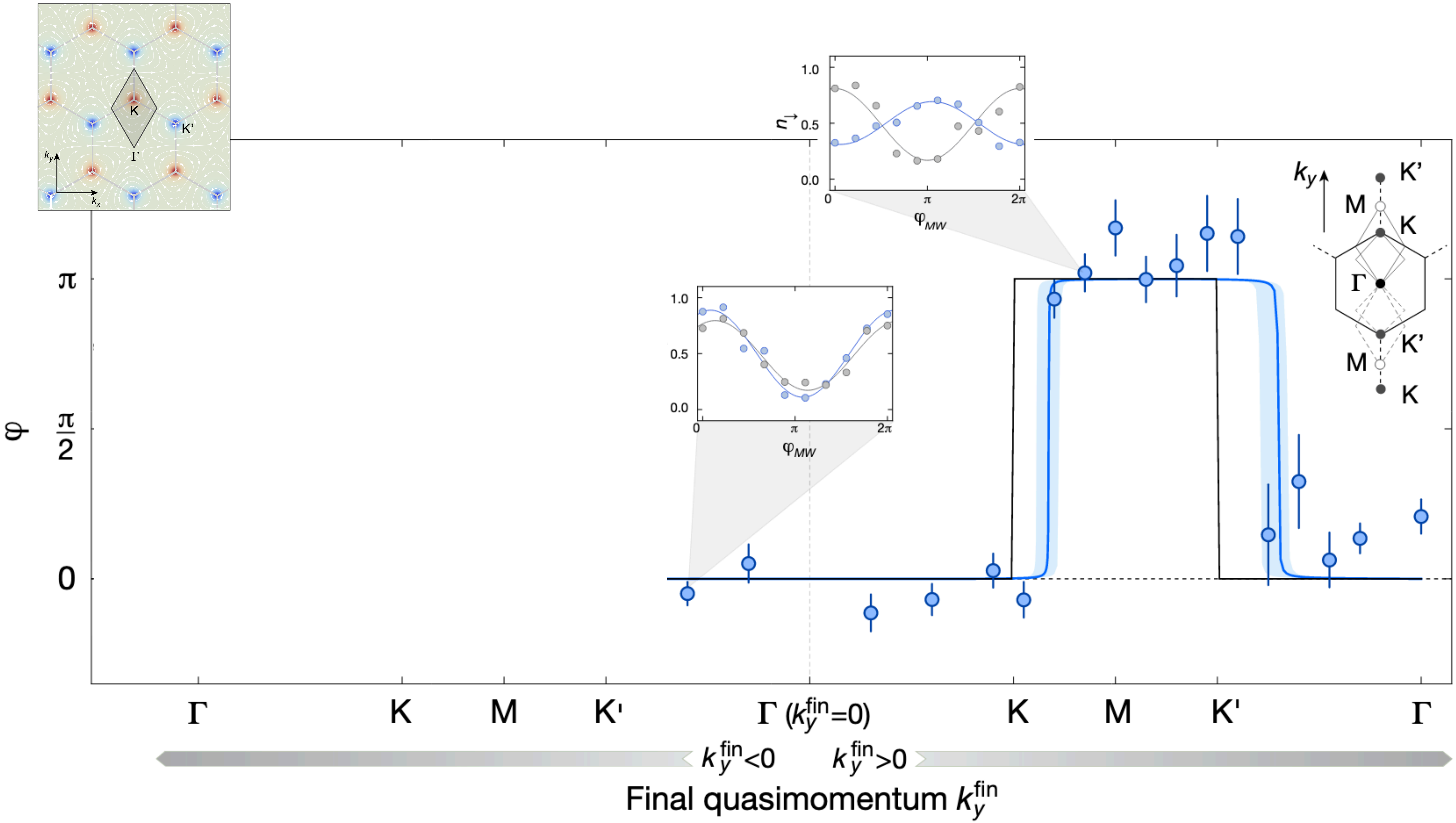

L. Duca *et al.* Science **347**, 288 (2015)

Interferometer in momentum space

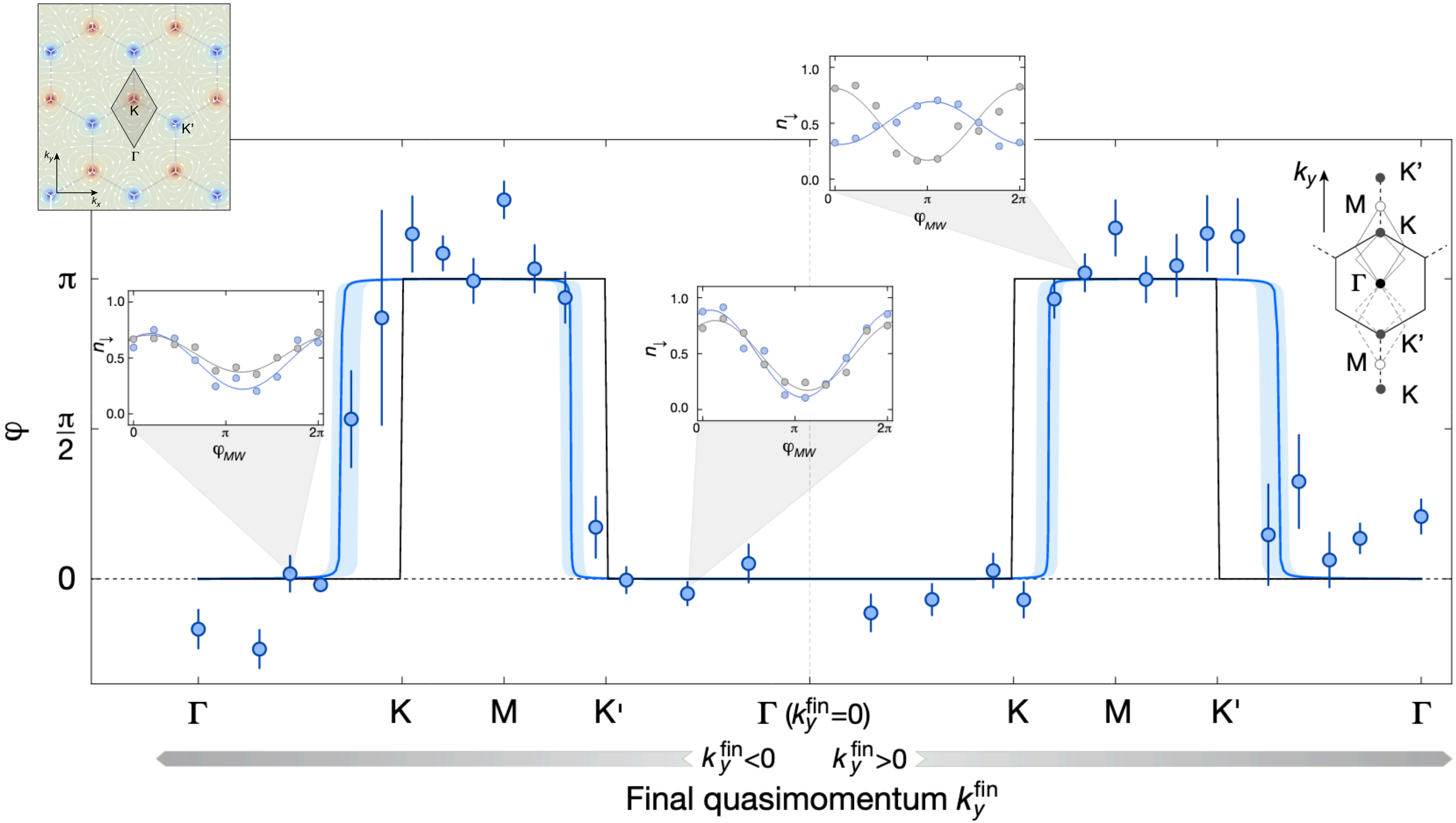

L. Duca *et al.* Science **347**, 288 (2015)

Berry phase

Cyclic adiabatic evolution (along closed path C)

$$\hat{H}(\mathbf{R}); \quad \mathbf{R}(t) = (R_1(t), R_2(t), \dots)$$

Instantaneous orthonormal basis

$$\hat{H}(\mathbf{R})\,|\,n(\mathbf{R})\rangle = E_n(\mathbf{R})\,|\,n(\mathbf{R})\rangle$$

Time-evolved state: $|\,\psi(t)\rangle = \mathrm{e}^{i\gamma_n(t)}\ \mathrm{e}^{-\frac{i}{\hbar}\int_0^t dt' E_n(\mathbf{R}(t'))}\,|\,n(\mathbf{R}(t))\rangle$

Geometric phase: $\boxed{\gamma_n(t) = \int_C \mathbf{A}_n(\mathbf{R}) \cdot d\mathbf{R}}$ $\quad \mathbf{A}_n(\mathbf{R}) = i\langle n(\mathbf{R})\,|\,\frac{\partial}{\partial \mathbf{R}}\,|\,n(\mathbf{R})\rangle$

Haldane model

The Haldane model

- no **net** magnetic field
- no breaking of lattice translational symmetry!

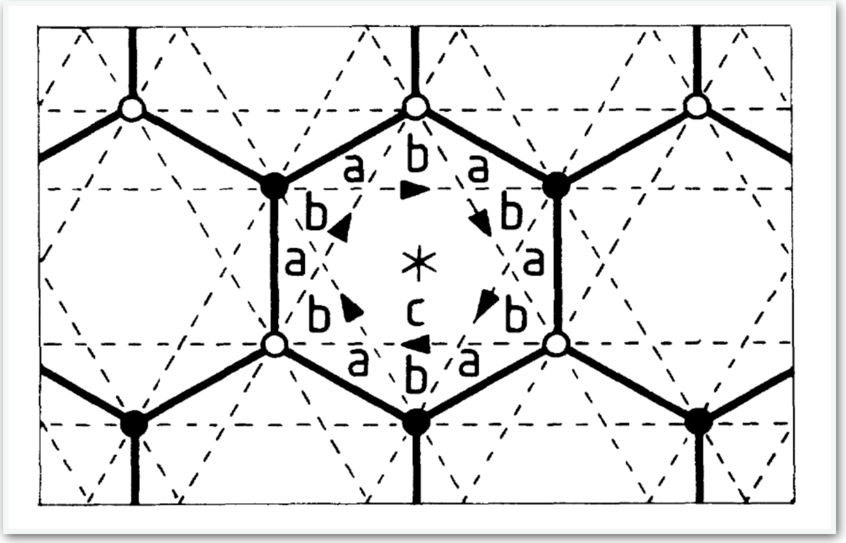

Tight-binding Hamiltonian:

$$\hat{H} = \sum_{\langle ij \rangle} t_{ij} \hat{c}_i^\dagger \hat{c}_j + \sum_{\langle\langle ij \rangle\rangle} \mathrm{e}^{i\Phi_{ij}} t'_{ij} \hat{c}_i^\dagger \hat{c}_j + \Delta_{AB} \sum_{i \in A} \hat{c}_i^\dagger \hat{c}_i$$

F. D. M. Haldane *et al. Phys. Rev. Lett.* **61**, 2015–2018 (1988)

Haldane model

Experimental realization:

T. Oka und H. Aoki, Phys. Rev. Lett. **79,** 081406 (2009)

Circular lattice shaking

$$\mathbf{r}_{\mathrm{lat}}(t) = -A\left(\cos(\omega t)\mathbf{e}_1 + \cos(\omega t - \varphi)\mathbf{e}_2\right)$$

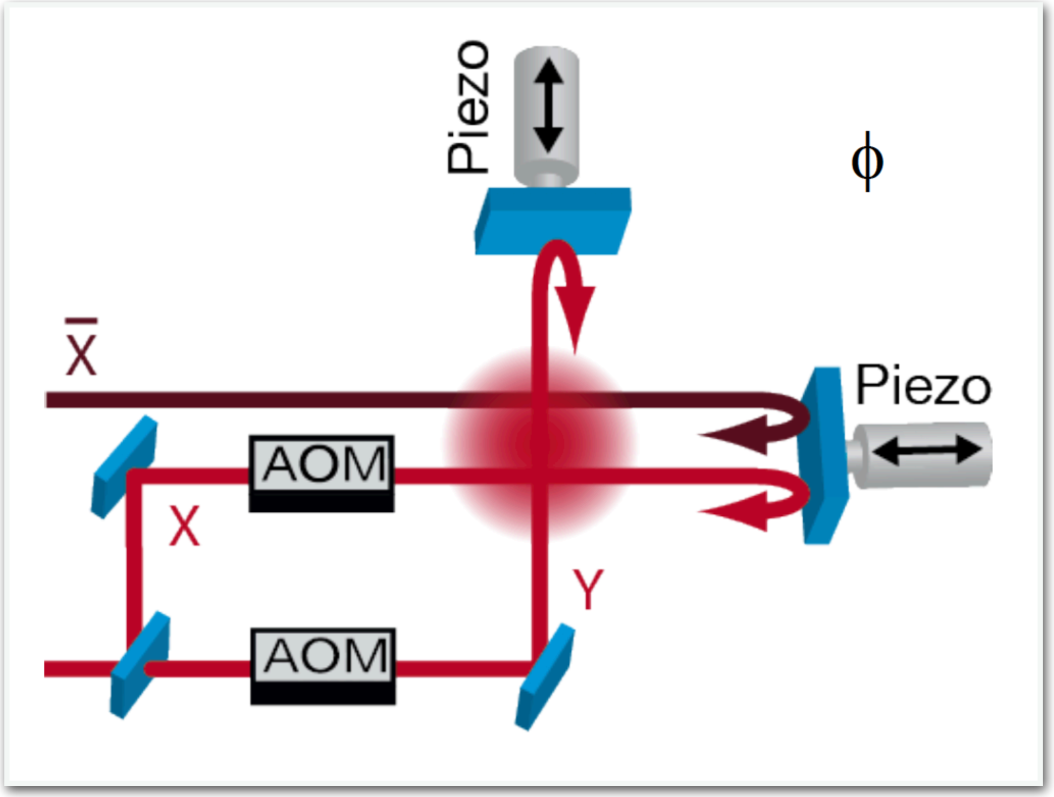

G. Jotzu *et al.* Nature **515**, 237 (2014)

Photonic systems:

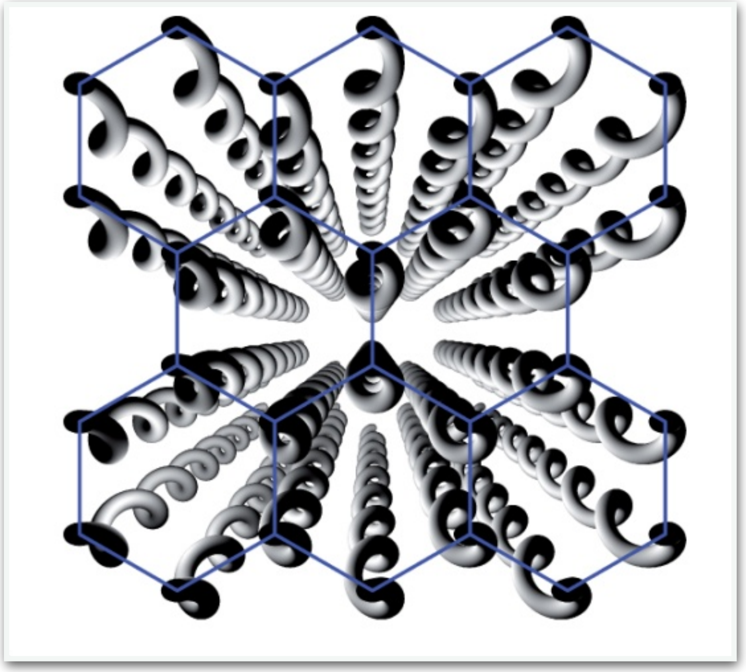

M. C. Rechtsman *et al.* Nature **496**, 196 (2013)

Haldane model

The Haldane model

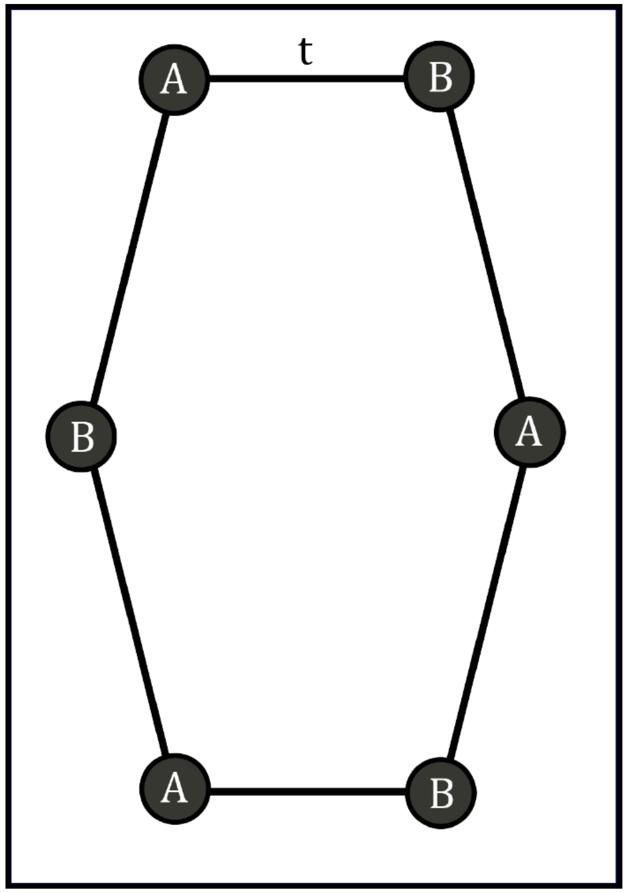

Starting point: honeycomb lattice
inversion + time-reversal symmetric

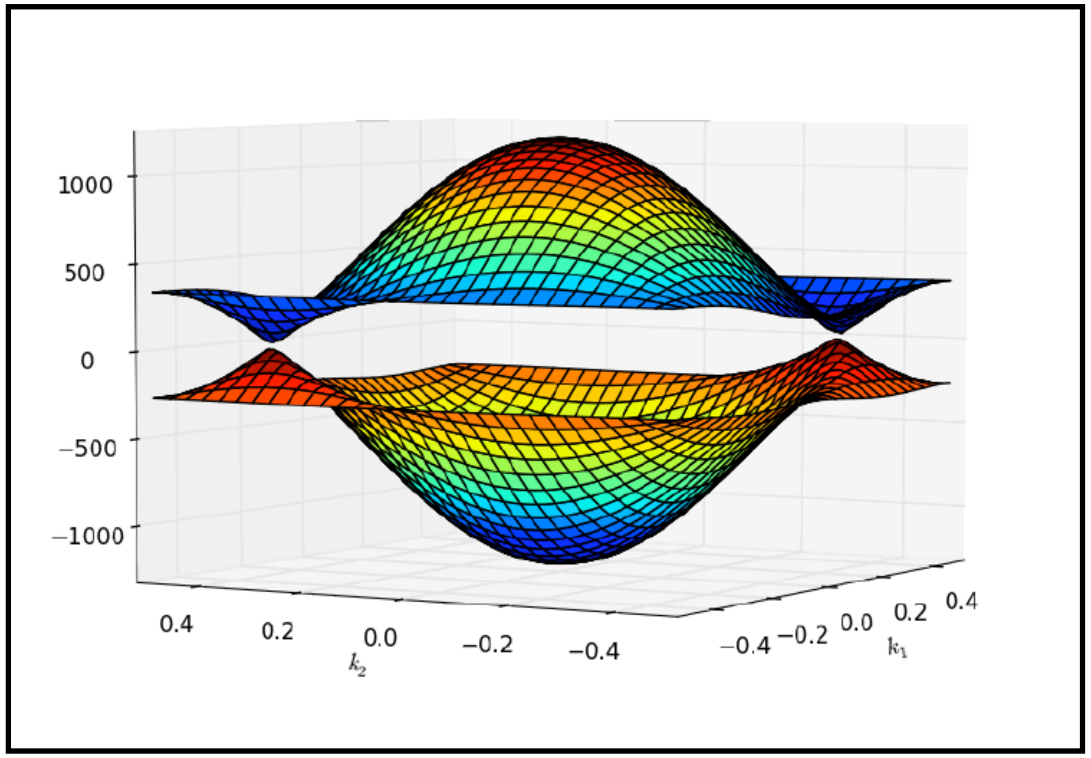

Haldane model

The Haldane model

1) break time-reversal symmetry

complex next-nearest neighbor hopping

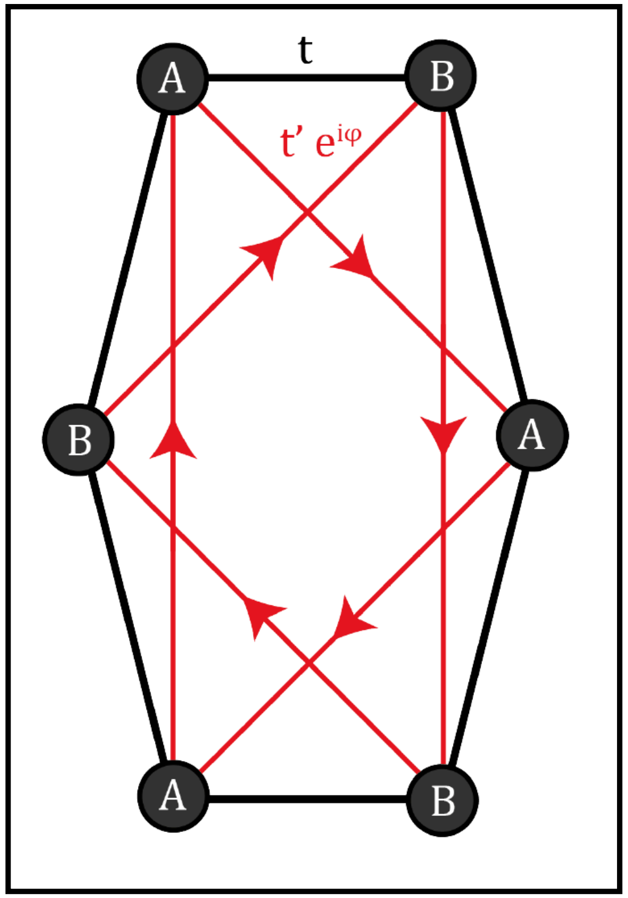

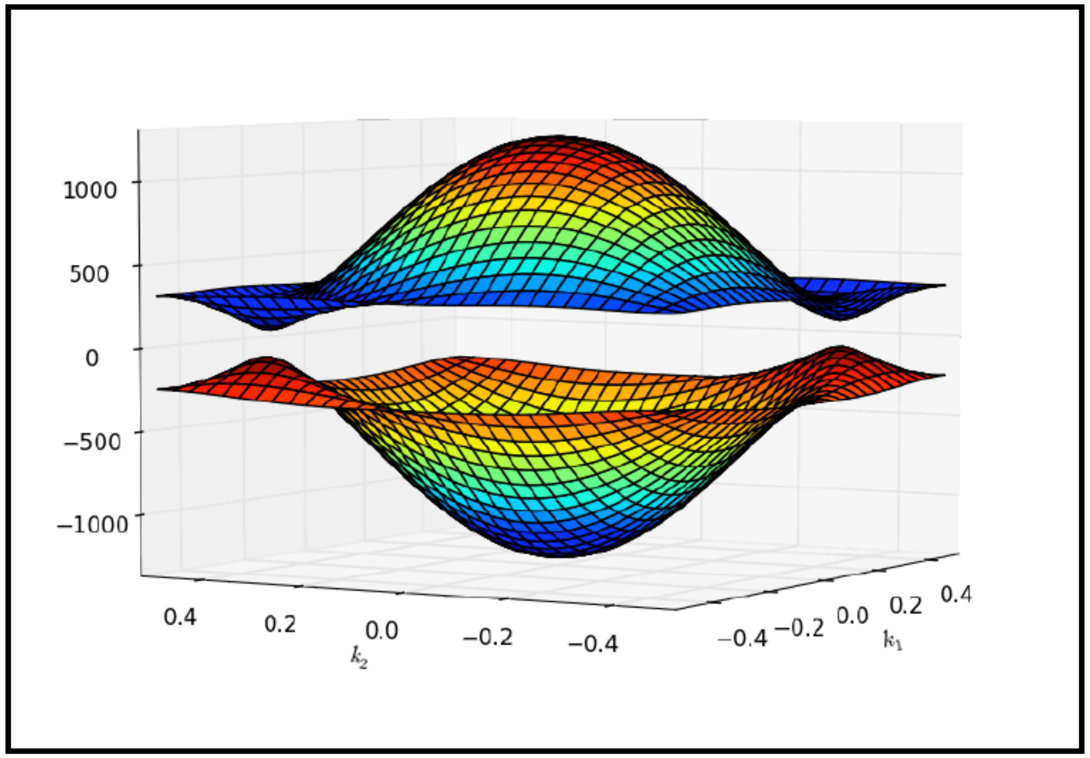

Chern bands!

Haldane model

The Haldane model

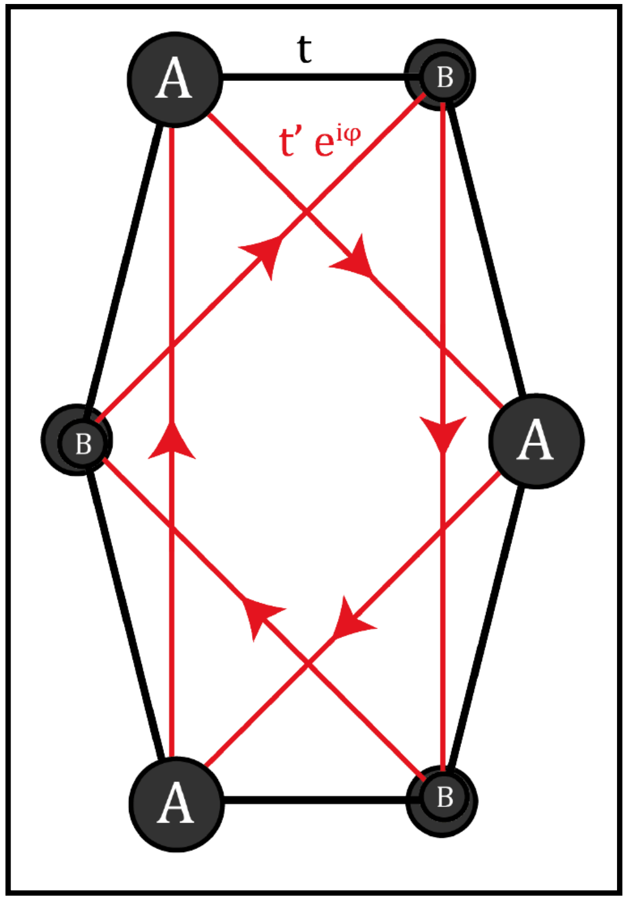

2) break inversion symmetry

AB-site energy offset

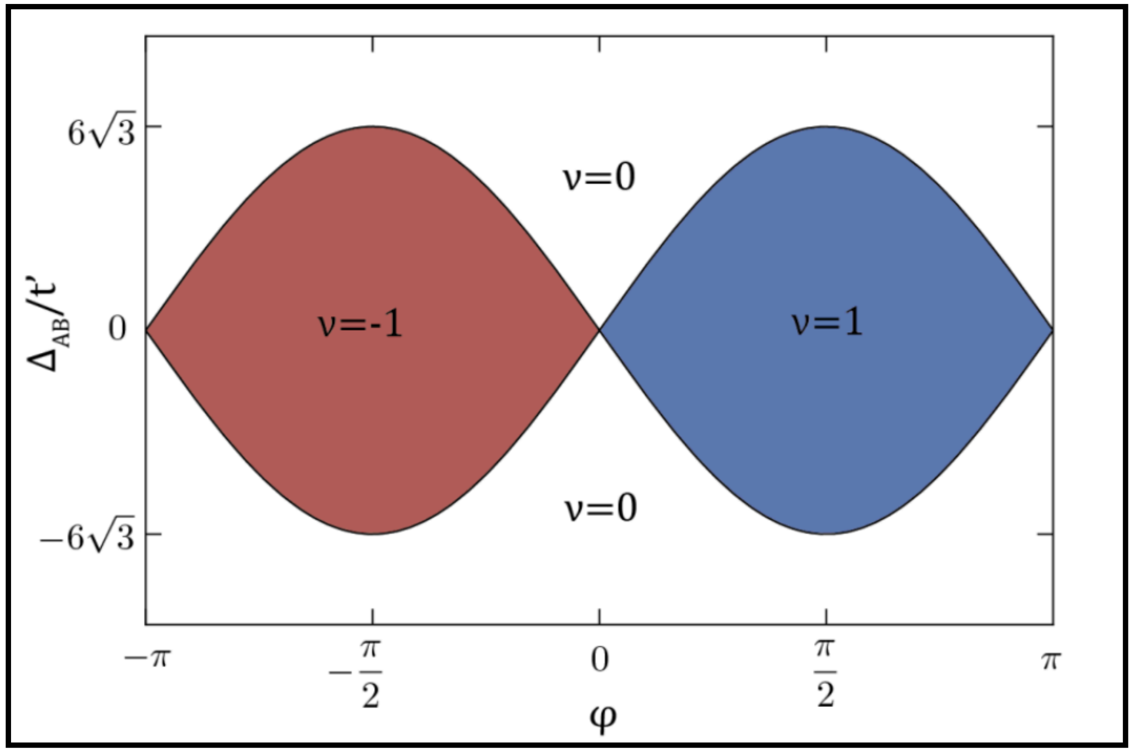

Quench protocol

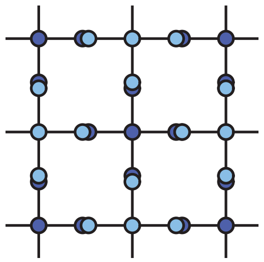

Experimental measurement of Berry curvature in Floquet bands

N. Fläschner *et al.* Science **352**, 1091 (2016)

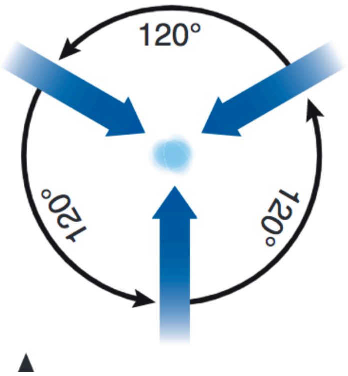

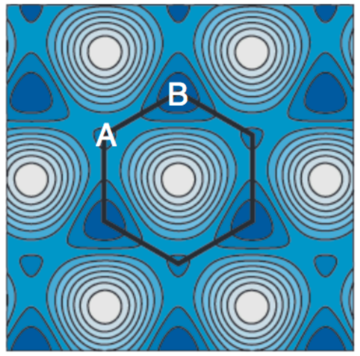

- Key ingredient: large A-B offset

  → **nearly flat bands** = reference lattice

  P. Hauke *et al.* PRL **113**, 045303 (2014)

- **Protocol:**

  Study geometric properties of Floquet-Bloch bands via quench to flat reference bands

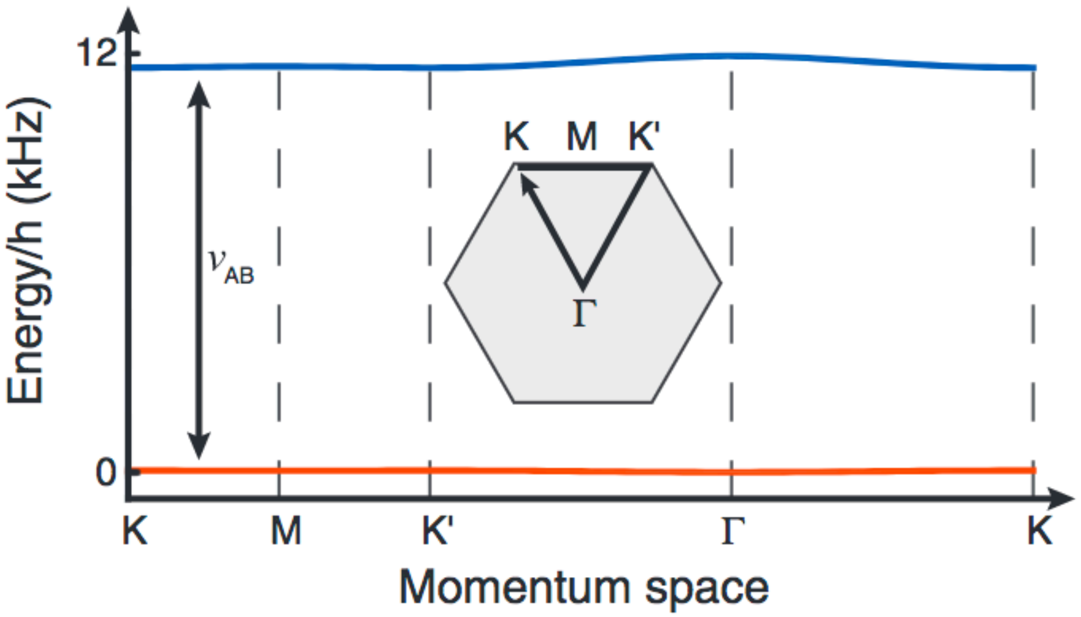

see also: T. Li *et al.* Science **352**, 1094 (2016)

Quench protocol Hamburg

fermionic 40K

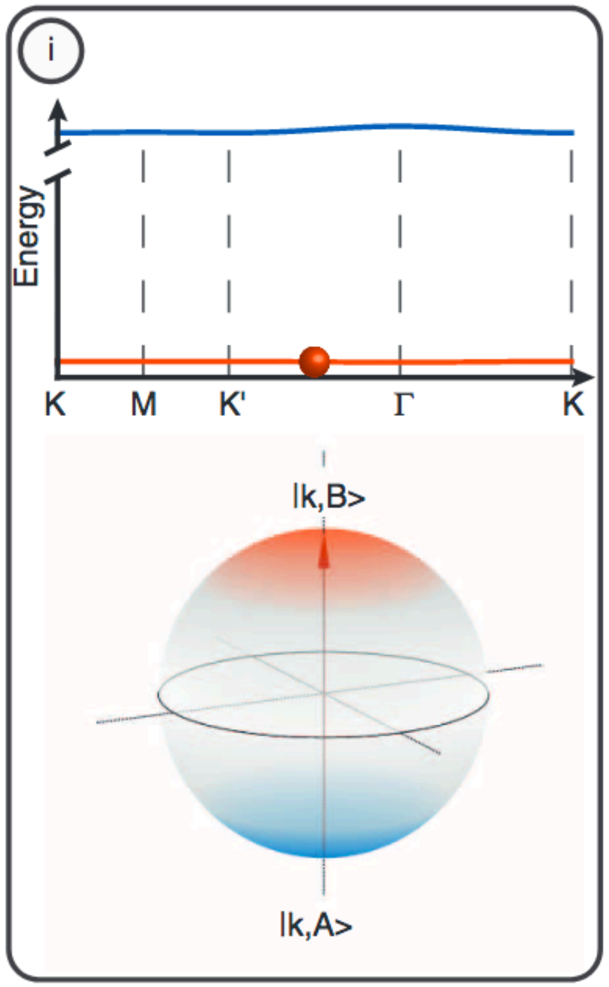

1) Start in flat bands: $|\mathbf{k}, B\rangle$

N. Fläschner *et al.* Science **352**, 1091 (2016)

Quench protocol Hamburg

fermionic 40K

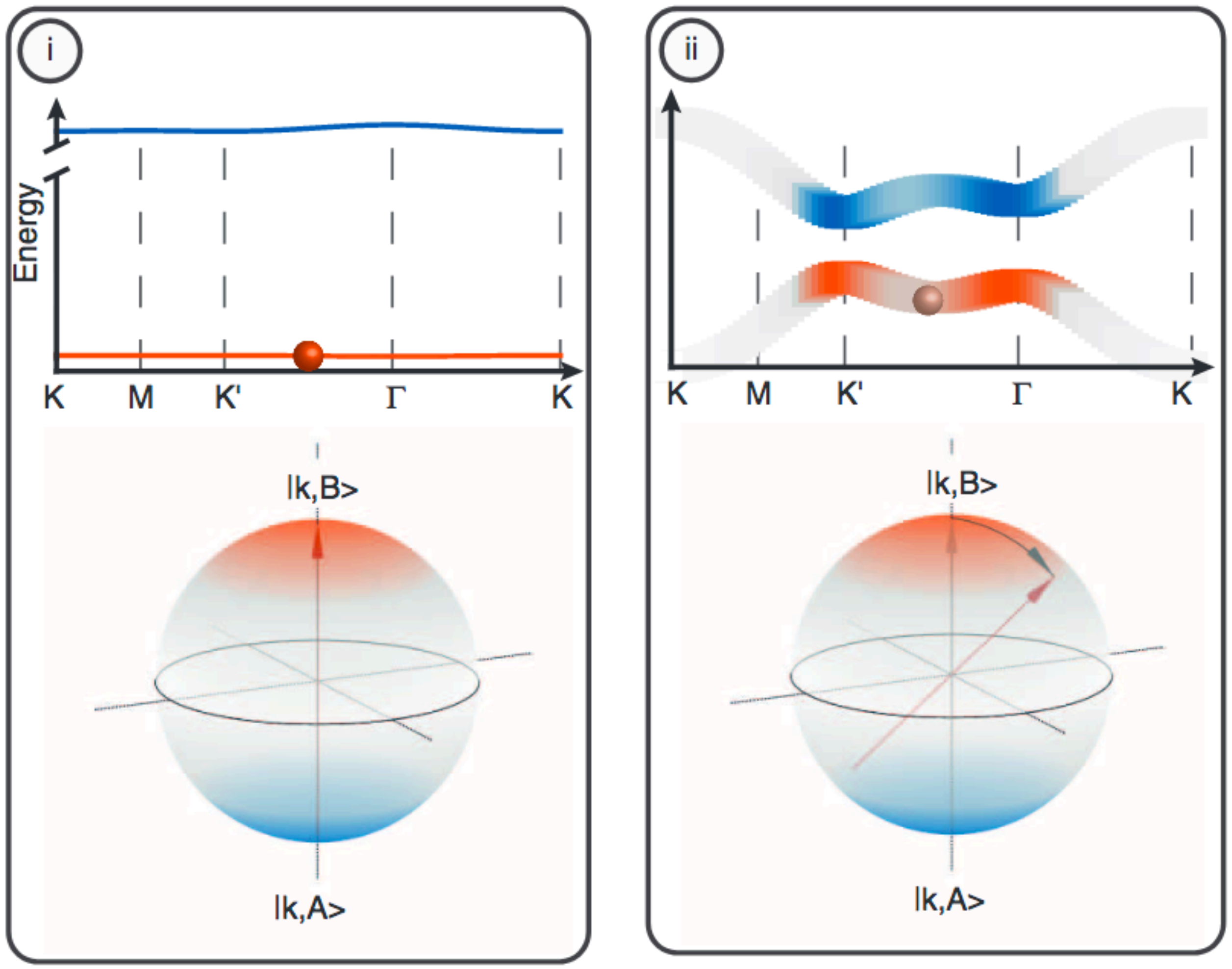

2) Prepare ground state in dressed bands

$$|\mathbf{k}\rangle = \sin(\theta_j/2)|\mathbf{k}, A\rangle - \cos(\theta_k/2)\mathrm{e}^{i\phi_k}|\mathbf{k}, B\rangle$$

N. Fläschner *et al.* Science **352**, 1091 (2016)

Quench protocol Hamburg

fermionic 40K

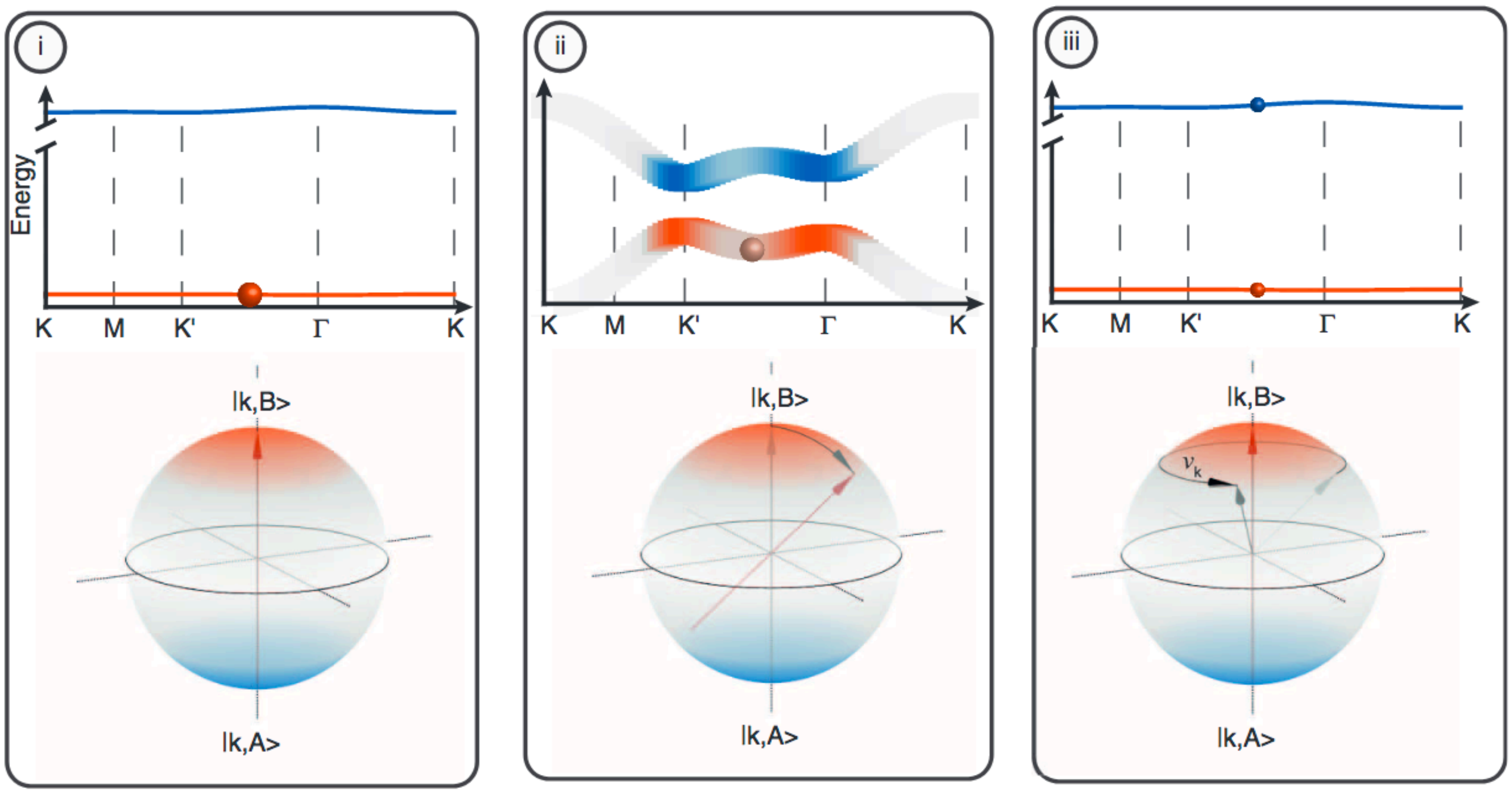

3) Quench to flat-band configuration

→ oscillation around $|\mathbf{k}, B\rangle$ with energy difference of flat bands ν_k

N. Fläschner *et al.* Science **352**, 1091 (2016)

Quench protocol Hamburg

Momentum-resolved oscillations after ToF

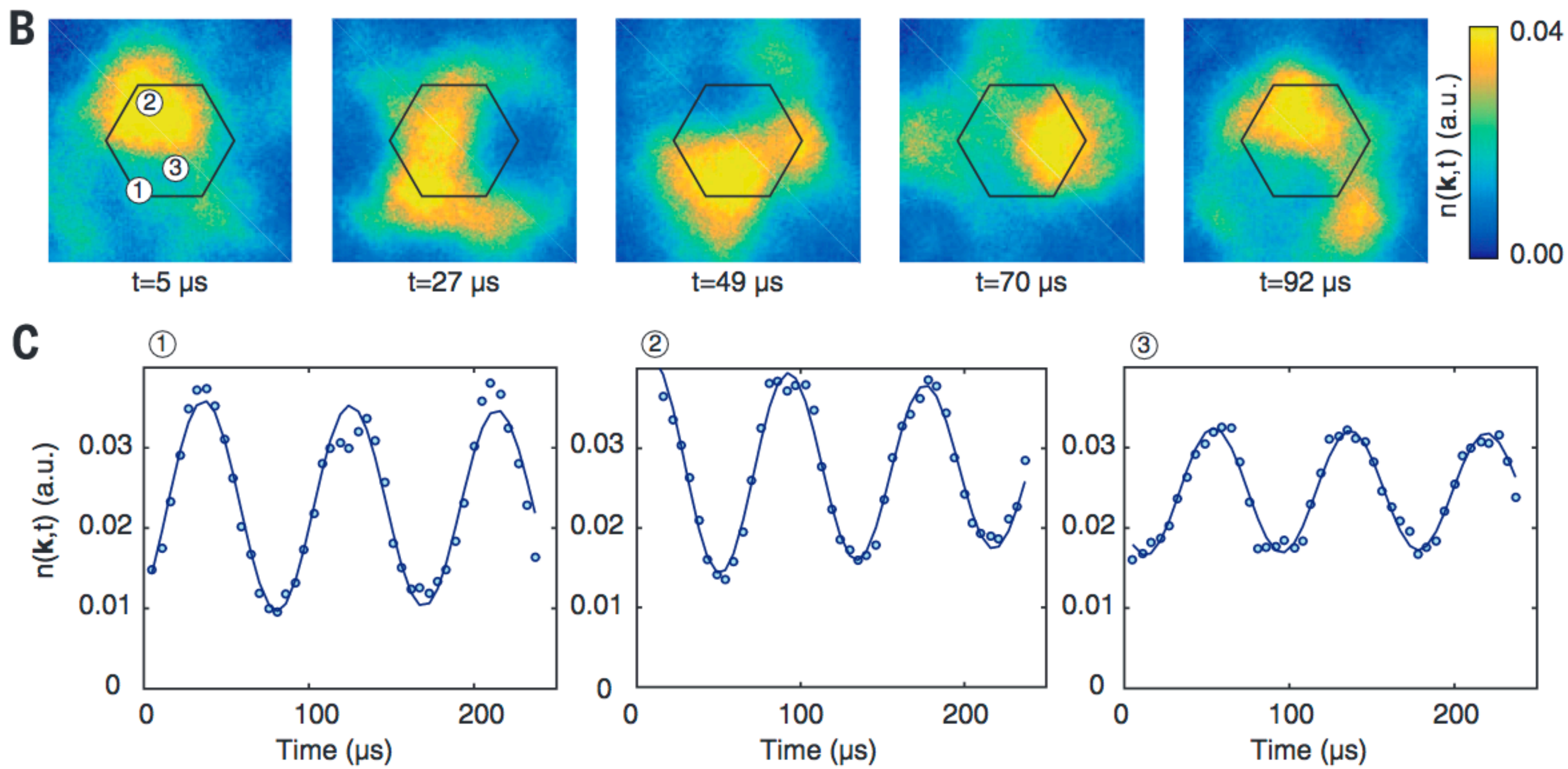

$$n(\mathbf{k},t) = f(\mathbf{k})[1 - \sin(\theta_k)\cos(\phi_k + 2\pi\nu_k t)]$$

Extract amplitude and phase to reconstruct the Berry curvature!

N. Fläschner *et al.* Science **352**, 1091 (2016)

Quench protocol Hamburg

Berry curvature reconstruction

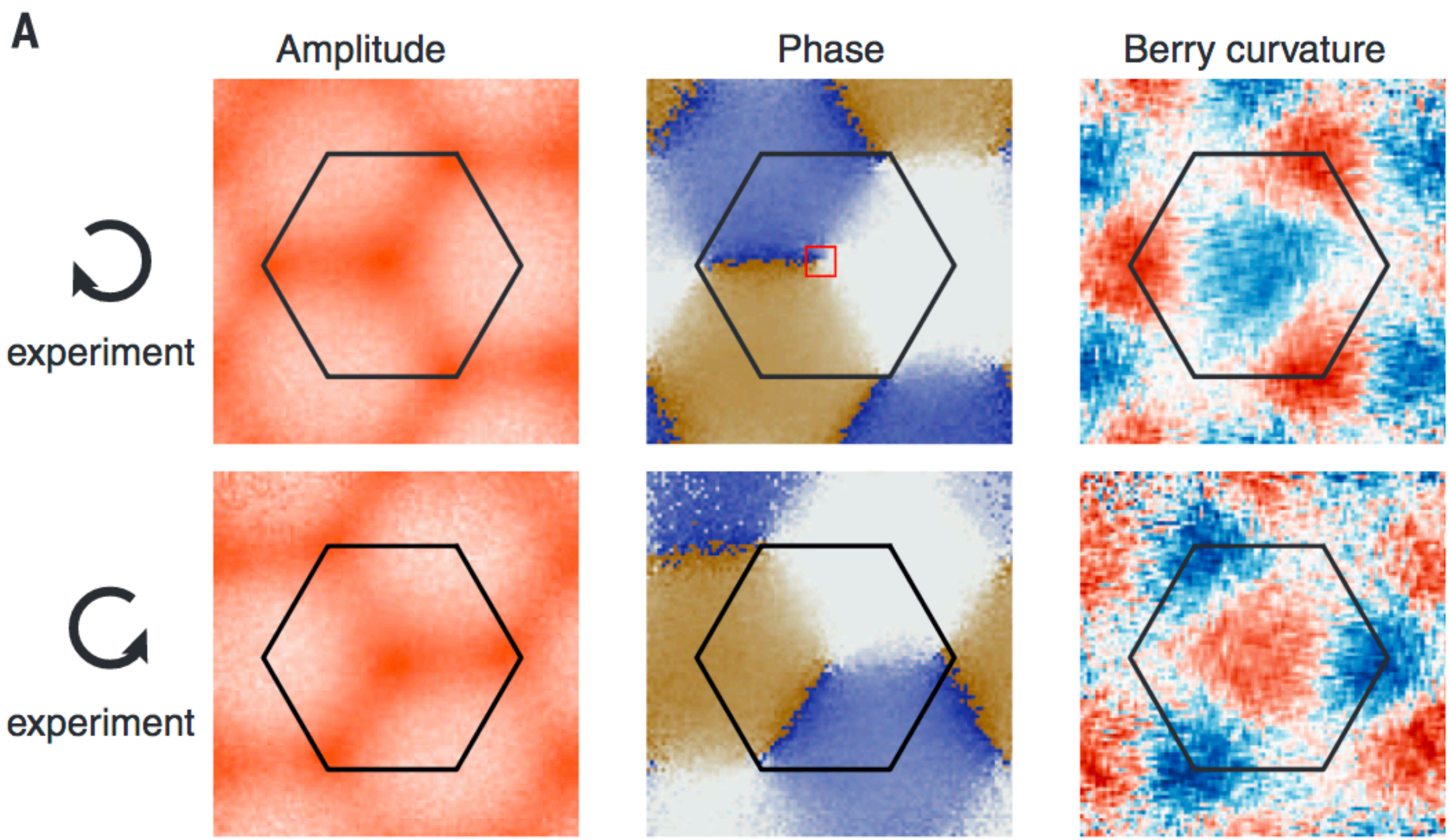

N. Fläschner *et al.* Science **352**, 1091 (2016)

Engineering genuine out-of-equilibrium topological phases

Anomalous Floquet phases

Floquet engineering:

- Engineer time-periodic system to *emulate properties* of *non-trivial static system*
- High-frequency limit:

  → known *bulk-edge correspondence*

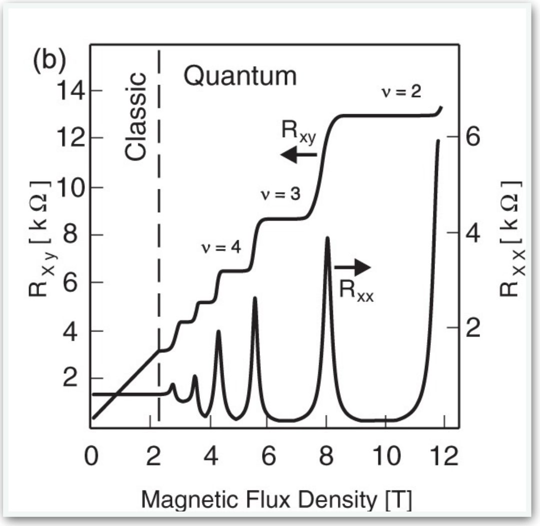

$$R_{xy} = \frac{1}{i}\frac{h}{e^2}\,,\; i = \sum_{\text{bands}} \mathcal{C}^{\mu}$$

Beyond static systems:

T. Kitagawa *et al.*, PRB **82**, 235114 (2010), M. Rudner *et al.*, PRX **3**, 031005 (2013)

- *Beyond the high-frequency limit*:

  → *top. protected edge modes*, while conventional *top. invariants are zero*!

- *Robust edge transport* ⟷ *localized bulk*!

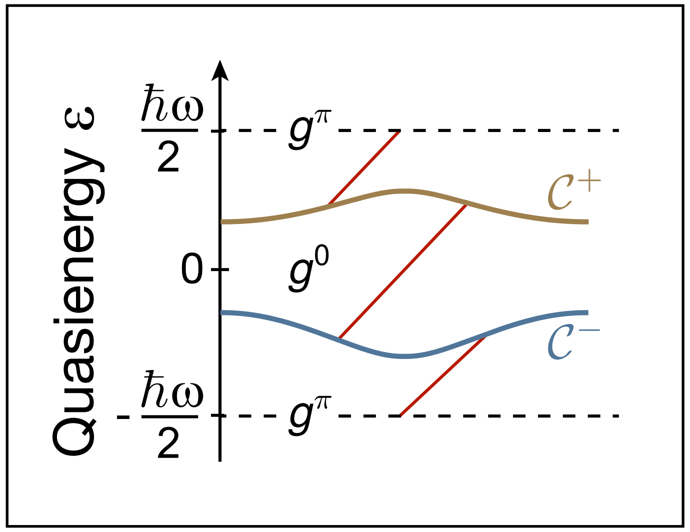

Anomalous Floquet phases

Simple example: Stepwise modulated square lattice

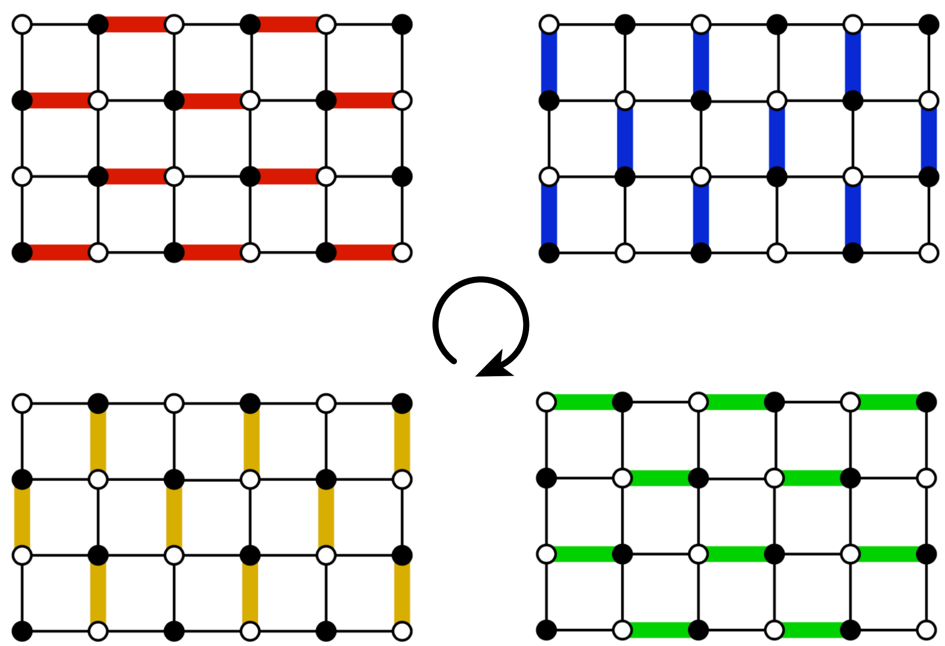

- Four equal time steps, with $JT/4 = \pi/2$
- After one period: *initial state reproduced* $\rightarrow \hat{U}(T) = \mathbf{1}$
- Effective Floquet Hamiltonian: *zero matrix* $\hat{H}_{\text{eff}} = 0$

$\rightarrow$ two degenerate flat bands at ε=0, with *trivial topology!*

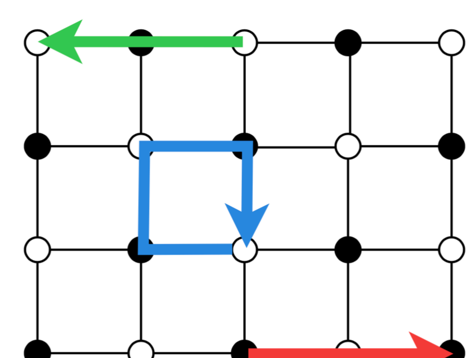

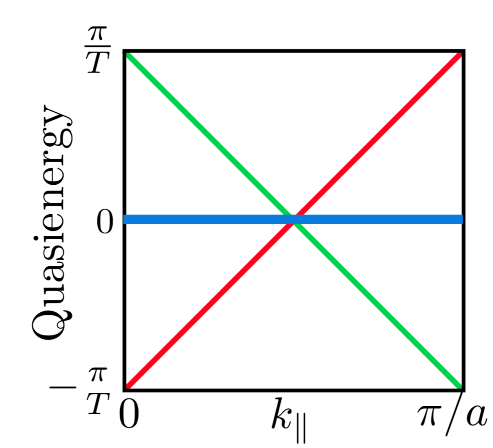

T. Kitagawa *et al.*, Phys. Rev. B **82**, 235114 (2010), M. Rudner *et al.*, PRX **3**, 031005 (2013)

Anomalous Floquet phases

Simple example: Stepwise modulated square lattice

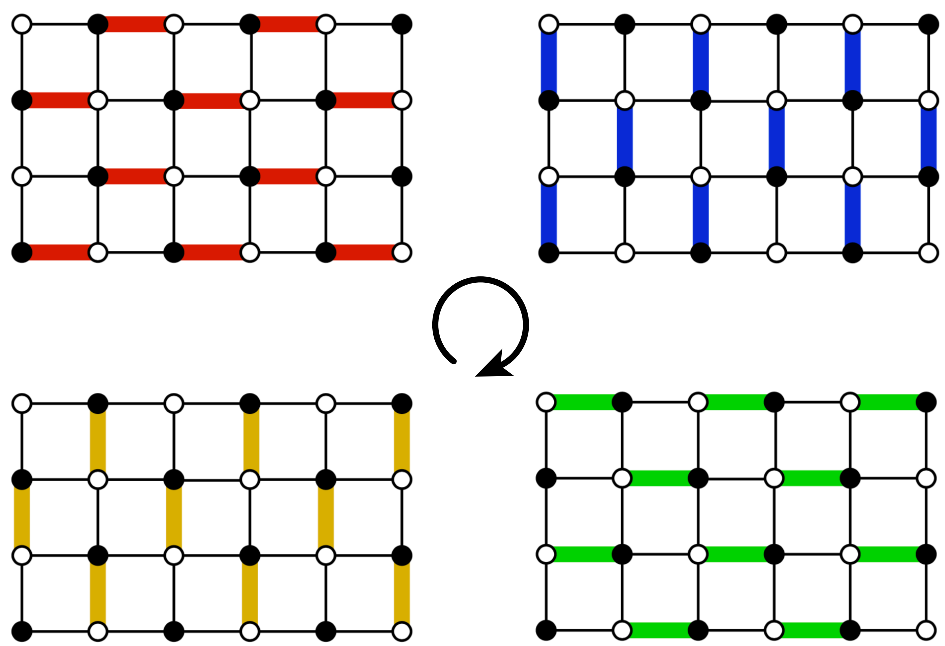

- Topology not determined by properties of $\hat{H}_{\text{eff}}$!
- Full time-dependence is important
- Non-trivial winding of quasi-energy spectrum

$\rightarrow$ two degenerate flat bands at ε=0, with *trivial topology!*

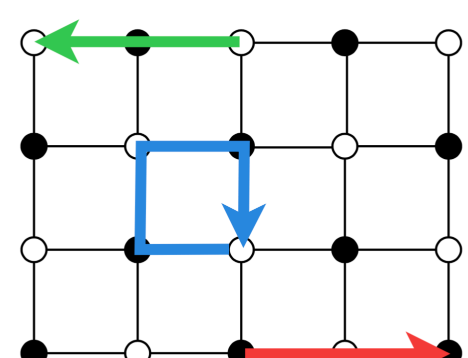

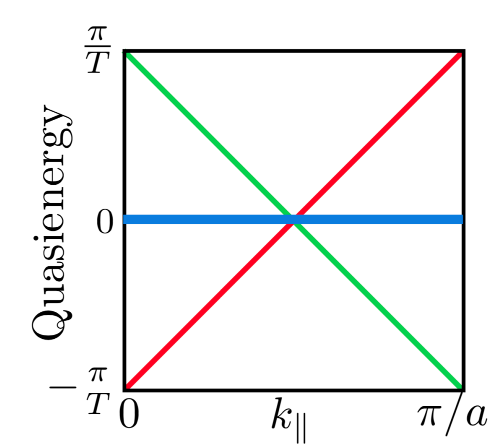

Photonics: S. Mukherjee *et al.*, Nat. Commun. **8**, 13918 (2017), L. J. Maczewsky *et al.*, Nat. Commun. **8**, 13756 (2017)

Anomalous Floquet phases

State-of-the art:

Modulated square lattice in coupled waveguide arrays

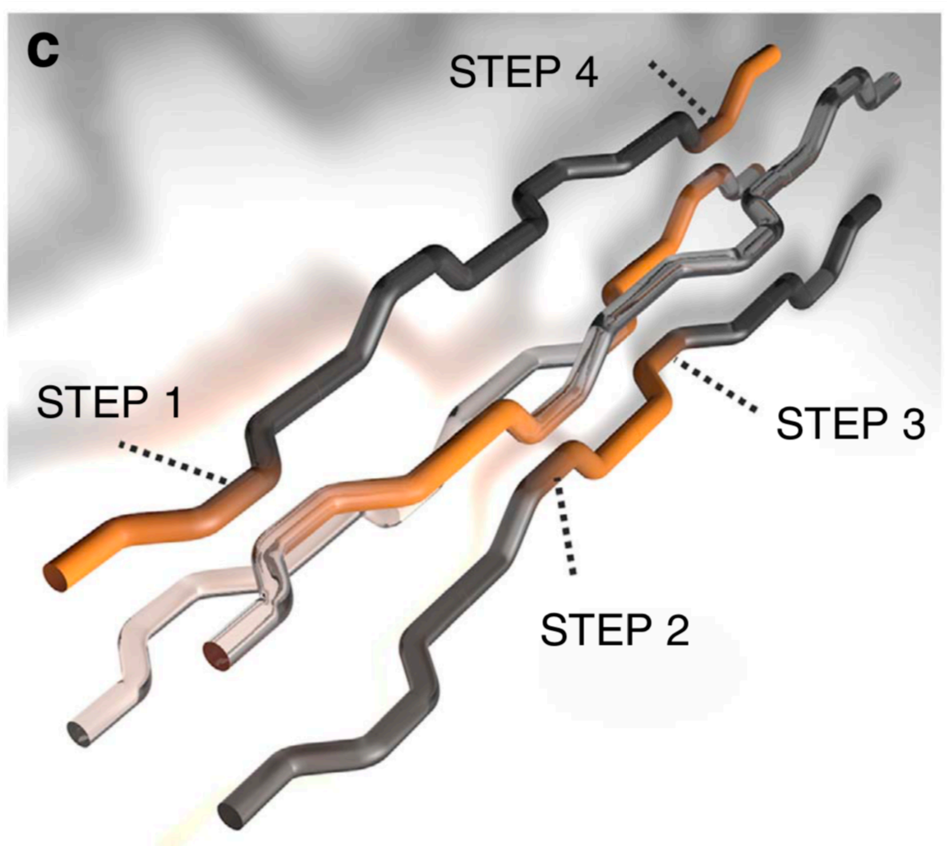

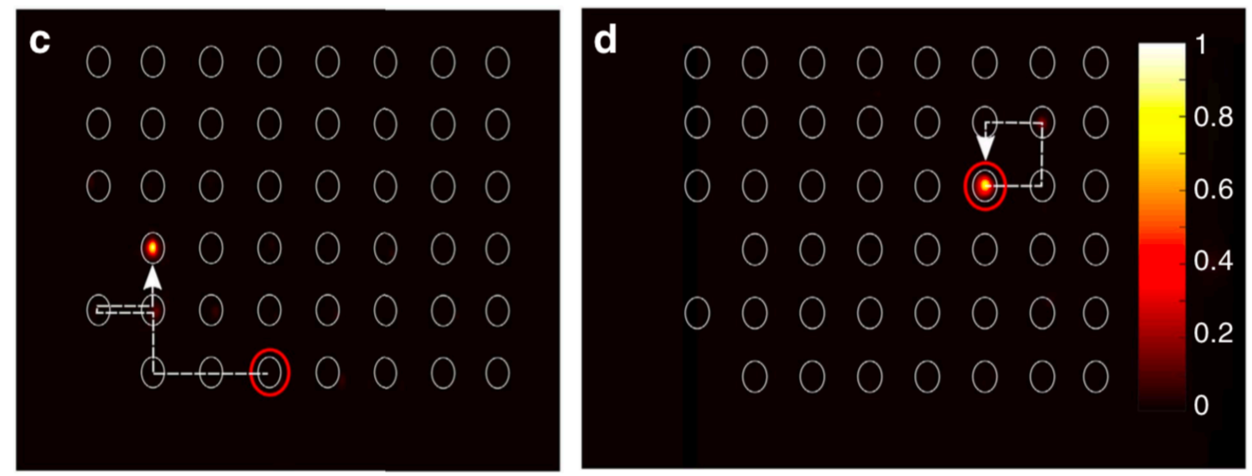

→ Robust edge transport

Cold atoms:

- Reveal *bulk and edge-state physics*
- Study *many-body phases*

S. Mukherjee *et al.*, Nat. Commun. **8**, 13918 (2017), L. J. Maczewsky *et al.*, Nat. Commun. **8**, 13756 (2017)

Topological Floquet phases

How to characterize top. properties?

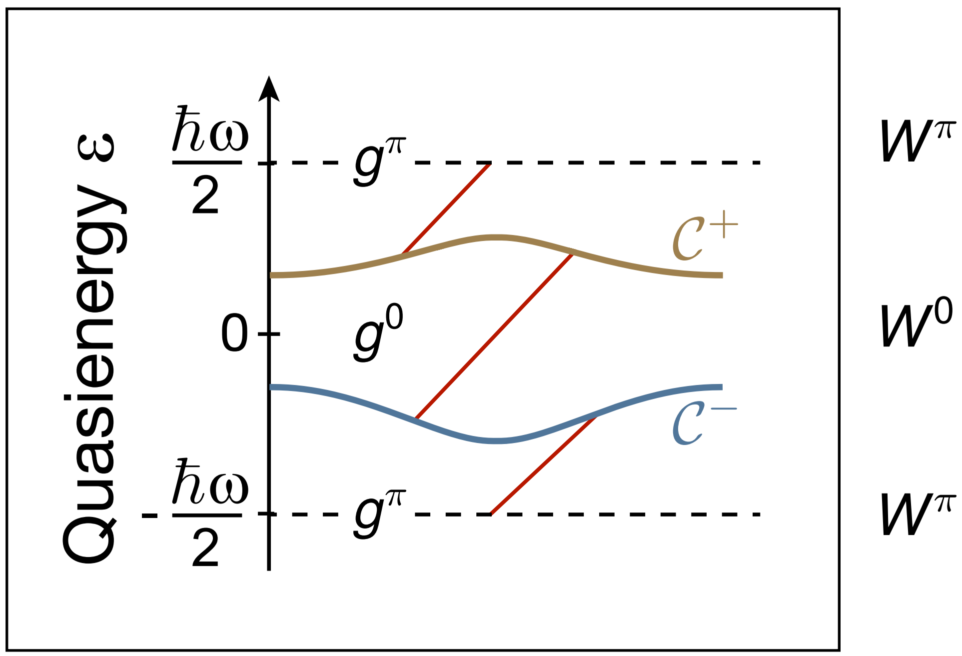

Winding number counts *# edge modes in gap!*

$$\mathcal{C}^{\pm} = \mp(W^0 - W^{\pi})$$

Chern number not sufficient to characterize Floquet systems

Complete set of invariants given by winding numbers!

T. Kitagawa *et al.*, Phys. Rev. B **82**, 235114 (2010)
M. Rudner *et al.*, PRX **3**, 031005 (2013), N. Ünal et al., PRL 122, 253601 (2019)

Topological Floquet phases

High-frequency limit: ***Haldane phase***

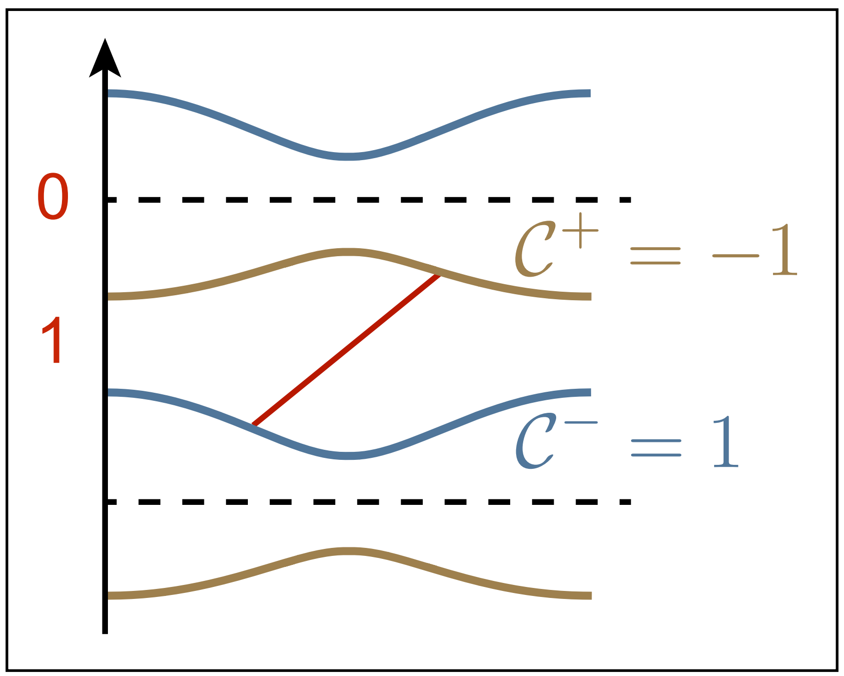

- High-frequency limit: $W^{\pi} \to 0$
  (mapping to static system via RWA)
- Edge state at zero energy
  $W^{0} = 1$

How to determine *bulk top. invariants* of the other phases?

T. Oka *et al.*, PRB (2009); M. C. Rechtsman *et al.*, Nature (2013); G. Jotzu *et al.*, Nature (2014)

Topology of gap-closing points

Band-touching singularities

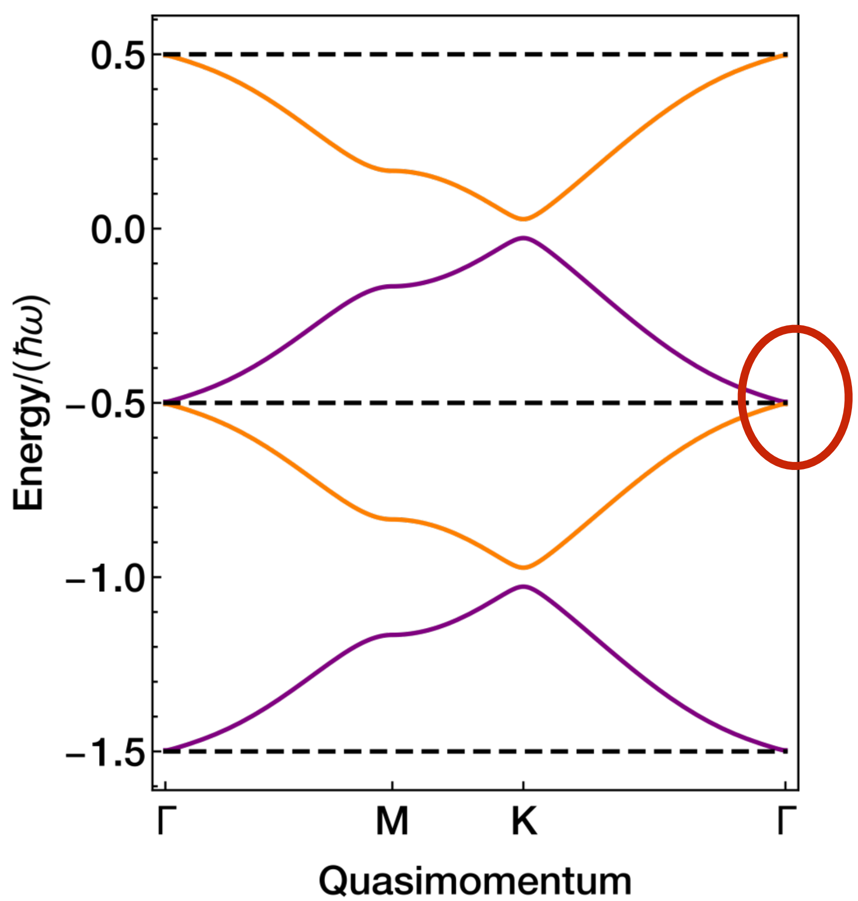

- Consider 3D-parameter space: (q_x, q_y, λ), where λ parametrizes mod.

Topological charge $Q_s = \pm 1$

- Topological charge describes the change in Winding number

$$W^j_{\lambda_s+\varepsilon} = W^j_{\lambda_s-\varepsilon} + Q^j_s$$

1) Identify energy gap
2) Measure topological charge Q_s

F. Nathan et al, New J. Phys. 17, 125014 (2015); N. Ünal et al., PRL 122, 253601 (2019)

Topology of gap-closing points

I) Measure Berry flux associated with Q_s

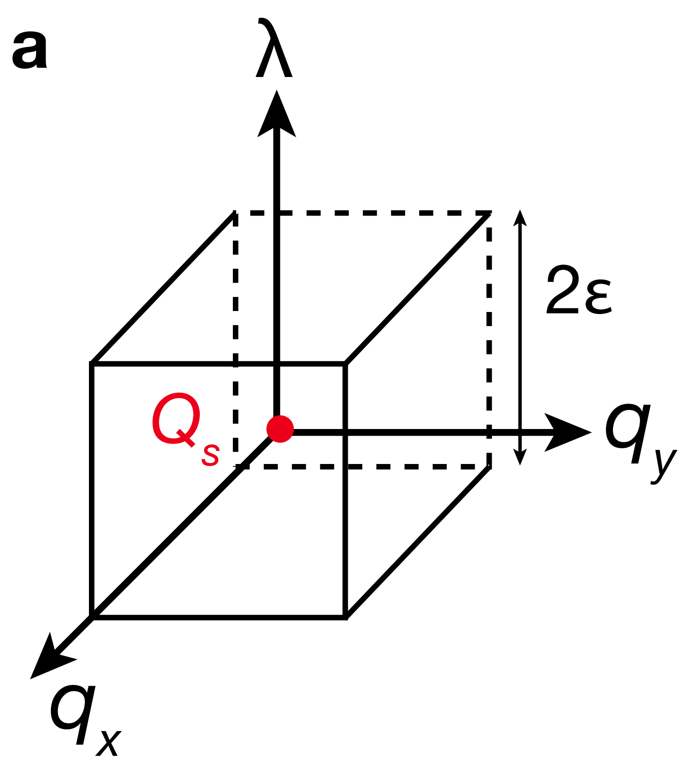

(a) Measure Berry-flux through all six faces!

Topology of gap-closing points

1) Measure Berry flux associated with Q_s

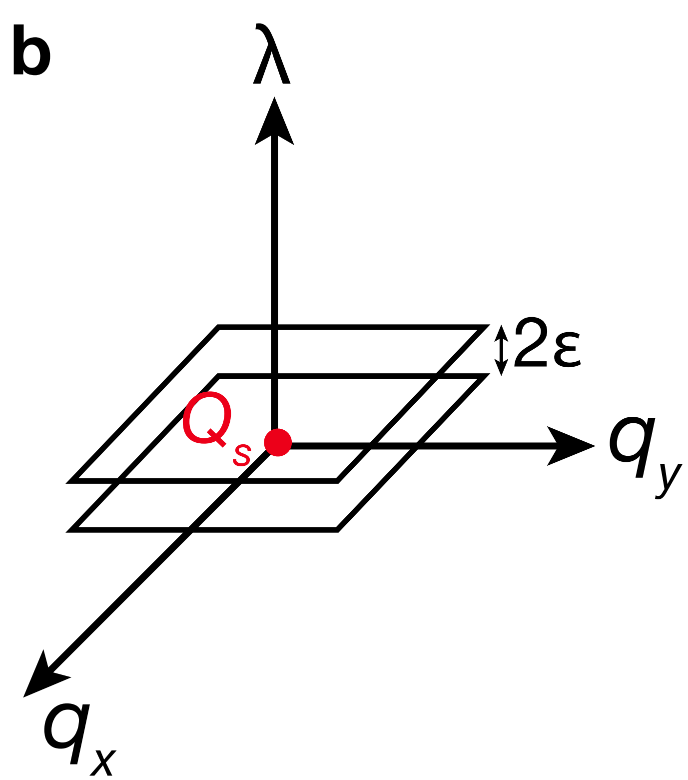

(b) Measure *Berry-flux locally shortly before and after* the gap-closing point!

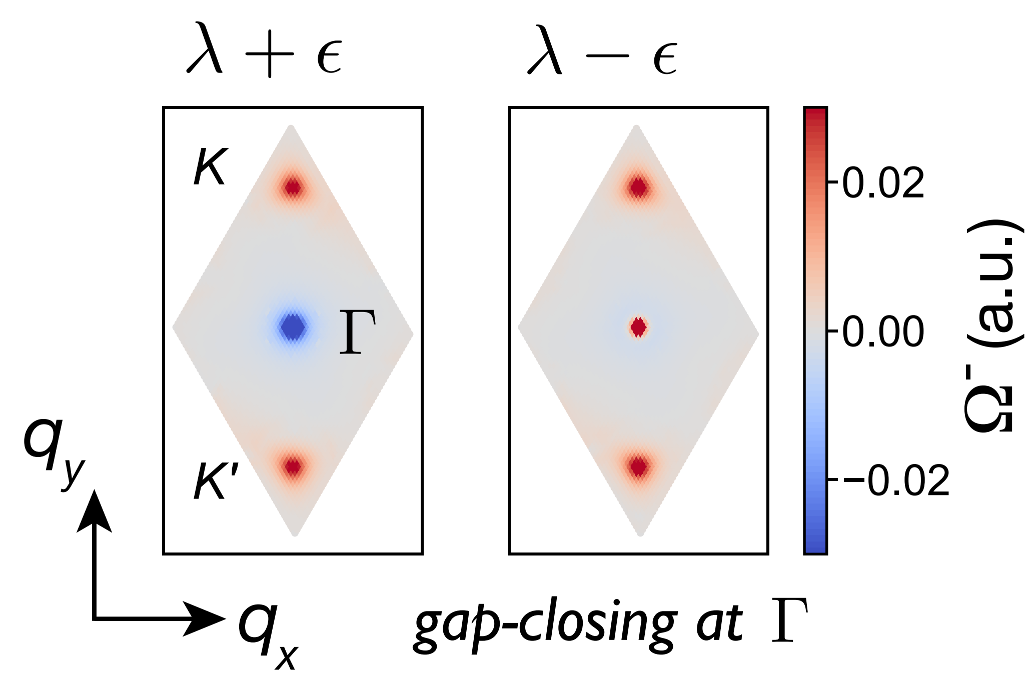

F. Nathan et al, New J. Phys. 17, 125014 (2015); N. Ünal et al., PRL 122, 253601 (2019)

Geometric properties of energy bands

Transport measurement

semiclassical dynamics when applying a force F

→ *Anomalous transverse velocity* prop. to *Berry curv.* Ω_μ

$$\mathbf{v}^x_\mu(\mathbf{q}) = -\frac{F}{\hbar}\Omega_\mu(\mathbf{q})$$

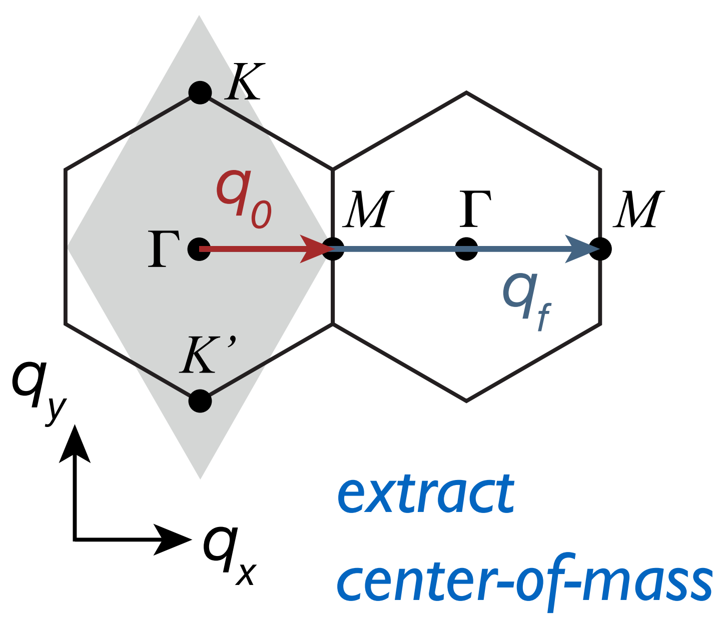

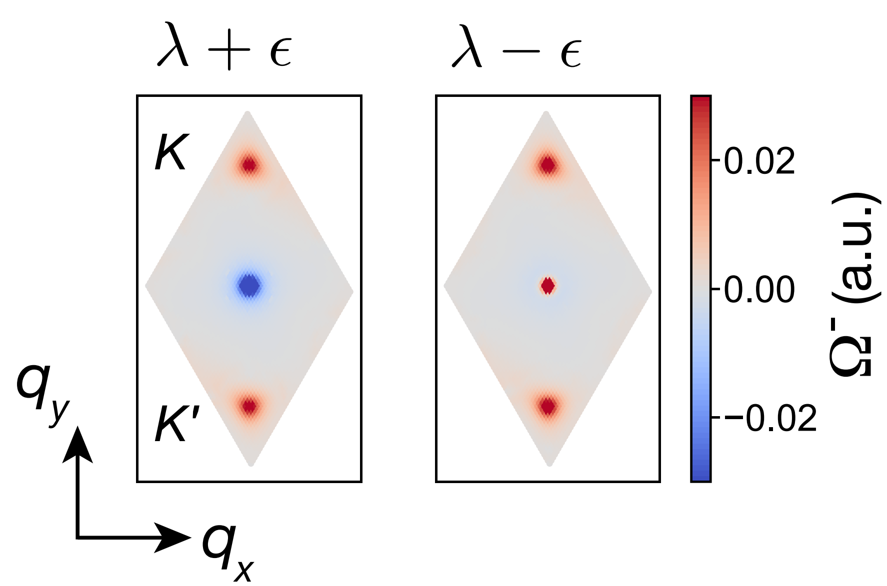

$$\Delta s^-_\perp(\mathbf{q}_s) = \mathrm{sgn}[s^-_\perp(\mathbf{q}_s, \lambda_s + \varepsilon)] - \mathrm{sgn}[s^-_\perp(\mathbf{q}_s, \lambda_s - \varepsilon)]$$

Geometric properties of energy bands

Transport measurement

semiclassical dynamics when applying a force F

→ *Anomalous transverse velocity*
prop. to *Berry curv.* Ω_μ

$$\mathbf{v}^x_\mu(\mathbf{q}) = -\frac{F}{\hbar}\Omega_\mu(\mathbf{q})$$

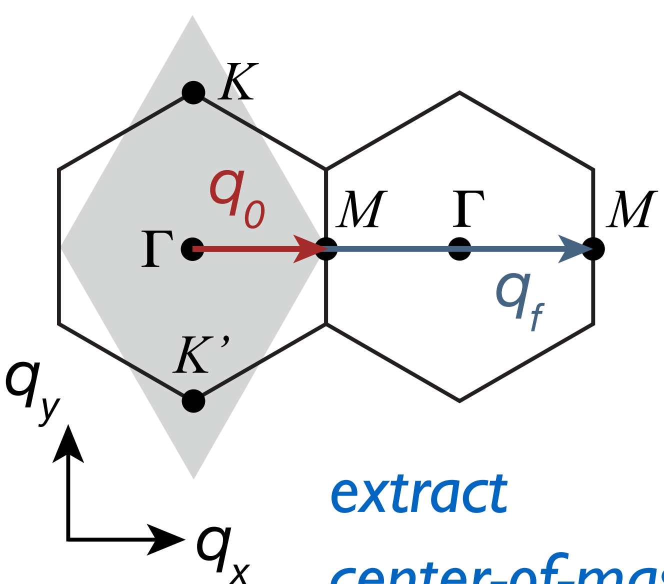

extract center-of-mass

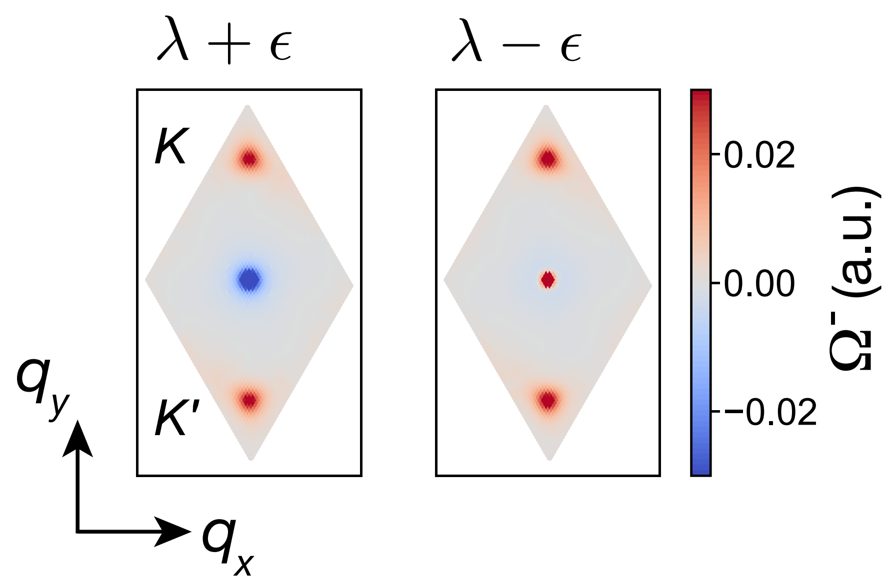

$$Q^0_s = \mathrm{sgn}\left(\Delta s^-_\perp(\mathbf{q}_s)\right)$$

Modulated hexagonal lattice

Modulate NN tunnelings between λJ and J

T. Kitagawa *et al.*, Phys. Rev. B **82**, 235114 (2010)

Here: Bosonic ^{39}K

$\lambda = 737\mathrm{nm}\ ,\quad a = 284\mathrm{nm}$

Continuous modulation scheme:

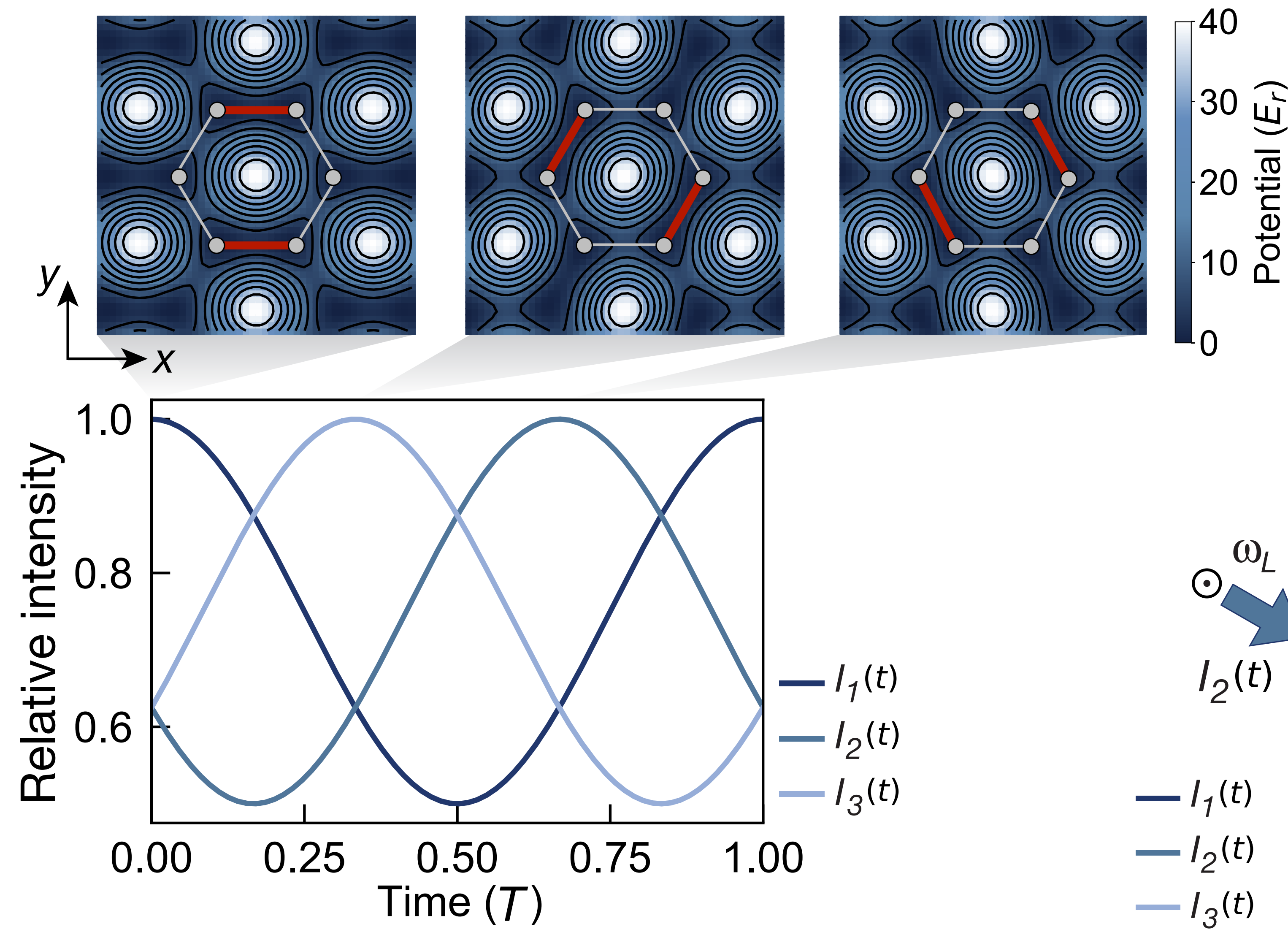

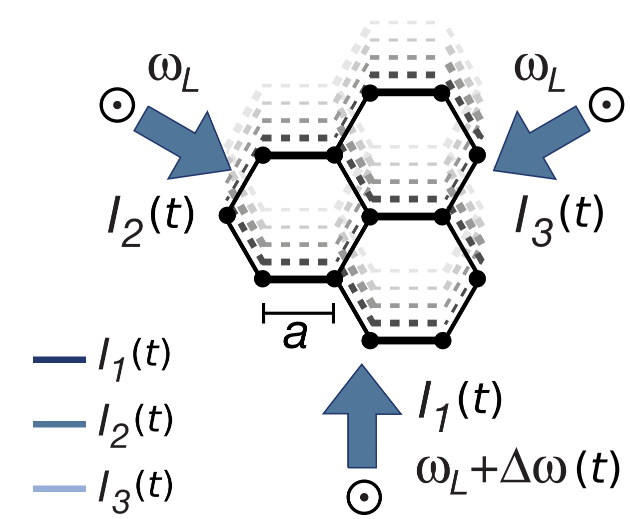

K. Wintersperger, ..., M.A., Nature Phys. **16**, 1058-1063 (2020)
see also: A. Quelle *et al.*, New J Phys. **19**, 113010 (2017)

Topological Floquet phases

Phase diagram

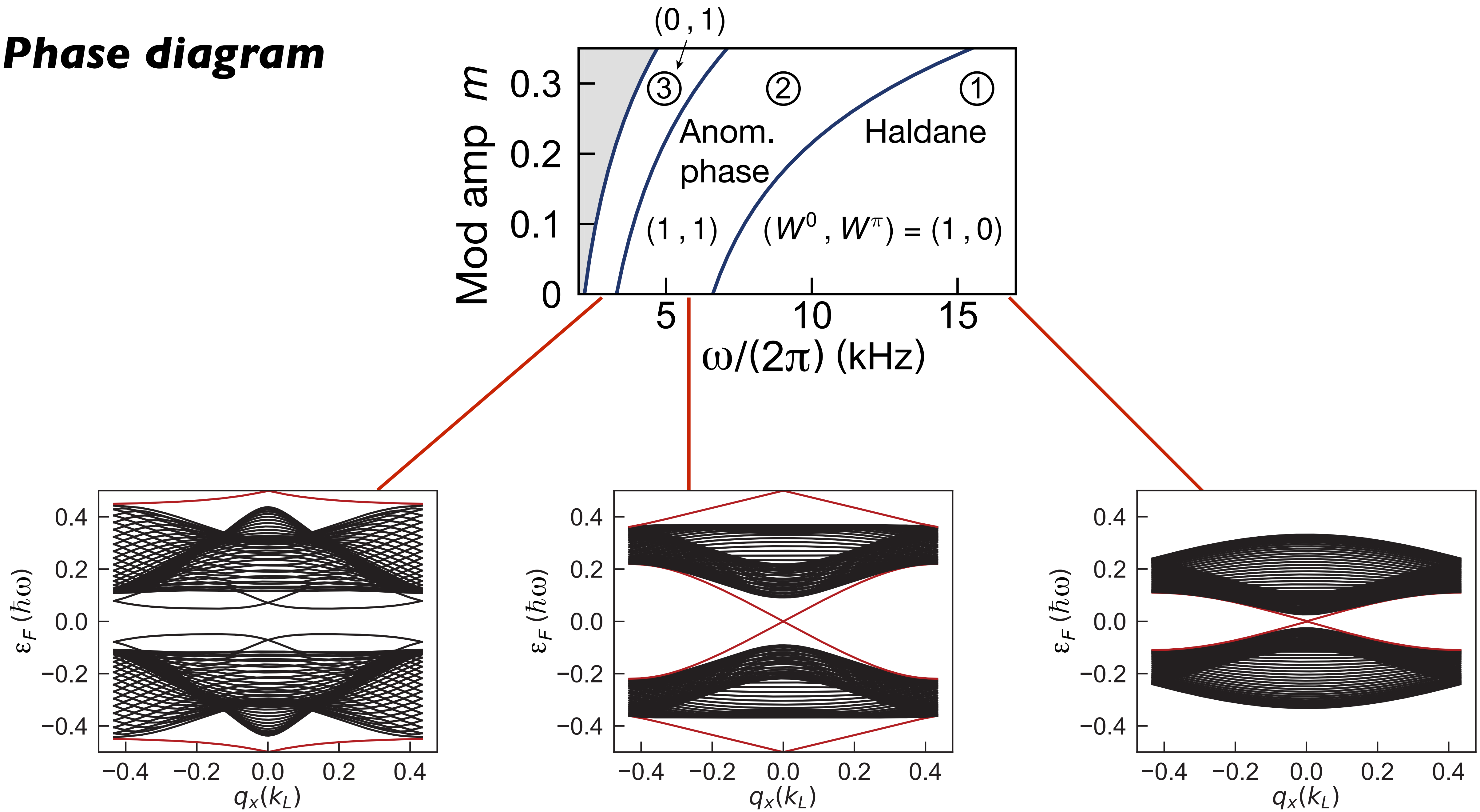

Haldane-like phase	Anomalous phase	Haldane phase
$\mathcal{C}^{\pm} = \pm 1$	$\mathcal{C}^{\pm} = 0$	$\mathcal{C}^{\pm} = \mp 1$

K. Wintersperger, ..., M.A., Nature Phys. **16**, 1058-1063 (2020)

Phase diagram

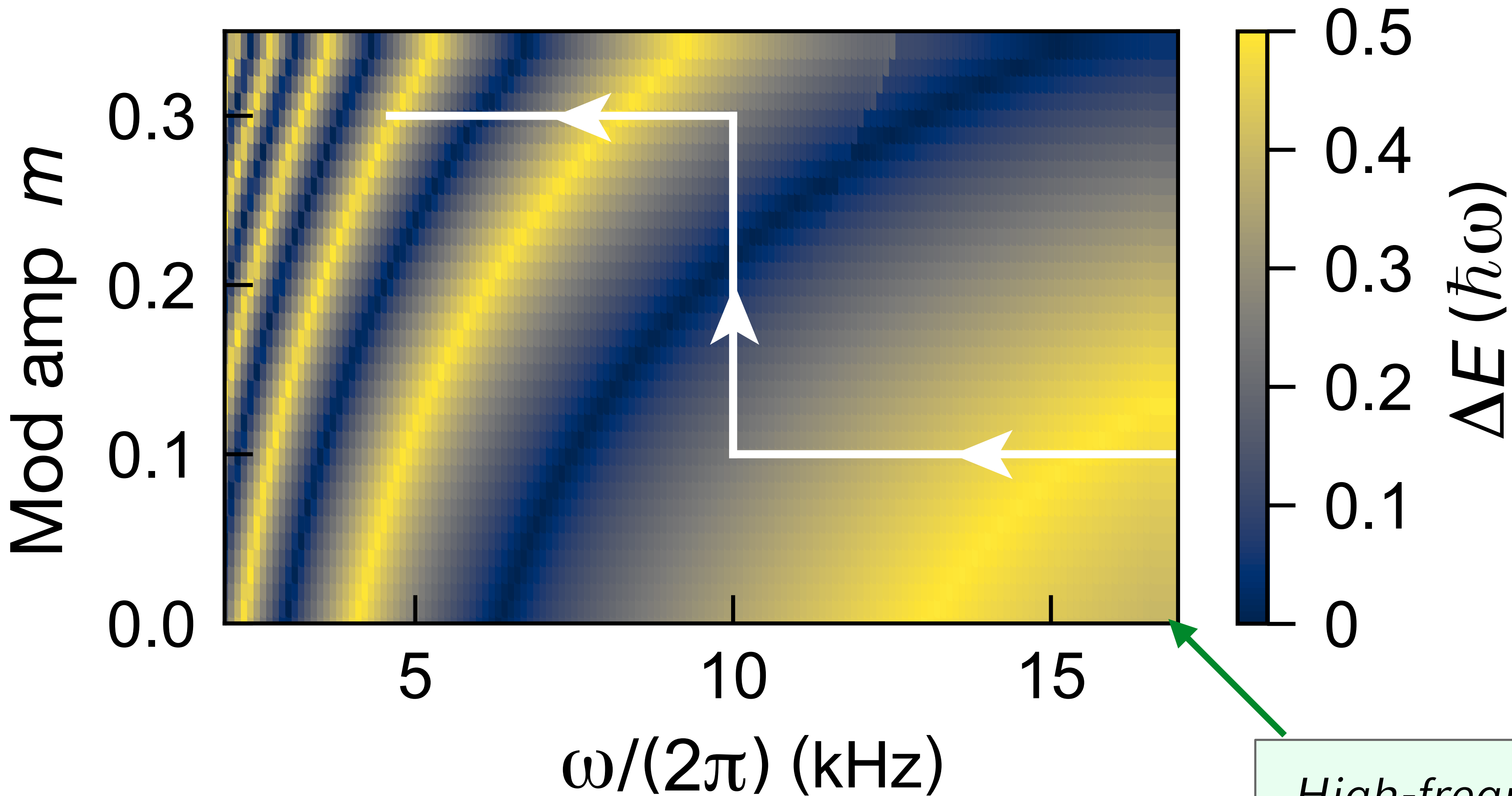

High-frequency limit!

Track gap-closing points

Γ-point:

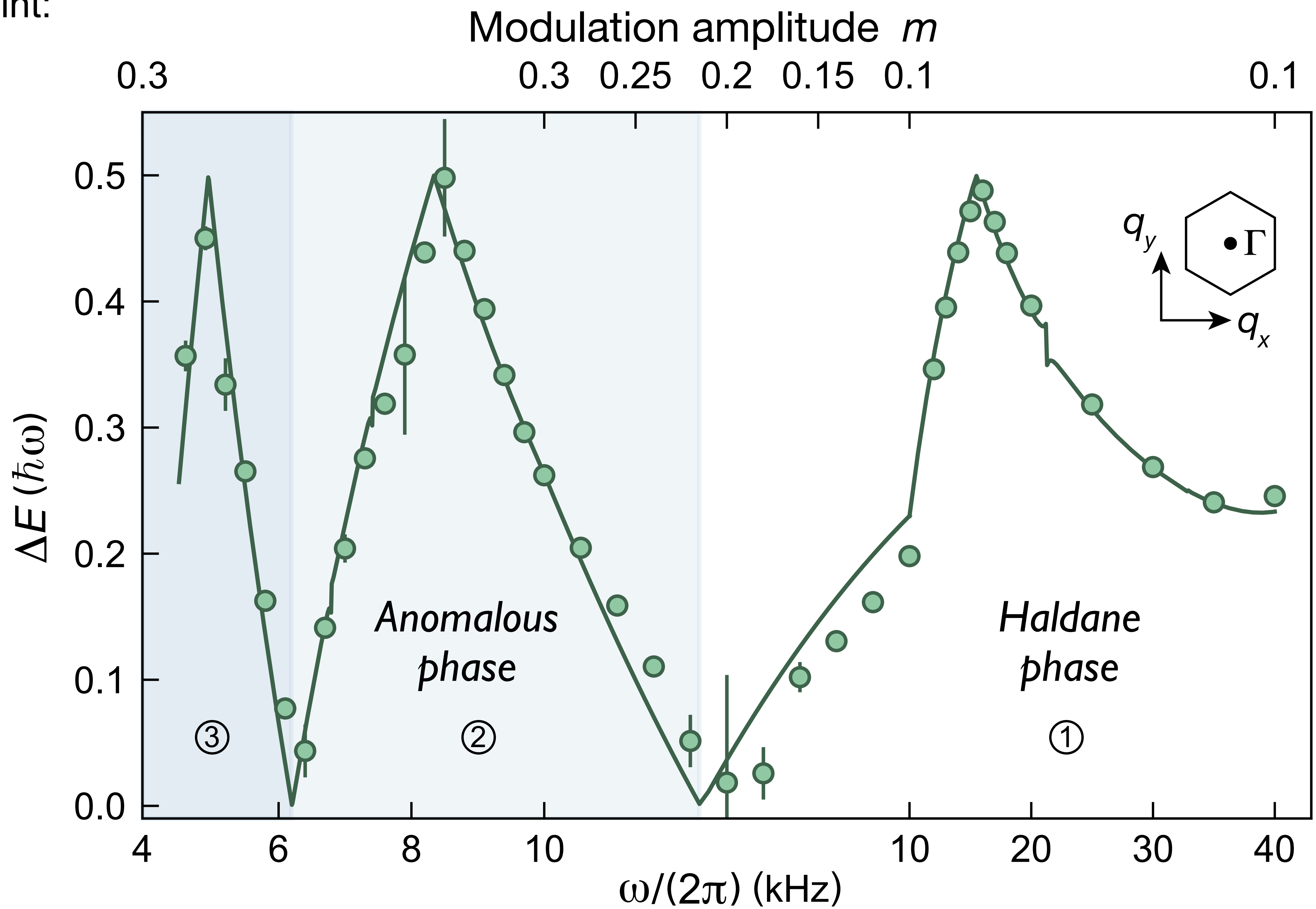

Track gap-closing points

Stückelberg oscillations:

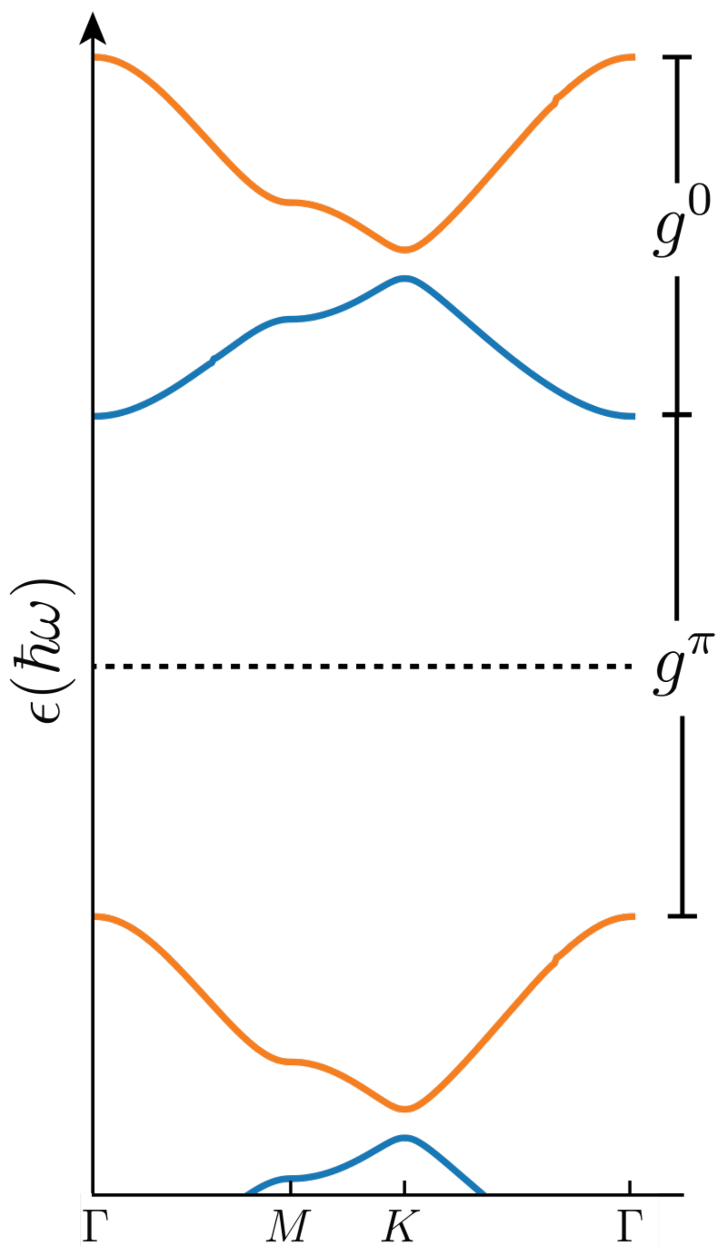

- We always measure the *smaller energy gap:* $\min(g^0, g^\pi)$
- In the *high-frequency limit* we probe g^0

N. Ünal et al., PRL 122, 253601 (2019)

Track gap-closing points

Stückelberg oscillations:

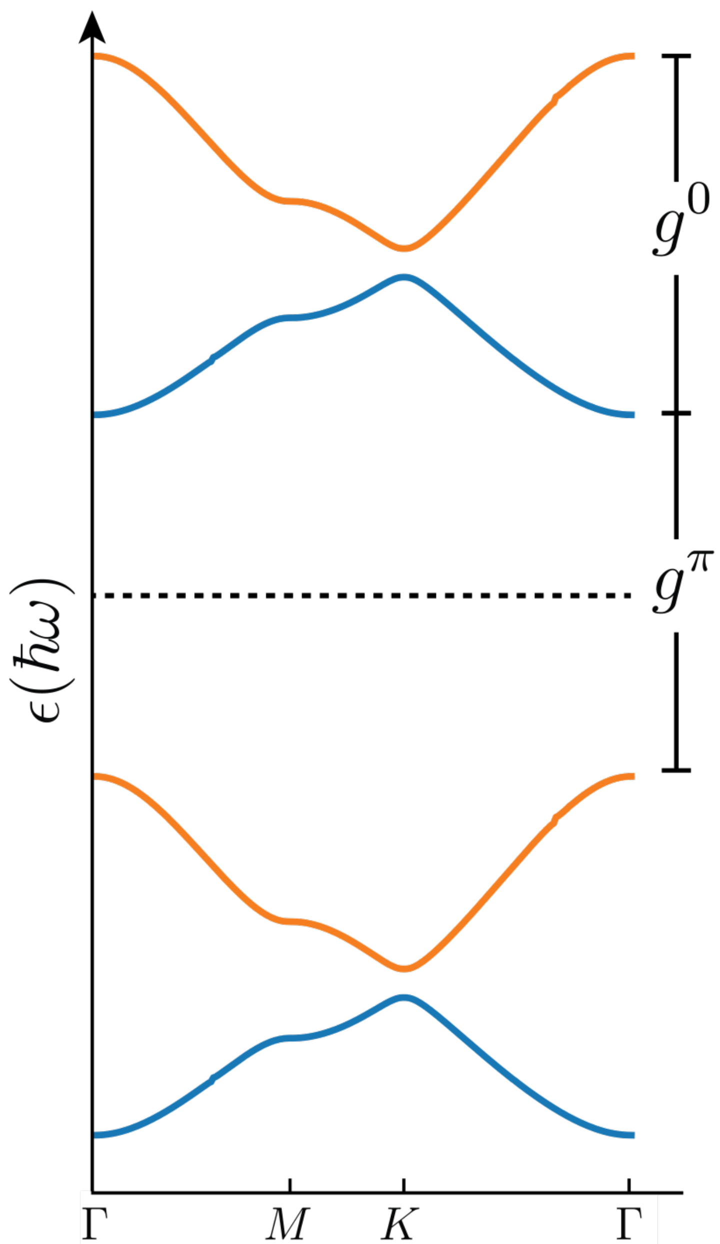

- We always measure the *smaller energy gap:* $\min(g^0, g^\pi)$
- In the *high-frequency limit* we probe g^0
- Transition, when
  $g^0 = g^\pi = \hbar\omega/2$

N. Ünal et al., PRL 122, 253601 (2019)

Track gap-closing points

Stückelberg oscillations:

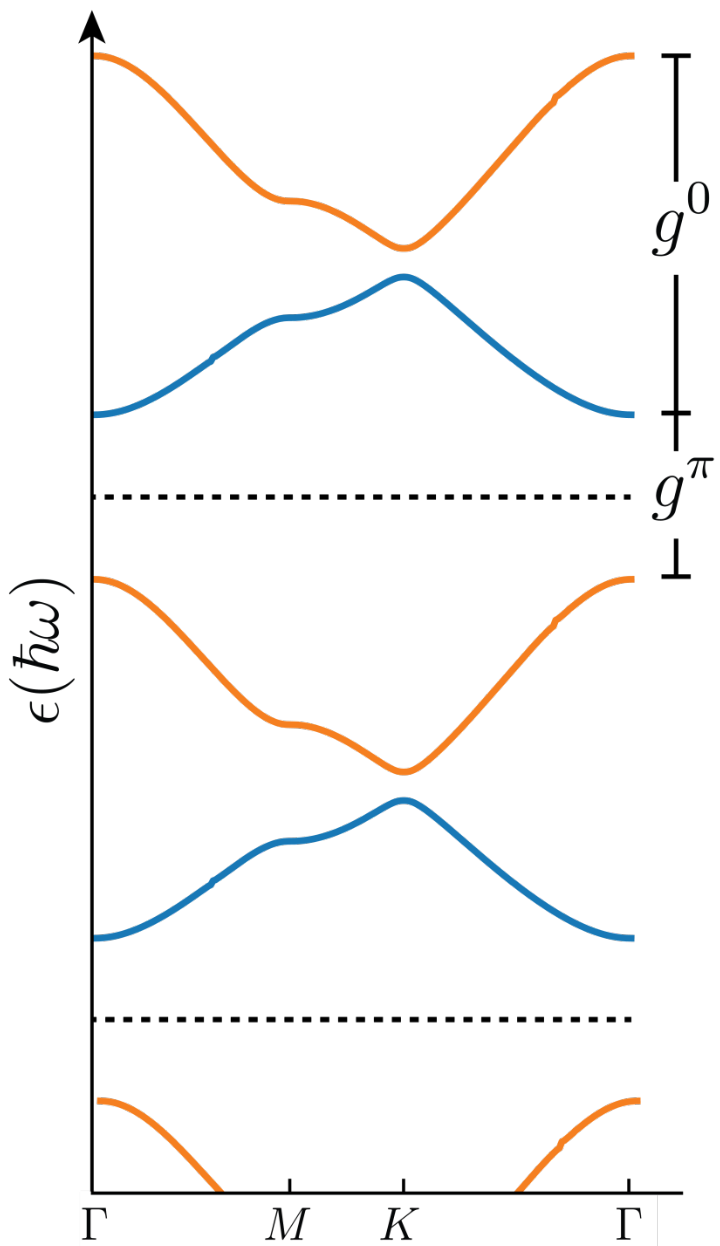

- We always measure the *smaller energy gap:* $\min(g^0, g^\pi)$
- In the *high-frequency limit* we probe g^0
- Transition, when
  $$g^0 = g^\pi = \hbar\omega/2$$

N. Ünal et al., PRL 122, 253601 (2019)

Identify different energy gaps

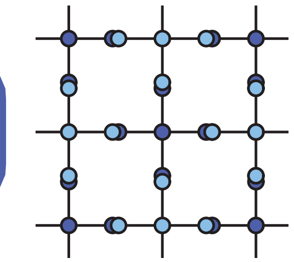

Γ-point:

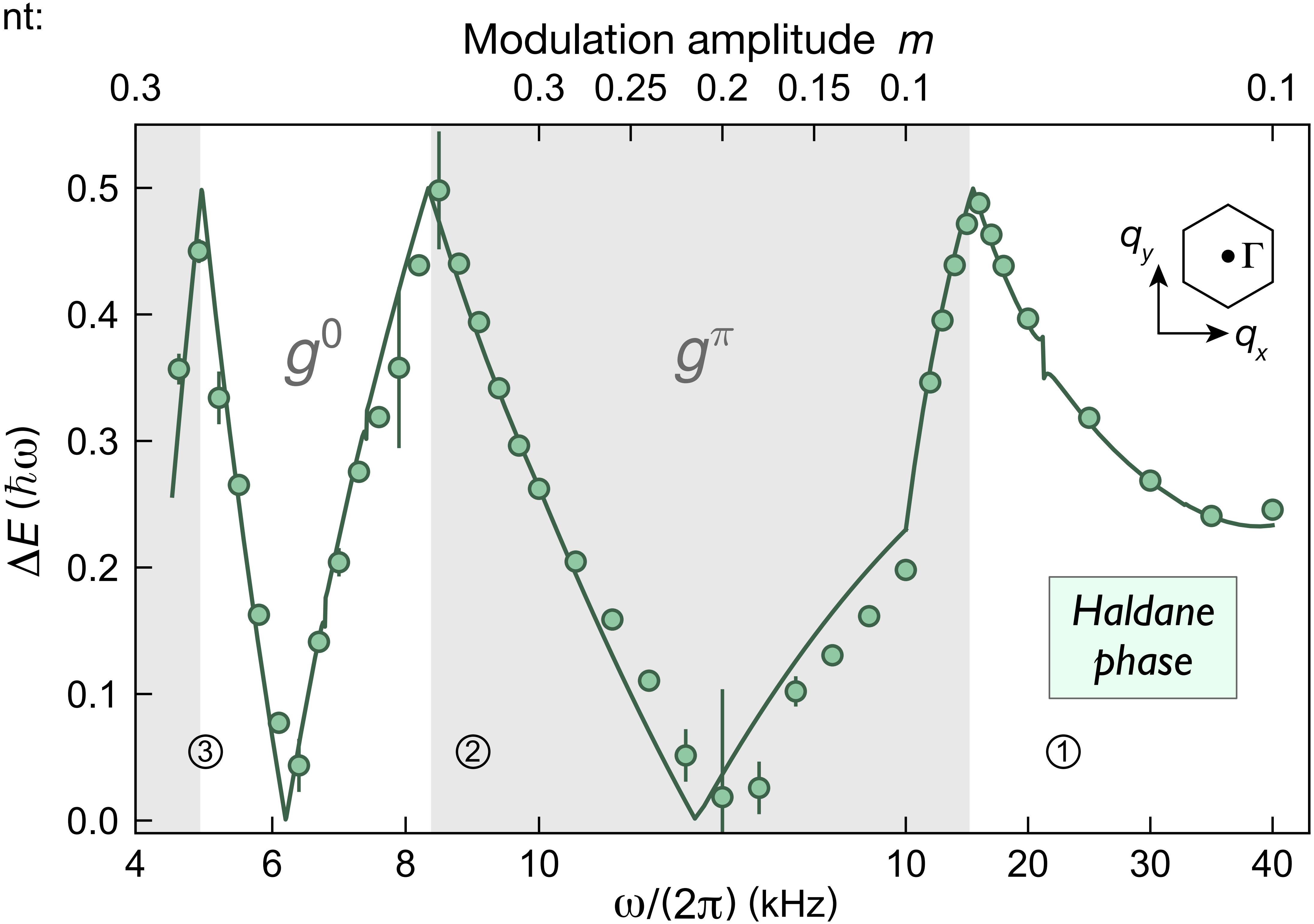

K. Wintersperger, ..., M.A., Nature Phys. **16**, 1058-1063 (2020)

Topology of gap-closing points

$\mathbf{\Gamma}$-point:

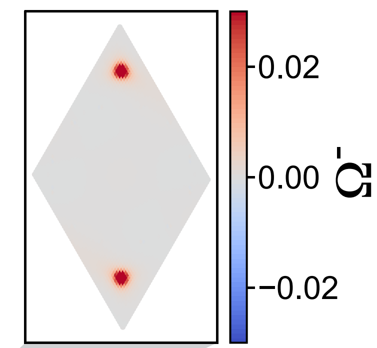

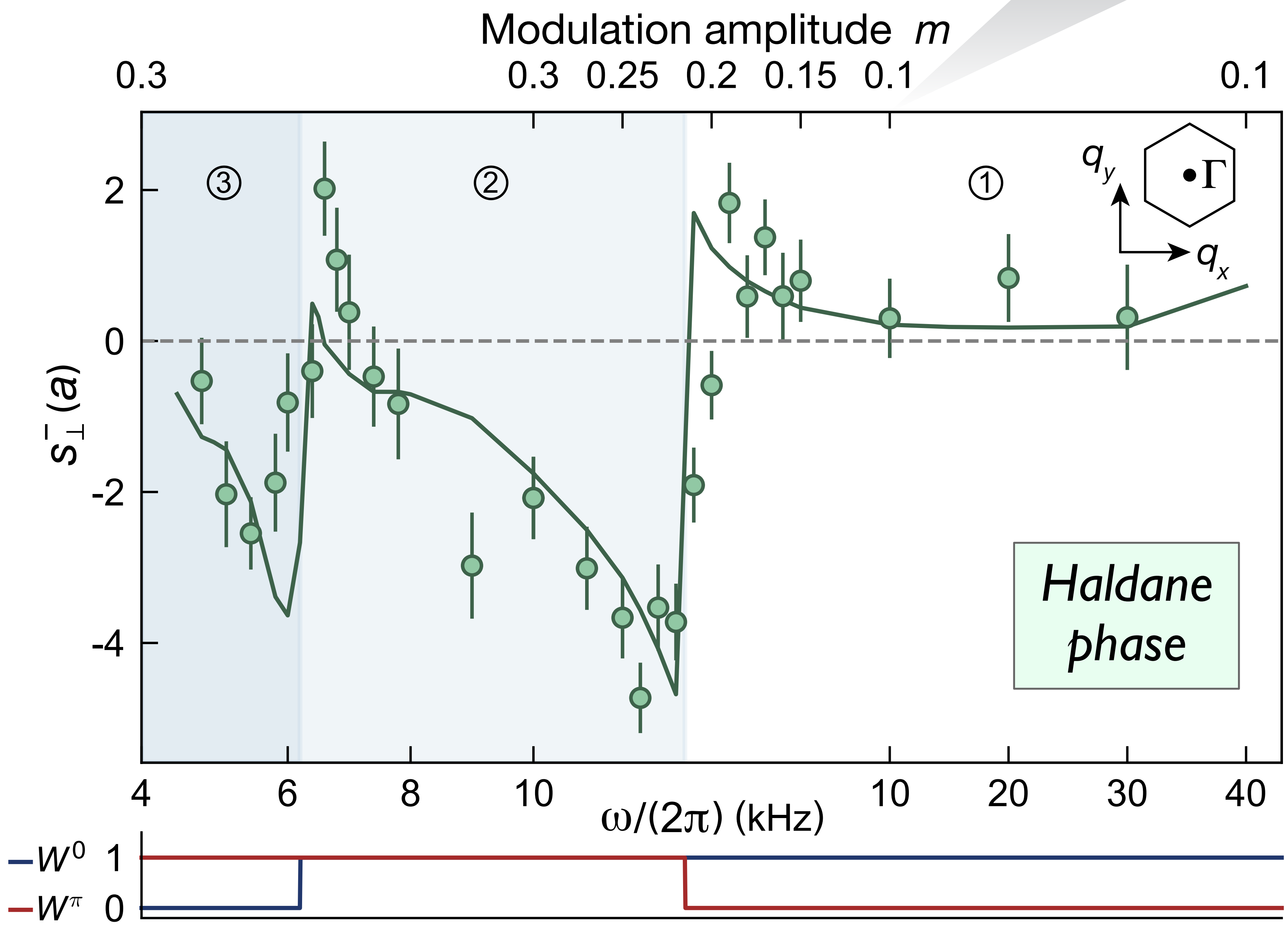

Topology of gap-closing points

Γ-point:

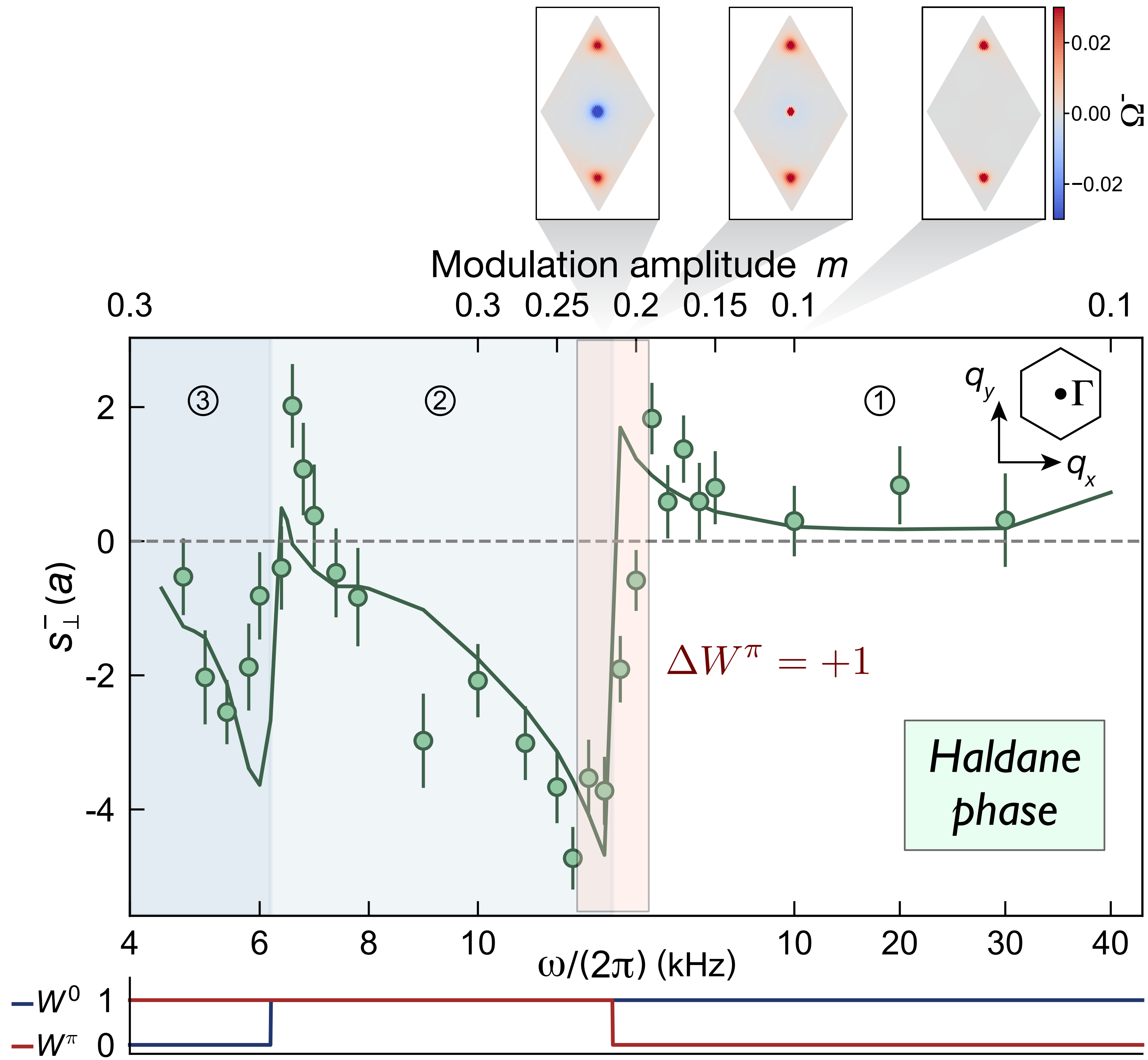

Topology of gap-closing points

Γ-point:

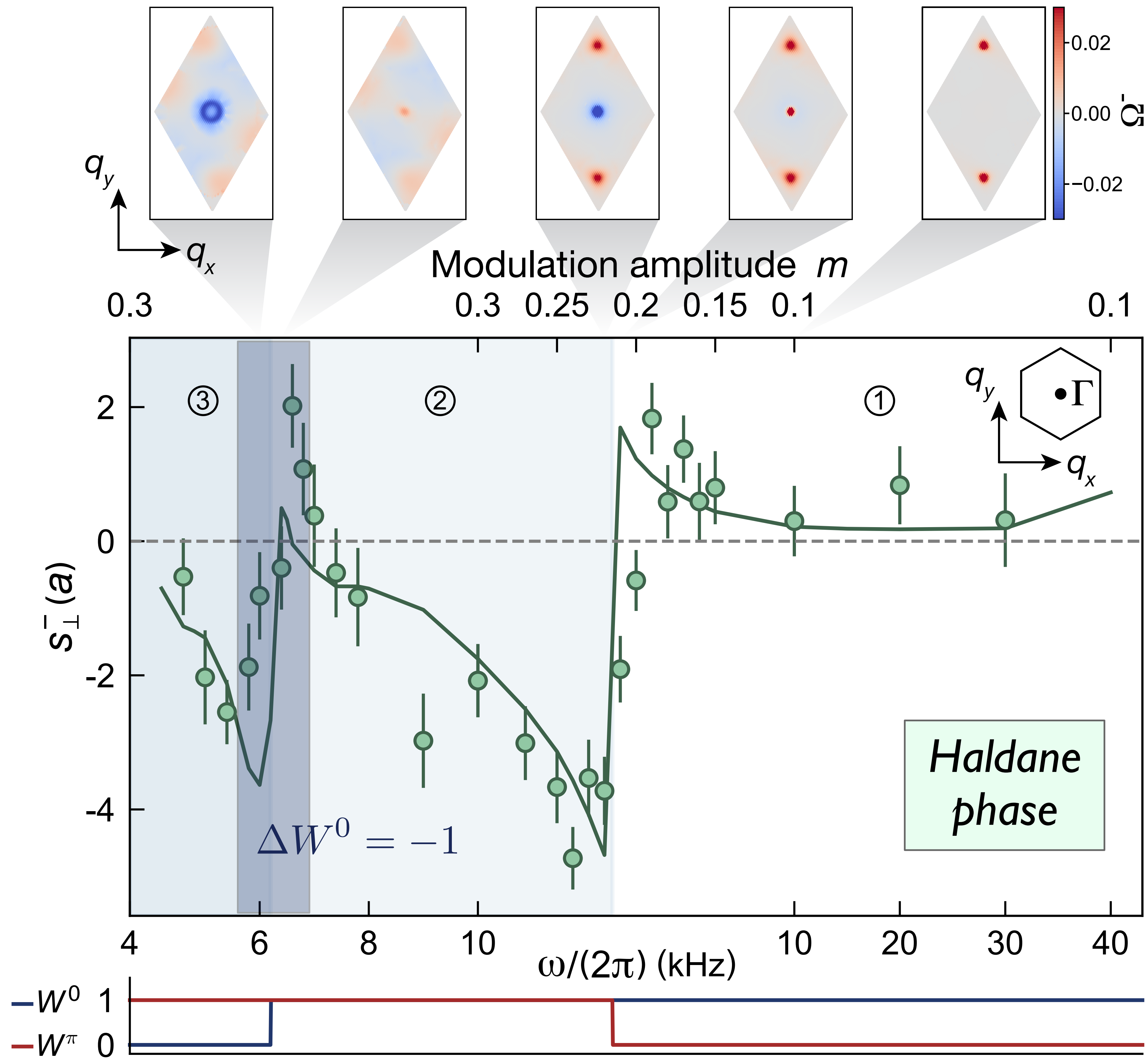

Local Hall-deflection measurements

Γ-point:

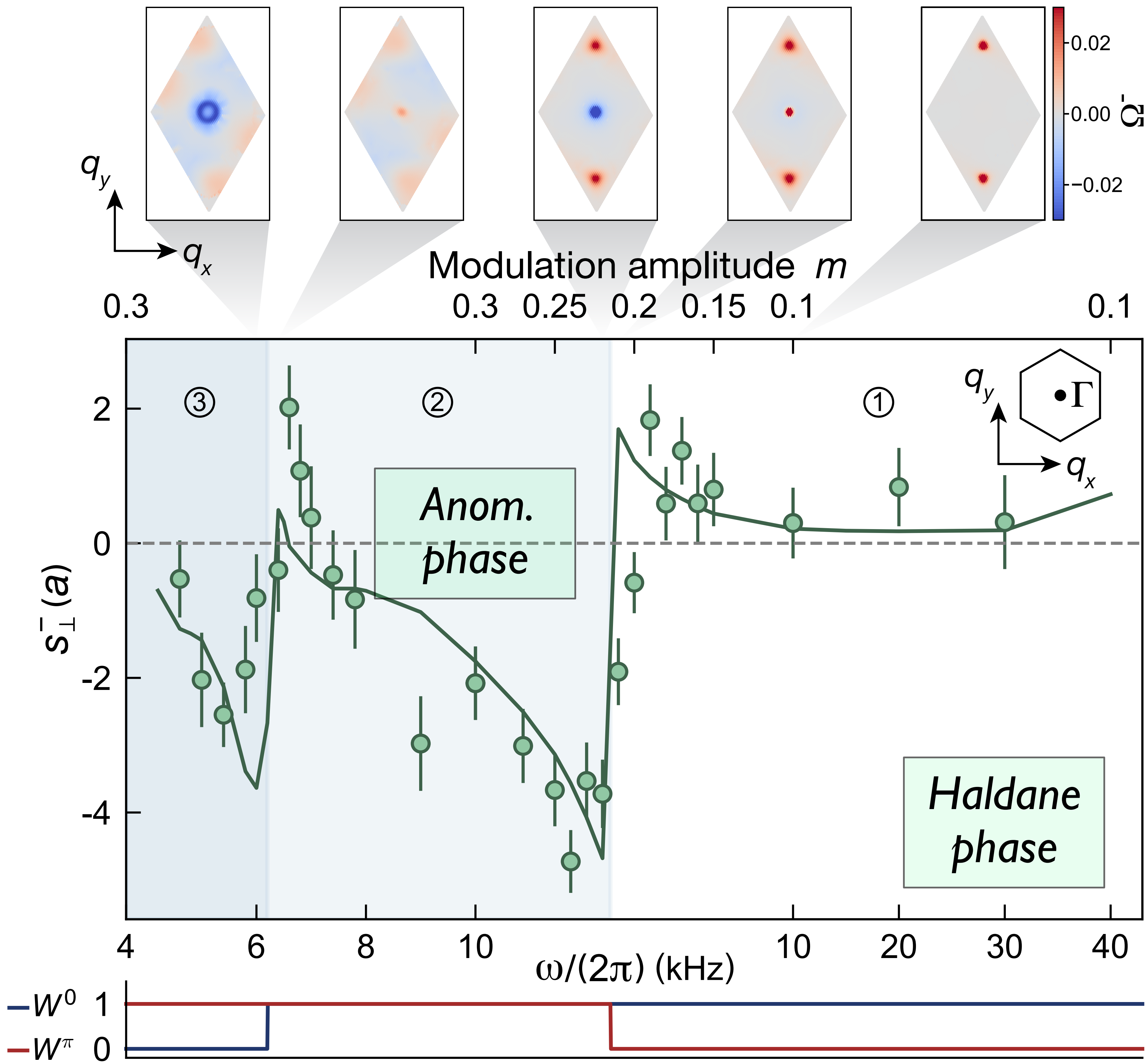

Complete set of top. invariants!

Making synthetic gauge fields dynamical

Density-dependent gauge fields

Non-trivial gauge-matter coupling

previously. *no backaction* of motion of particles onto fields

Use periodic driving
to control amplitude and
phase of *density-assisted tunneling processes*

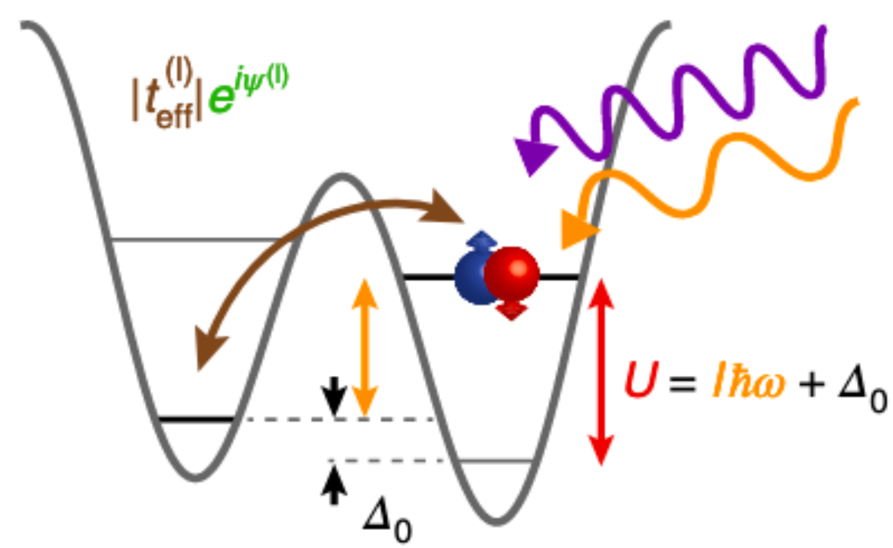

How to engineer local symmetries?

L. W. Clark *et al.* Phys. Rev. Lett. **121**, 030402 (2018); F. Görg *et al.* Nat. Phys. **15**, 1161-1167 (2019)

Gauge theories

Lattice gauge theories:

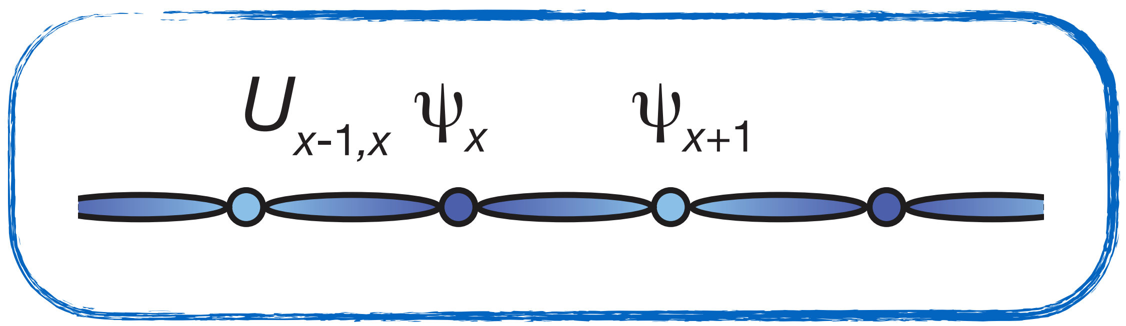

Matter (fermionic) & *gauge (bosonic) fields*

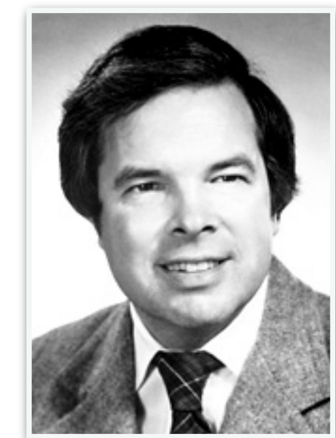

K. G. Wilson

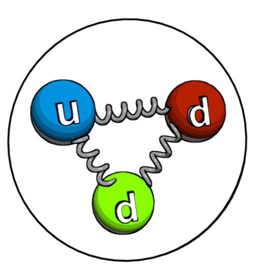

High Energy Physics

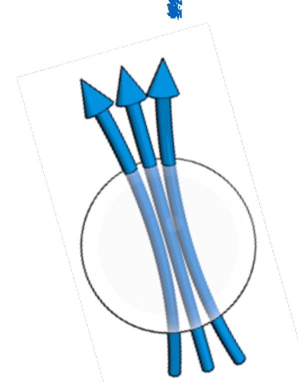

Condensed Matter Physics

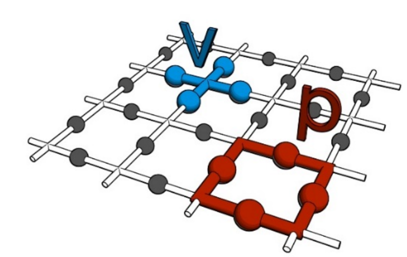

Top. Quantum Computation

Simulating lattice gauge theories

Lattice gauge theories:

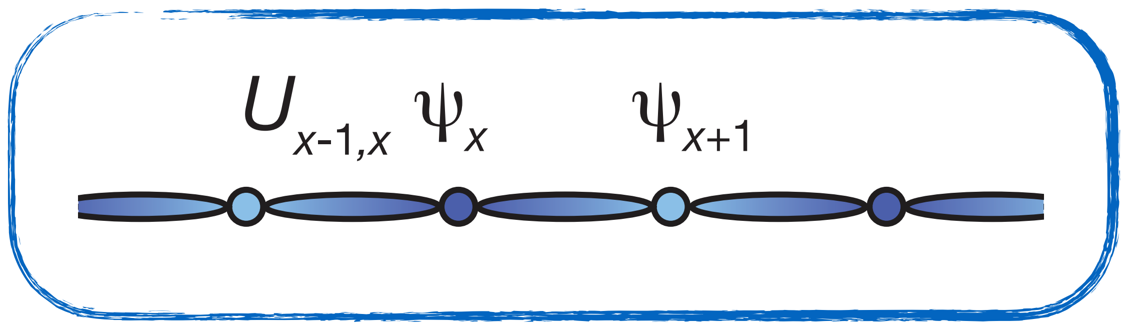

Matter (fermionic) & *gauge (bosonic) fields*

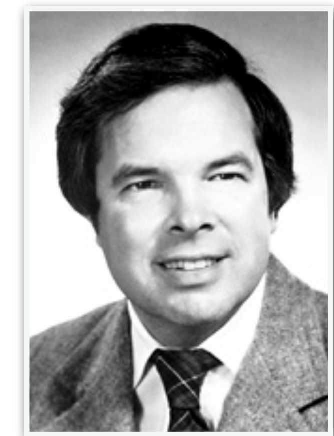

K. G. Wilson

Microscopically engineered quantum systems
in table-top experiments

Challenges:

- **matter- and gauge-field** coupling
- **local symmetry** (Gauss's law)

U.-J. Wiese *et al.* Ann. Phys. **525**, 777-796 (2013); E. Zohar *et al.* Rep. Prog. Phys. **79**, 014401 (2015);
M. Dalmonte *et al.* Contemp. Phys. **57**, 388-412 (2016); M. Banuls *et al.* Eur. Phys. J. D **74**, 165 (2020)

Quantum link models: implementations

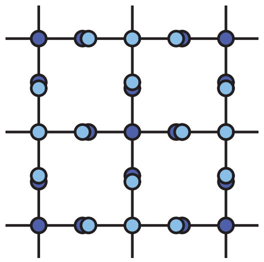

- Staggered 1D Bose-Hubbard chains

  B. Yang *et al.* Nature **587**, 392-396 (2020)

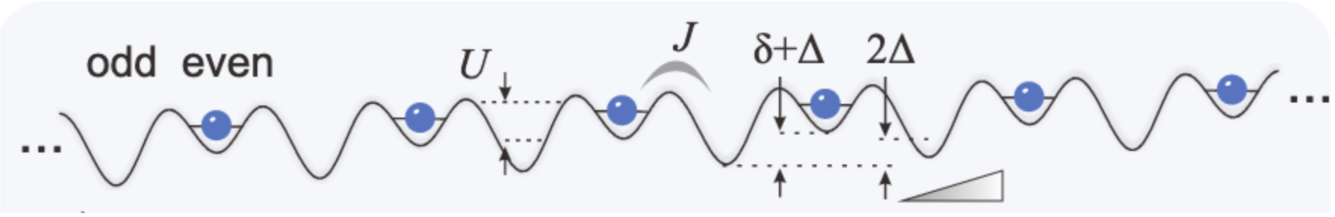

- Rydberg atom quantum simulator

  H. Bernien *et al.* Nature **551**, 579 (2017); F. M. Surace *et al.* Phys. Rev. X **10**, 021041 (2020)

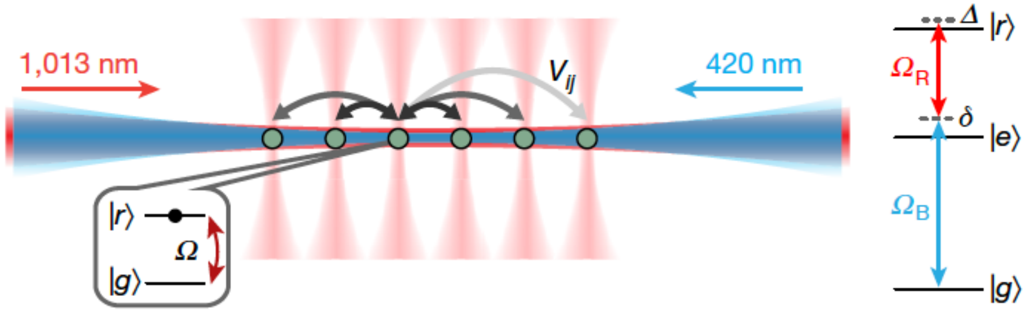

- Atomic mixtures / spin-changing collisions

  E. Zohar *et al.* Phys. Rev. A **88**, 023617 (2013); A. Mil *et al.* Science **367**, 1128-1130 (2020)

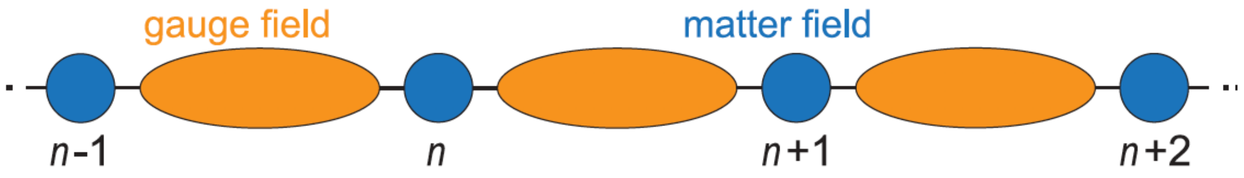

$\mathbb{Z}_2$ lattice gauge theory coupled to matter

$$\hat{H}_{\mathbb{Z}_2} = +\sum_j J_a \left(\hat{\tau}^z_{\langle j,j+1\rangle} \hat{a}^\dagger_j \hat{a}_{j+1} + \text{h.c.} \right) - \sum_j J_f \hat{\tau}^x_{\langle j,j+1\rangle}$$

$\mathbb{Z}_2$ charge

$\hat{Q}_j = e^{\mathrm{i}\pi \hat{n}^a_j}$

$\mathbb{Z}_2$ gauge field

$\tau^z = +1$

$\mathbb{Z}_2$ electric field

$\tau^x = +1$

- matter-gauge field coupling with strength J_a
- energy of electric field J_f

a matter field f gauge field

C. Schweizer,..., MA, *et al.*, Nat. Phys. **15**, 1168-1173 (2019)

Gauss's law

Z_2 symmetry:

$$\hat{G}_j = \hat{Q}_j \prod_{i:\langle i,j \rangle} \hat{\tau}^x_{\langle i,j \rangle}, \qquad \left[\hat{H}, \hat{G}_j\right] = 0 \quad \forall j$$

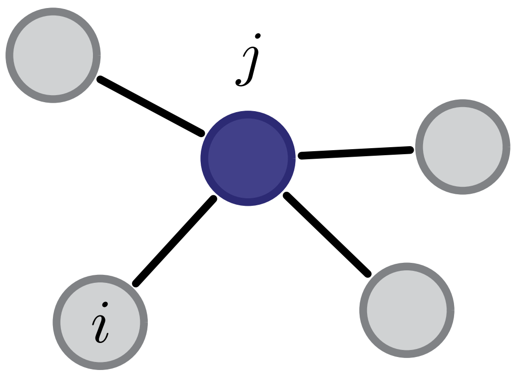

eigenvalues: $g_j = \pm 1$

Z_2 Gauss's law:

$$\boxed{\hat{G}_j |\psi\rangle = g_j |\psi\rangle}$$

g_j : local conserved quantities

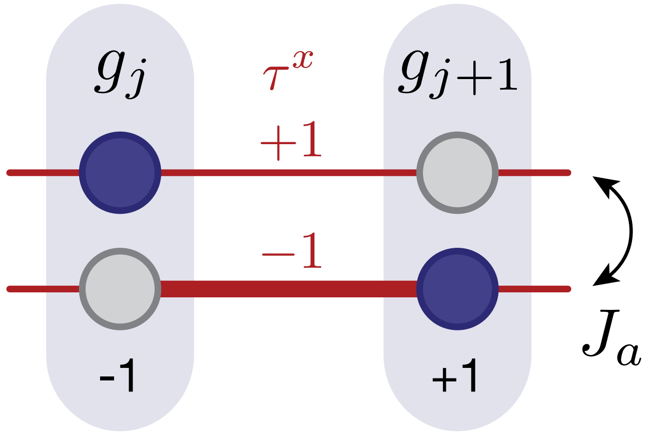

→ Subsectors characterized by set of conserved quantities $\{g_j\}$

C. Schweizer,..., MA, *et al.*, Nat. Phys. **15**, 1168-1173 (2019)

Dynamics in 1D

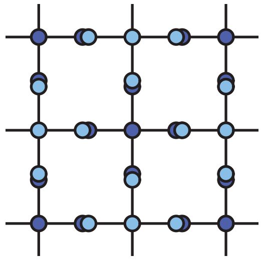

Initial state:

Single charge on site j=0

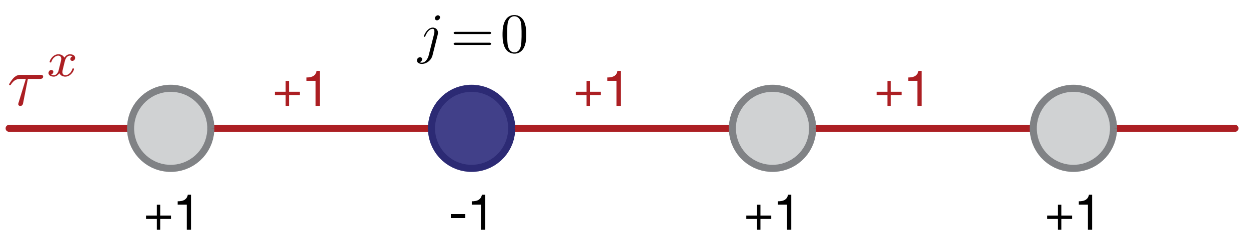

electric field $J_f \rightarrow 0$

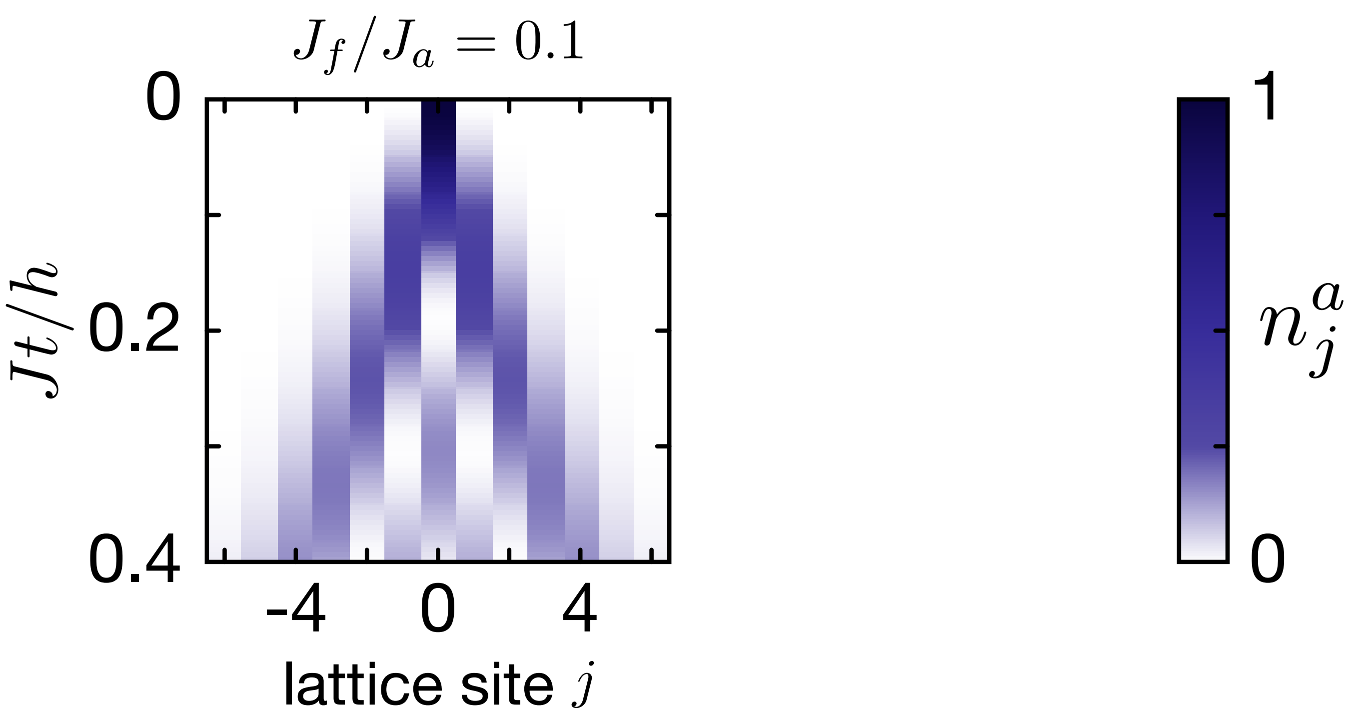

electric field dominated: $J_f \gg J_a$

C. Schweizer,..., MA, *et al.*, Nat. Phys. **15**, 1168-1173 (2019)

Dynamics in 1D

Initial state:

Single charge on site *j*=0

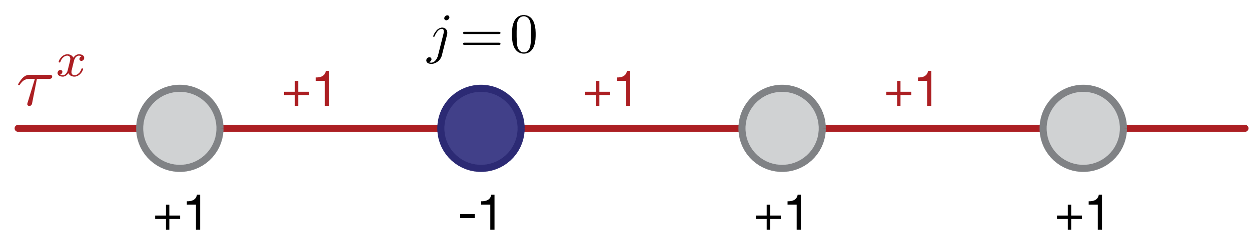

electric field
$J_f \to 0$

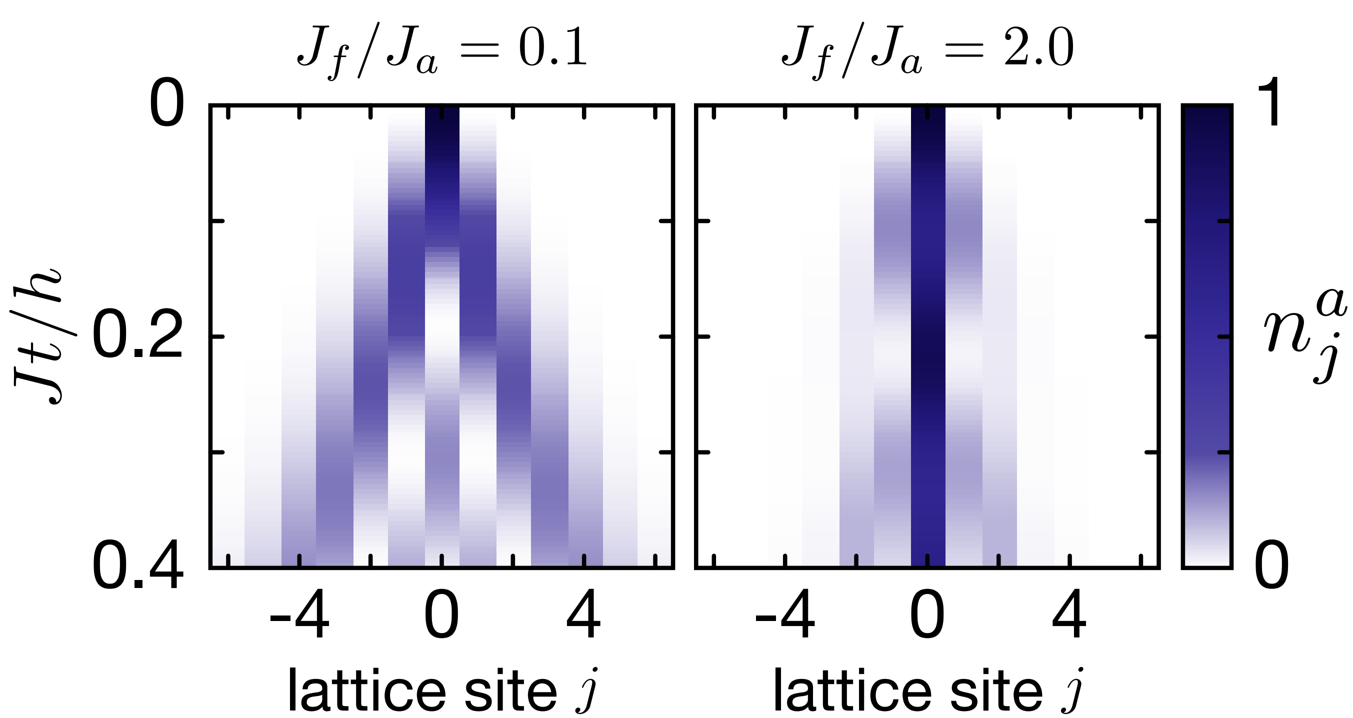

electric field dominated:
$J_f \gg J_a$

C. Schweizer,..., MA, *et al.*, Nat. Phys. **15**, 1168-1173 (2019)

$\mathbb{Z}_2$ lattice gauge theory coupled to matter

$$\hat{H}_{\mathbb{Z}_2} = + \sum_j J_a \left(\hat{\tau}^z_{\langle j,j+1 \rangle} \hat{a}^\dagger_j \hat{a}_{j+1} + \text{h.c.} \right) - \sum_j J_f \hat{\tau}^x_{\langle j,j+1 \rangle}$$

Building block:

$$\hat{\tau}^z = \hat{n}^f_1 - \hat{n}^f_2$$

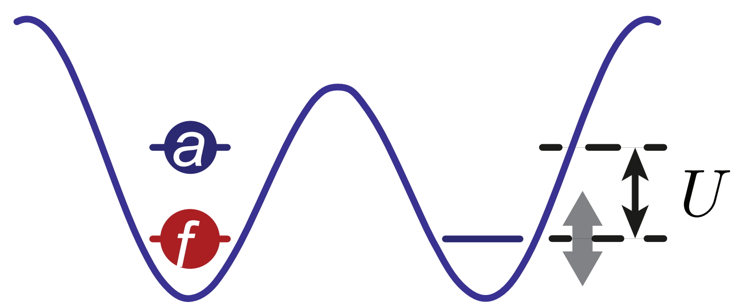

Implementation:

- mixture of two-component bosons
- resonant modulation at interaction U

a matter field *f* gauge field

C. Schweizer,..., MA, *et al.*, Nat. Phys. **15**, 1168-1173 (2019)

Floquet scheme

Resonant driving: $\hbar\omega = U$, $\hbar\omega \gg J$ and $\phi = \{0, \pi\}$

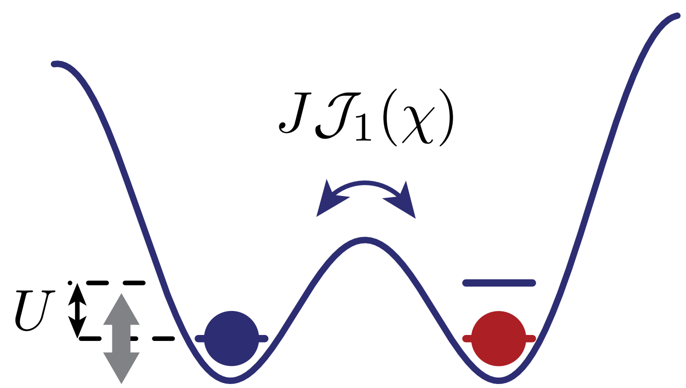

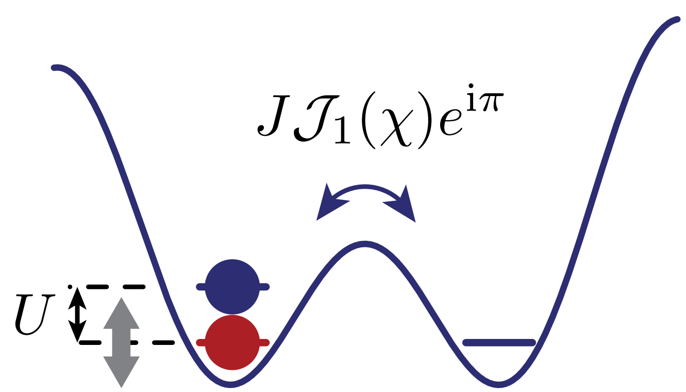

Tunneling of matter particle:

Link variable: $\hat{\tau}^z = \hat{n}_1^f - \hat{n}_2^f$

$$\boxed{\hat{H}_{\text{eff}} = J_a\,\hat{\tau}^z\left(\hat{a}_2^\dagger \hat{a}_1 + \hat{a}_1^\dagger \hat{a}_2\right)} \quad J_a = J\mathcal{J}_1(\chi)$$

Reflection properties of Bessel function:

$$\mathcal{J}_{-\nu}(\chi) = (-1)^\nu \mathcal{J}_\nu(\chi)$$

a matter field *f* gauge field

C. Schweizer,..., MA, *et al.*, Nat. Phys. **15**, 1168-1173 (2019)

Floquet scheme

Resonant driving: $\hbar\omega = U$, $\hbar\omega \gg J$ and $\phi = \{0, \pi\}$

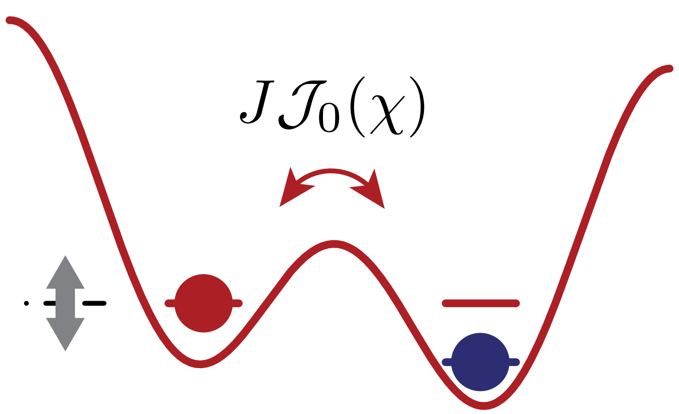

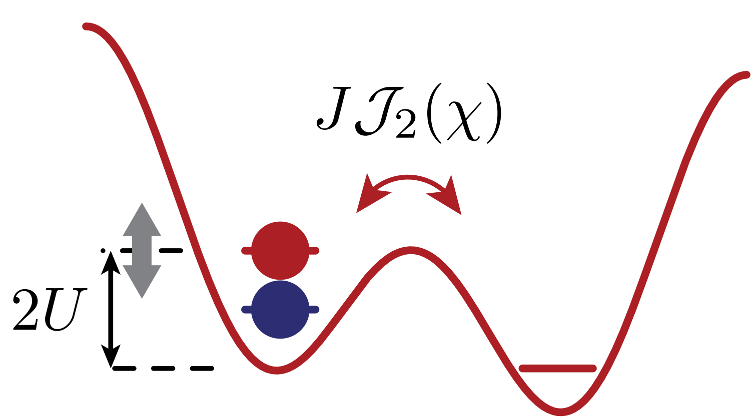

Tunneling of gauge-field particle:

Needs to be real: $\hat{\tau}^x = \hat{f}_1^\dagger \hat{f}_2 + \hat{f}_2^\dagger \hat{f}_1$

Depend weakly on position of a-particle:

$$\boxed{\hat{J}_f = J\mathcal{J}_0(\chi)\,\hat{n}_1^a + J\mathcal{J}_2(\chi)\,\hat{n}_2^a}$$

Can be avoided for:

$\chi = 1.84:\quad \mathcal{J}_0(\chi) = \mathcal{J}_2(\chi)$

a matter field *f* gauge field

C. Schweizer,..., MA, *et al.*, Nat. Phys. **15**, 1168-1173 (2019)

Dynamics double-well

Initial state I:

eigenstate of electric-field operator $\hat{\tau}^x$

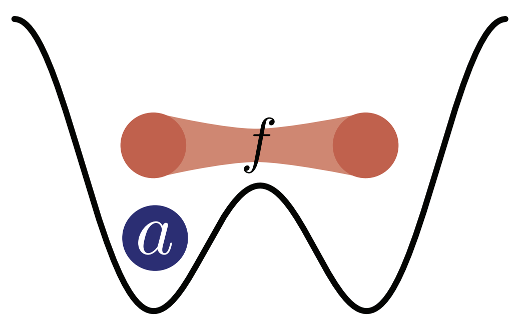

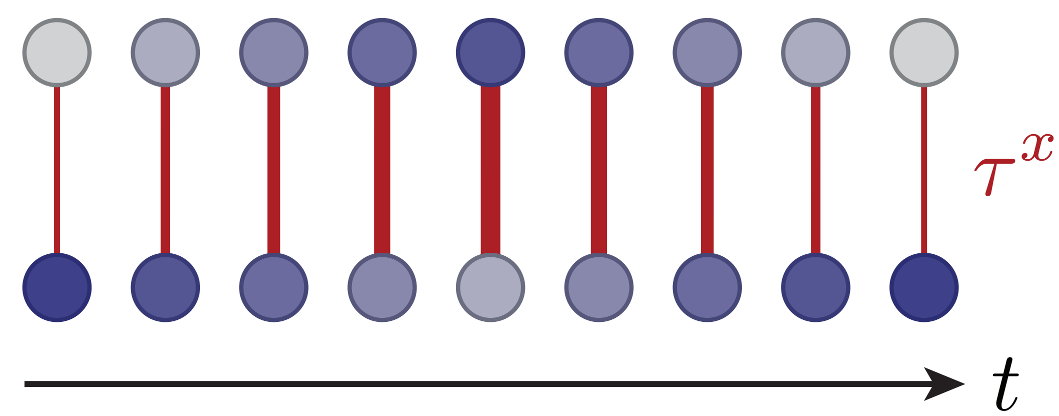

$$|\psi_0^x\rangle = |a, 0\rangle \otimes (|f, 0\rangle + |0, f\rangle)\,/\sqrt{2}$$

eigenvalues $g_1 = -1$ and $g_2 = +1$

⇒ oscillation amplitude / frequency depends on ratio $J_f\,/\,J_a$!

C. Schweizer,..., MA, *et al.*, Nat. Phys. **15**, 1168-1173 (2019)

Dynamics double-well

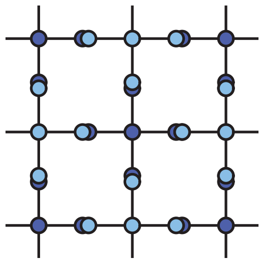

Observed dynamics:

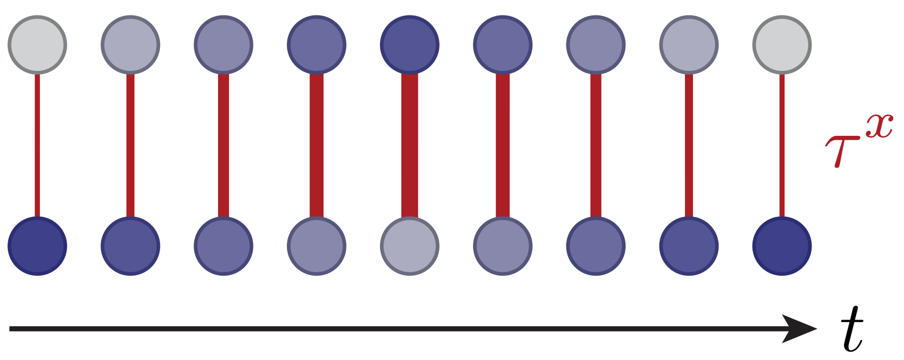

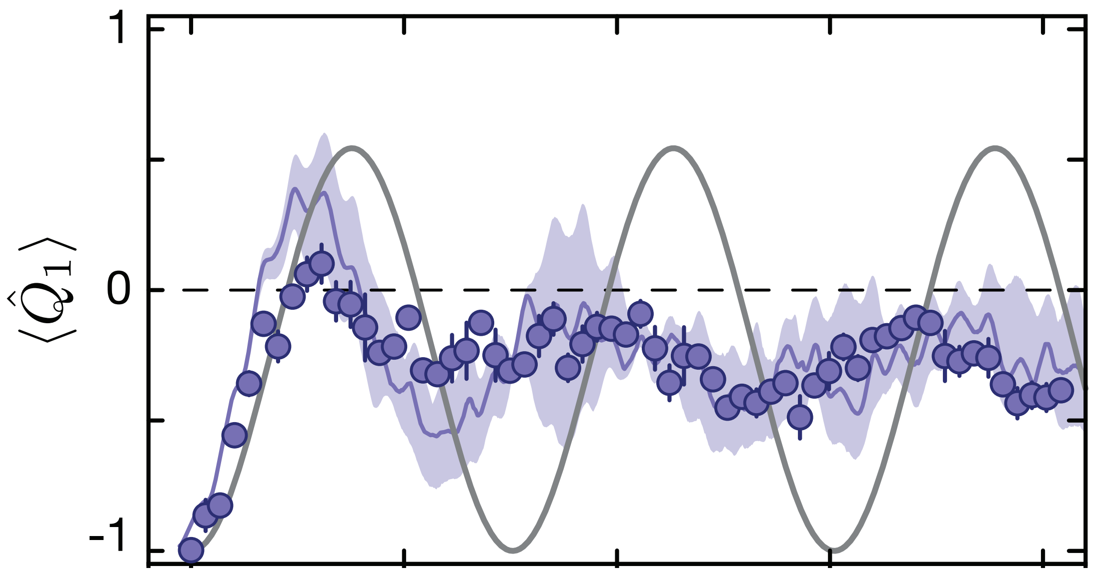

Observable: site occupations

⇒ *Z_2 charge* + *Z_2 gauge field*

Parameters: $J_f / J_a \approx 0.54$

C. Schweizer,..., MA, *et al.*, Nat. Phys. **15**, 1168-1173 (2019)

Dynamics double-well

Observed dynamics:

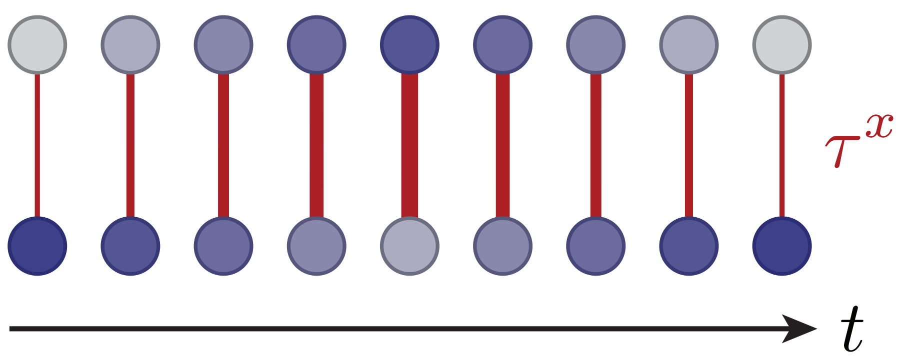

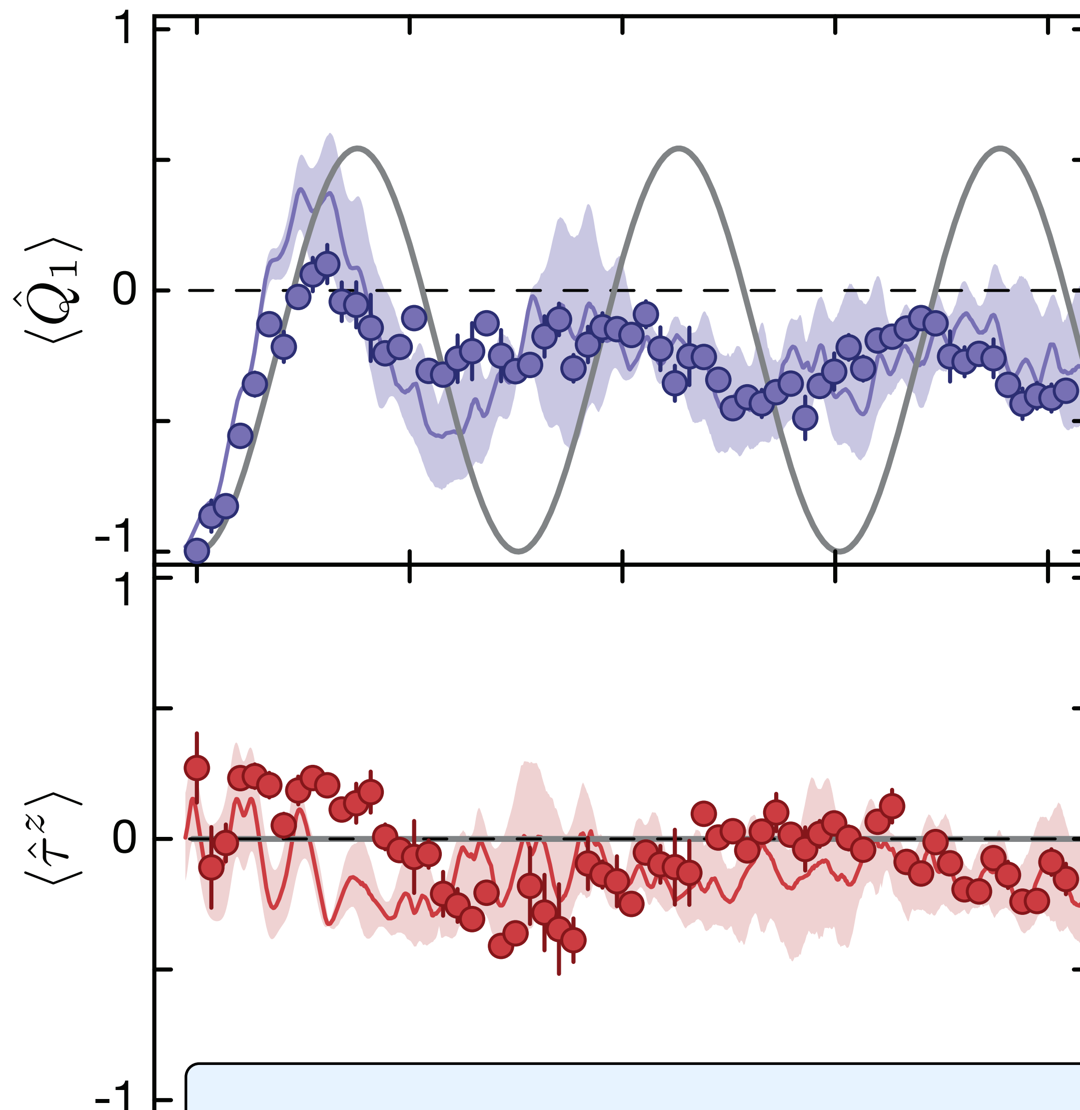

Observable: site occupations

$\Rightarrow$ *Z_2 charge* + *Z_2 gauge field*

Parameters: $J_f / J_a \approx 0.54$

Gauge-field dynamics suppressed!

C. Schweizer,..., MA, *et al.*, Nat. Phys. **15**, 1168-1173 (2019)

Dynamics double-well

Initial state II:

eigenstate of electric-field operator $\hat{\tau}^z$

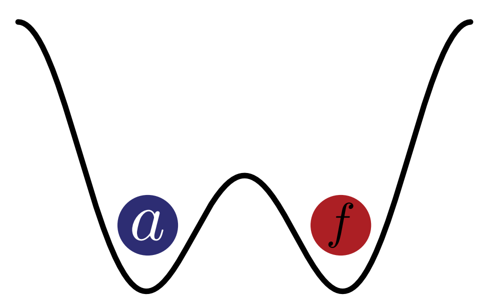

$$|\psi_0^z\rangle = |a,0\rangle \otimes |0,f\rangle$$

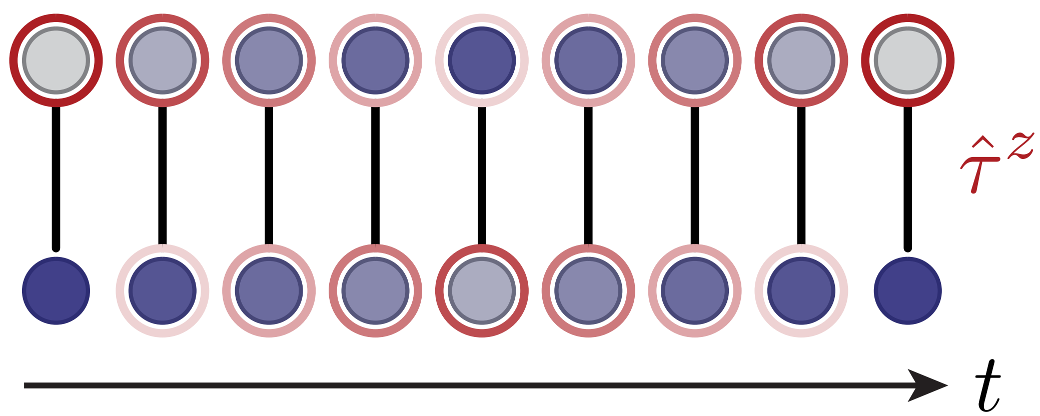

coherent superposition of two subsectors
with $g_1 = -g_2 = \pm 1$

$$\boxed{\langle \hat{G}_1\rangle = \langle \hat{G}_2\rangle = 0}$$

- Note, subsectors are *not coupled*
- Dynamics of charge unchanged!

C. Schweizer,..., MA, *et al.*, Nat. Phys. **15**, 1168-1173 (2019)

Dynamics double-well

Observed dynamics:

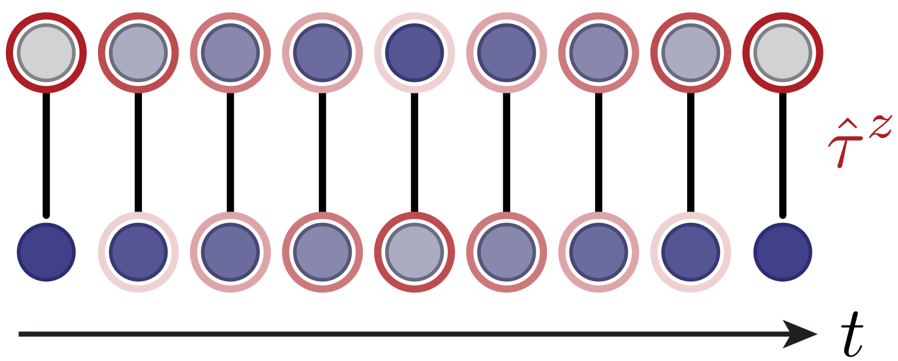

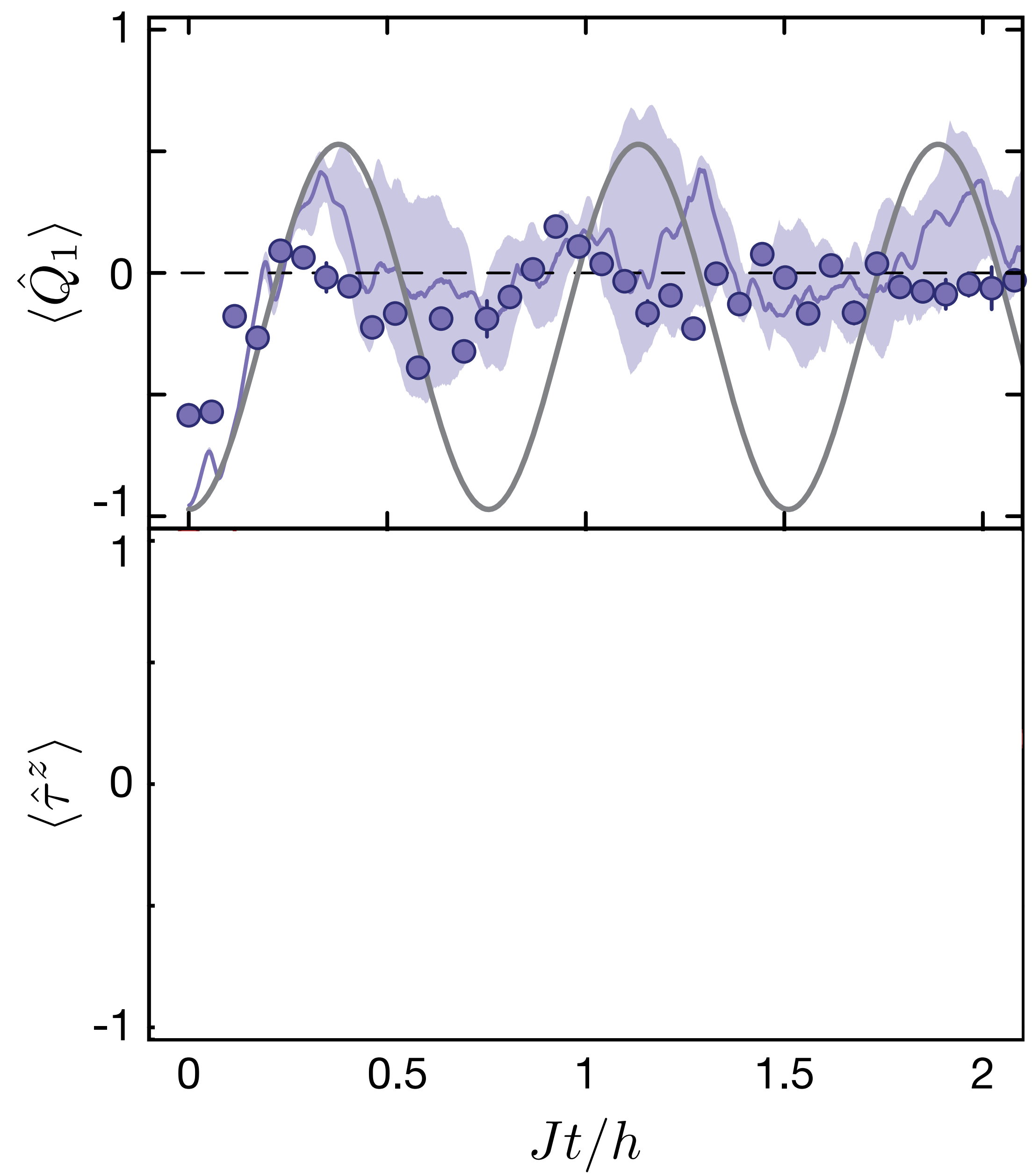

Observable: site occupations

$\Rightarrow$ *Z_2 charge* + *Z_2 gauge field*

Parameters: $J_f/J_a \approx 0.54$

C. Schweizer,..., MA, *et al.*, Nat. Phys. **15**, 1168-1173 (2019)

Dynamics double-well

Observed dynamics:

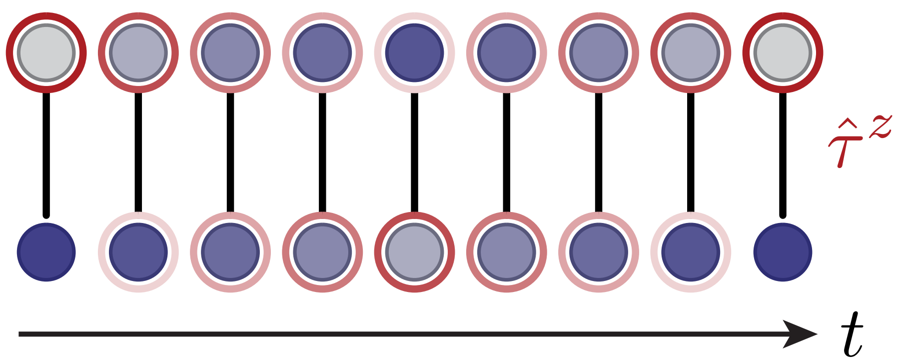

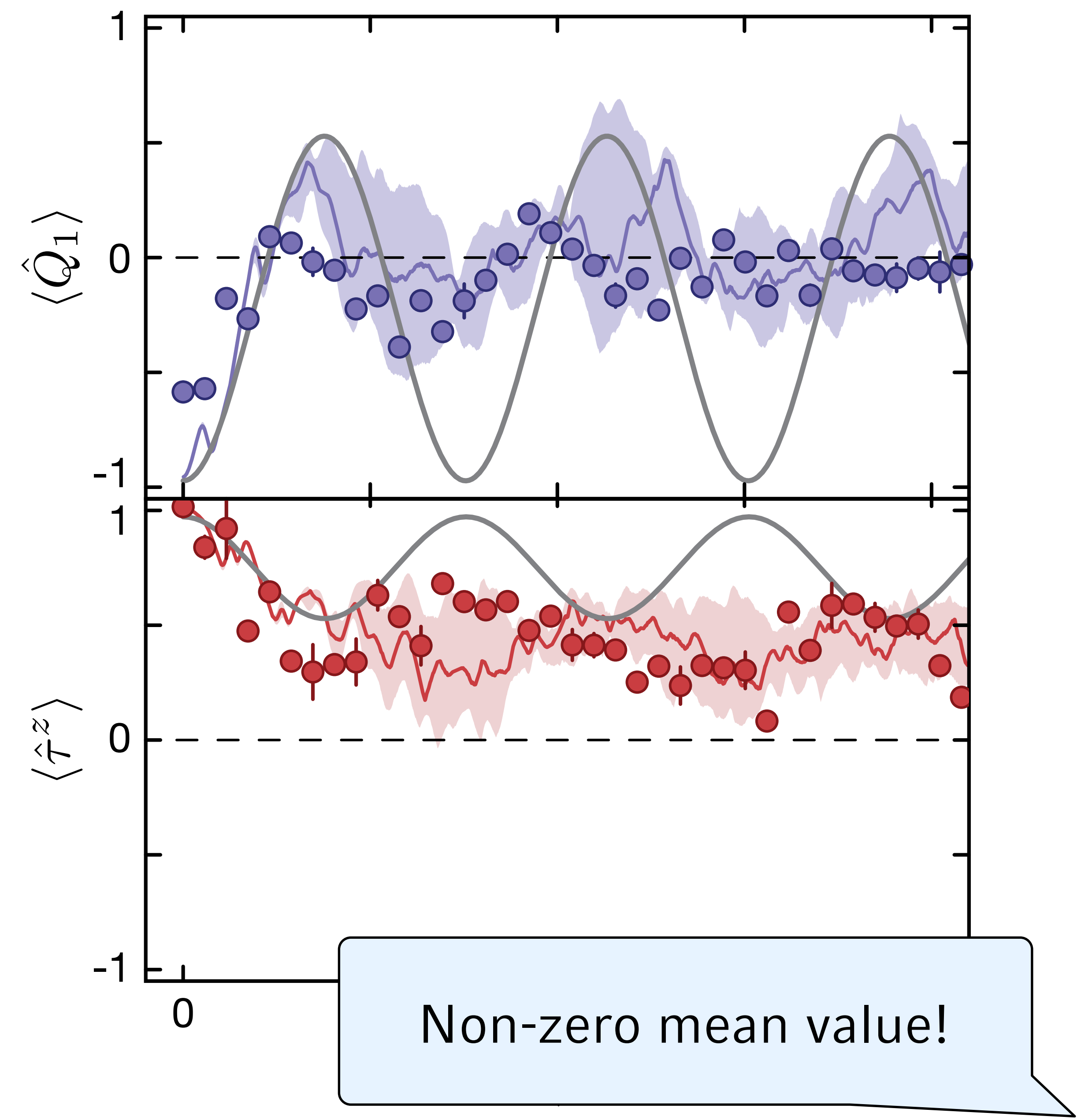

Observable: site occupations

⇒ *Z_2 charge* + *Z_2 gauge field*

Parameters: $J_f/J_a \approx 0.54$

C. Schweizer,..., MA, *et al.*, Nat. Phys. **15**, 1168-1173 (2019)

Corrections

Symmetry-breaking terms

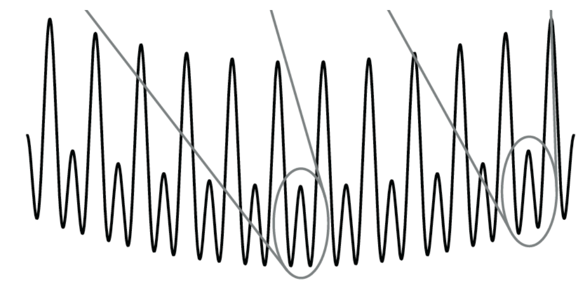

- tilt distribution ➞ create *homogeneous potential*
- correlated tunneling processes due to *higher-order Floquet corrections & extended Bose-Hubbard terms* *(deeper lattices)*

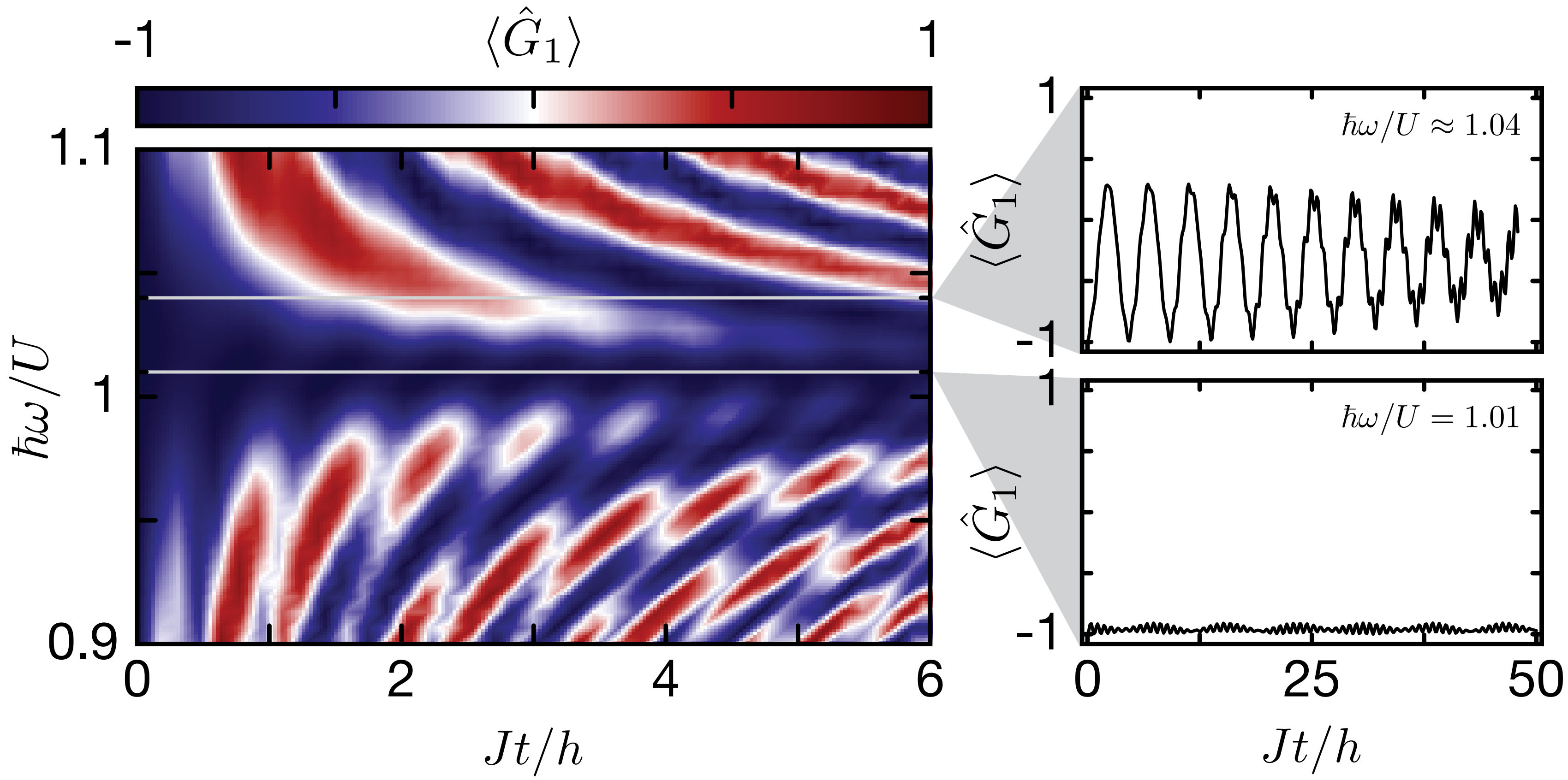

C. Schweizer,..., MA, *et al.*, Nat. Phys. **15**, 1168-1173 (2019)

Thank you!